# INVESTIGATION OF RELATIVE EXPRESSION LEVEL OF

# *SLC4* BICARBONATE TRANSPORTER FAMILY

# IN MOUSE AND HUMAN CORNEAL ENDOTHELIAL CELLS

WILLIAM SHEI (A) KHAING HLAING TUN
*(M.B.,B.S. University of Medicine 1, Myanmar)*

A THESIS SUBMITTED

FOR THE DEGREE OF MASTER OF SCIENCE

DEPARTMENT OF OPHTHALMOLOGY

NATIONAL UNIVERSITY OF SINGAPORE

2011

# Acknowledgements

# Table of Contents

# Summary

The solute carrier 4 (SLC4) family, composed of 10 integral membrane proteins (SLC4A1-SLC4A11), mediates transportation of bicarbonate ions and solutes across plasma membrane. Bicarbonate ions have been implicated as playing a central role in human corneal endothelial ion pump to maintain corneal transparency. Several members of *SLC4* gene family have been linked to ocular diseases in human. Given the involvement of at least two genes (*SLC4A11* and *SLC4A4*) within the *SLC4* family in corneal dystrophies, we hypothesized that this family of proteins are important to the normal function of the corneal endothelium, and that there could be other members of the family equally important but as yet unrecognized to be so in the cornea. Therefore in this study we aimed to characterize the relative expression levels of all *SLC4* gene family members in mouse and human corneal endothelium, using real time qRT-PCR, in order to identify further members from this family that can serve as candidate genes for analysis in corneal dystrophies. Furthermore, as important proteins in the cornea, SLC4A11 and SLC4A4 will be subject to study in *in vitro* systems (i.e. corneal endothelial cell culture system), we therefore wanted to explore how close to the base line levels the gene expression levels remain after cells have been subject to expansion and culture. Our analyses revealed that all *SLC4* bicarbonate transporter family members were expressed in both mouse and human primary corneal endothelium. The *SLC4A11* showed the highest expression and its expression was approximately 2.75 times higher (2.75±0.1 [p=0.0004]) than that of *SLC4A4* in human corneal endothelium. Hence, based on their level of expression in human corneal endothelium, the *SLC4* family members can be categorized into three groups: *SLC4A11* and *SLC4A4* in 'high expression', *SLC4A2, SLC4A3, SLC4A7* and *SLC4A5* in 'moderate expression', *SLC4A1, SLC4A8, SLC4A10* and *SLC4A9* in 'very low expression'. Interestingly, during culturing of

HCECs the expression of *SLC4A11* in cultured cells was significantly reduced by approximately 40% (0.59±0.04 [p=0.0026]) in early passage and by approximately 70% (0.31±0.01 [p=0.00007]) in late passage compared to uncultured tissue. Meanwhile, the expression of another important gene *SLC4A4* showed a significant 3-fold increase (3.74±0.16 [p=0.0011]) in early passage and 4-fold increase (4.04±0.5 [p=0.0088]) in late passage. Given the known involvement of *SLC4A4* and *SLC4A11* in corneal dystrophies, we speculate that the other two highly expressed genes, *SLC4A2* and *SLC4A7* are worthy of being considered next as potential candidate genes for corneal endothelial diseases. Moreover, the similar expression profile observed for the *SLC4* family members within the primary corneal endothelium of mouse and human suggests similar forces at play in the regulation of expression of these genes in these two mammalian species, as well as possible conservation of the functional role played by each member in solute transport in the corneal endothelium through evolution. The drastically altered expression levels of the main genes *SLC4A11* and *SLC4A4*, seen in late endothelial cell culture passages co-incident with altered cellular morphology indicate that further study should be undertaken to explore the possible link between *SLC4* gene expression and endothelial mesenchymal transition.

# List of Tables

# List of Figures

# List of Abbreviations

-/-, KO          Knockout

*18S*          18s ribosomal RNA

*ACTB*          β-actin

AD          Autosomal dominant

AE          Anion exchanger

*AQP1*          Aquaporin 1

AR          Autosomal recessive

ATP          Adenosine triphosphate

*B2M*          β2 microglobulin

bp          Base pair

BSA          Bovine serum albumin

CA          Carbonic anhydrase

cDNA          Complementary deoxyribonucleic acid

CHED2          Corneal hereditary endothelial dystrophy recessive

$Cl^-$          Chloride anion

$CO_2$          Carbon dioxide

*COL1A1*          Collagen group I A1

*COL8A2*          Collagen group VIII A2

Ct          Cycle threshold

C-terminal          Carboxyl terminal

DNA          Deoxyribonucleic acid

dNTP          Deoxy-ribonucleotide tri-phosphate

| | |
|---|---|
| E | Amplification efficiency |
| EDTA | Ethylene diamine tetra-acetate |
| EGF | Epidermal growth factor |
| EMT | Endothelial mesenchymal transition |
| EtBr | Ethidium bromide |
| FCS | Fetal calf serum |
| FECD | Familial endothelial corneal dystrophy |
| *GADPH* | Glyceraldehyde-3-phosphate dehydrogenase |
| GOI | Gene of interest |
| $H^+$ | Proton |
| $H_2CO_3$ | Carbonic acid |
| HCEC | Human corneal endothelial cells |
| $HCO_3^-$ | Bicarbonate ion |
| HKG | Housekeeping gene |
| *HPRT1* | Hypoxanthine-guanine phosphoribosyl transferase 1 |
| HS | Harboyan syndrome |
| IHCEn | Immortalized human corneal endothelial cell line |
| $K^+$ | Potassium cation |
| MCEC | Mouse corneal endothelial cells |
| MEM | Modified Eagle's Medium |
| MIM | Mandelian inheritance in man |
| mRNA | Messenger RNA |
| $Na^+$ | Sodium cation |

| | |
|---|---|
| NaHCO$_3$ | Sodium bicarbonate |
| NBC | Sodium bicarbonate cotransporter |
| NDCBE | Sodium‑driven chloride/bicarbonate exchangers |
| NGF | Nerve growth factor |
| N-terminal | Amino terminal |
| PBS | Phosphate buffered saline |
| pCO$_2$ | Partial pressure of carbon dioxide |
| PCR | Polymerase chain reaction |
| PPCD | Posterior polymorphous corneal dystrophy |
| qPCR | Quantitative polymerase chain reaction |
| RBC | Red blood corpuscle |
| RNA | Ribonucleic acid |
| RT-PCR | Reverse transcription Polymerase chain reaction |
| SAGE | Serial analysis of gene expression |
| SD | Standard deviation |
| *SLC4* | Solute carrier 4 |
| TAE | Tris-acetate-EDTA buffer |
| *TCF8* | Transcription factor 8 |
| TGF | Transforming growth factor |
| TNF | Tumour necrosis factor |
| UV | Ultraviolet |
| XR | X-linked recessive |
| ZO 1 | Zona occludens 1 |

# I.  INTRODUCTION

## 1.1  Introduction to the eye

The eye, one of the vital sense organs, is mainly composed of three coats and three structures. The outer layer is made up of the transparent cornea and the protective sclera. The intermediate layer consists of the choroid, the ciliary body, the iris and the innermost is the retina which sends neural signals to the brain through the optic nerve. Within these coats lie the aqueous humor, the lens and the vitreous body. The aqueous humor is a clear fluid that fills the anterior chamber between the cornea and the lens. The lens, which converges the light on the retina to create a sharp image, is suspended to the ciliary body by the suspensory ligament. The vitreous body fills the posterior chamber bordered by the sclera and the lens.
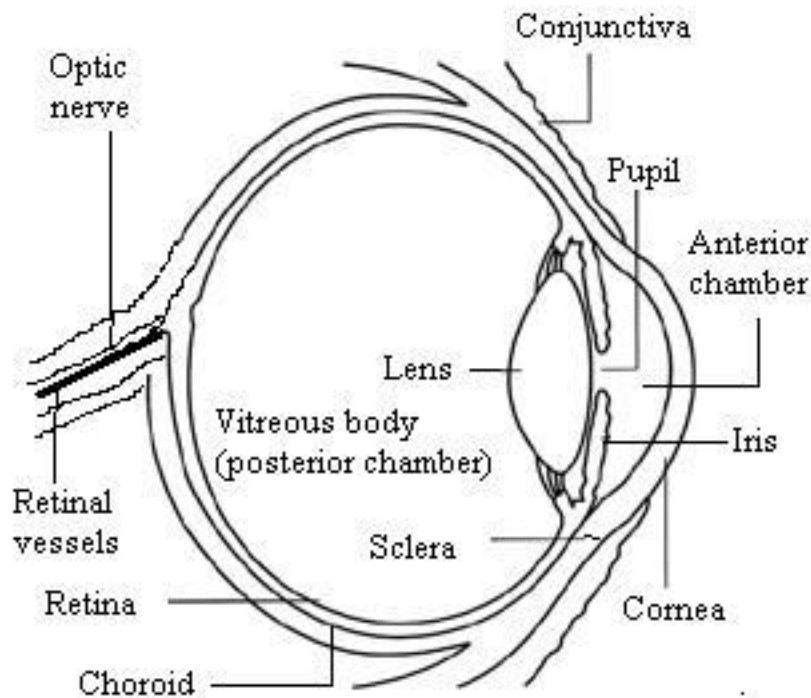
**Figure 1.1. Structure of the eye**

### 1.1.1 The cornea

The cornea, the anterior structure of the eye, is a colorless, transparent and completely avascular tissue inserted into the sclera at the limbus. The average adult cornea has approximately 550 µm thickness in the center, although there are racial variations, and is about 11.75 mm in diameter horizontally and 10.6 mm vertically. It has five distinct layers: the epithelium, Bowman's layer, the stroma, the Descemet's membrane, and the endothelium.

The stratified squamous nonkeratinized epithelium rests firmly on the thick homogeneous Bowman's layer, which is a clear acellular layer composed of thin collagen fibrils embedded in a matrix of glycosaminoglycans and is a modified portion of the stroma. The corneal stroma, the thickest component, consists of approximately 60 layers of long type I collagen fibers alternating with keratocytes that produce collagen and ground substance. Beneath the corneal stroma is a thick elastic layer known as Descemet's membrane, produced by the endothelial cells posterior to it and considered to be the basement membrane of the endothelial cells. It serves as a barrier to infections.

The endothelium is a nonvascular monolayer of highly metabolic, mitotically inactive, simple cuboidal cells held together by tight junctions. It is formed by the migration and proliferation of neural crest derived mesenchymal cells located at the periphery of the embryonic cornea. The endothelium is responsible for maintaining the essential deturgescence of the corneal stroma by transporting water or tissue fluid from the cornea. A reduction in endothelial cell density can lead to failure of endothelial function, loss of corneal transparency and visual loss.
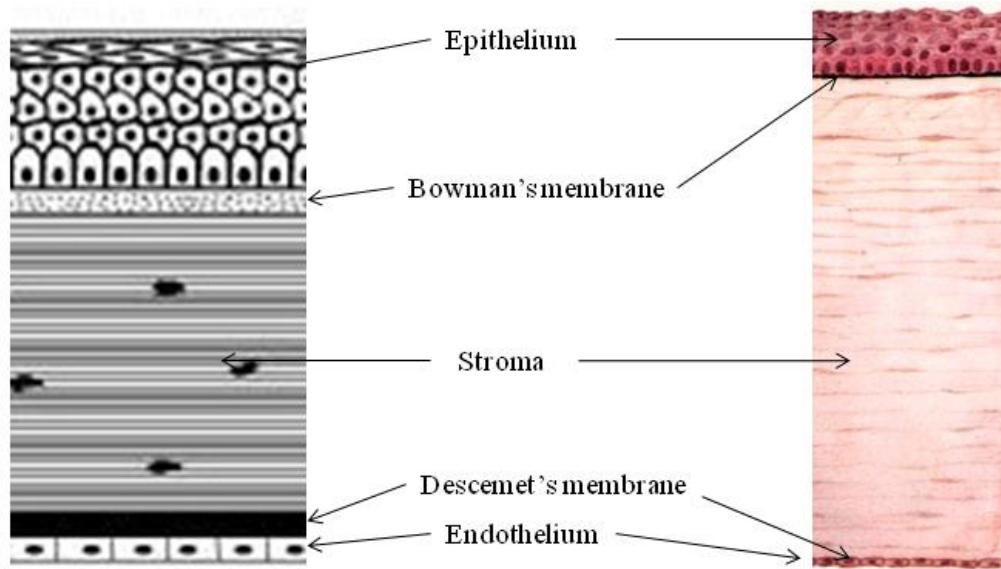
**Figure 1.2. Illustration and H & E staining of cross section of cornea.**

## 1.1.2 Maintenance of corneal transparency

Corneal transparency depends on regulation of the hydration of the corneal stroma and the mechanism by which the cornea maintains the fluid transport and its thickness has been a huge area of interest to researchers for decades. The still accepted pump leak hypothesis (Maurice DM, 1951) stated that there is the water balance between the corneal stroma and the aqueous humour caused by the leak of aqueous fluid into the stroma and the pump that moves fluid out of the stroma. The corneal stroma has a high concentration of dissolved solutes, in the form of hydrophilic glycosaminoglycans, which present osmotic driving force for water accumulation in the cornea through ionic permeability of the endothelium. To counter-balance this continuous leak, the endothelium is also active in ion transport, which pumps fluid reabsorbed from the stroma into the aqueous humour, using numerous membrane transporters and channels. (Bonanno JA *et. al.*, 2003) Hence there is no net fluid transport under normal in vivo physiological conditions and the corneal thickness is maintained. (Fischbarg J *et. al*., 2003)

### 1.1.3 Bicarbonate and corneal endothelial pump

The bicarbonate ion has been implicated as playing a central role in the transport of corneal endothelial ion pump when it was discovered that the endothelial cell fluid reabsorption required the bicarbonate and this process was inhibited by carbonic anhydrase inhibitors. Studies confirmed that the electrogenic sodium-bicarbonate cotransporter NBC1 (*SLC4A4*) is located at the basolateral membrane and is responsible for $HCO_3^-$ uptake into the endothelial cells. (Bok D *et. al.*, 2004, Jentsch TJ *et. al.*, 1984)

### 1.2 Overview of bicarbonate transporters

The Human Genome Organization has applied a systematic nomenclature to human genes, where membrane proteins facilitating movement of soluble substrates are classed as solute carriers or 'SLC' (Wain HM *et. al.,* 2004), According to this nomenclature, there are two gene superfamilies which encode the bicarbonate transporters: *SLC4* and *SLC26*. The main difference is that while most *SLC4* transporters mediate the cotransport of $Na^+$, *SLC26* proteins predominantly carry out the $Na^+$-independent anion transport. The expressed proteins of these two gene families also have different tissue distribution, phylogenetic relationships, anion selectivity, and regulatory properties. Moreover, unlike *SLC26* anion transporters, *SLC4* homologues have not been detected in prokaryotic genomes. The characteristic phenotypes and various genetic diseases result from abnormalities in either membrane targeting and/or function of their genetic products. (Pushkin *et. al.,* 2006, Alper SL 2005)

All *SLC4* polypeptides have in common three structural domains: an N-terminal hydrophilic, cytoplasmic domain, a hydrophobic, polytopic transmembrane domain, and a C-

terminal cytoplasmic domain. (Romero MF *et. al.,* 2004, Cordat E, 2009) The similarities and differences among them are tabulated in the table 1.1.

| Similarities | Differences |
|---|---|
| (1) membrane topology: a dimer with 10–14 transmembrane (TM) segments separating the hydrophilic N and C termini <br> (2) inhibition by disulfonic stilbene derivatives such as DIDS <br> (3) glycosylation | (1) nature of transport activity <br> (2) cotransport of a cation or an anion <br> (3) electrogenicity causing a shift in membrane potential (Vm) <br> (4)  third cellular loop |

**Table 1.1. Similarities and differences among *SLC4* family members**

### 1.2.1   *SLC4* family and genetic diseases

The *SLC4* family members can be functionally divided into three  groups (Figure 1.3) namely:

1. Anion exchangers (AEs) which mediate sodium-independent exchange of chloride for base ($HCO_3^-$, $CO_3^{2-}$)

2. Sodium bicarbonate cotransporters (NBCs) which mediate cotransport of sodium and base ($HCO_3^-$, $CO_3^{2-}$)

3. Sodium dependent chloride-bicarbonate exchangers (NDCBEs) which mediate exchange of chloride for sodium and base ($HCO_3^-$, $CO_3^{2-}$)

The table 1.2 describes *SLC4* family with its gene locus, protein names, aliases, functions and electrogenicity while the table 1.3 summarizes its tissue distribution/subcelllar location, link to disease and mouse knockout phenotypes.
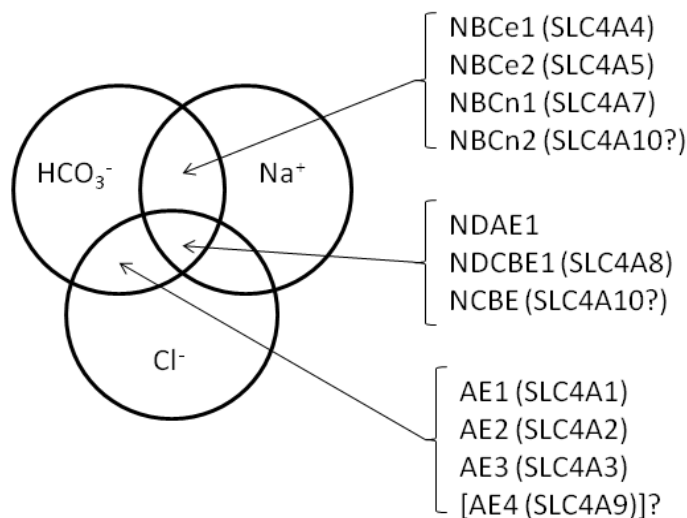
**Figure 1.3. Molecular entities subdivided by functional activity.** Sodium bicarbonate cotransporters (NBCs), sodium-dependent chloride-bicarbonate exchangers (NDCBE) and anion exchangers (AEs). (Modified from Romero MF, 2005)

| Human Gene | Protein Name | Aliases | Human gene locus | Electrogenicity | Splice variants |
|---|---|---|---|---|---|
| *SLC4A1* | AE1 | Band 3 | 17q21-q22 | electroneutral | 2 |
| *SLC4A2* | AE2 | | 7q35-36 | electroneutral | Many |
| *SLC4A3* | AE3 | | 2q36 | electroneutral | Many |
| *SLC4A4* | NBCe1 | NBC, NBC1 | 4q21 | electrogenic | 3 |
| *SLC4A5* | NBCe2 | NBC4 | 2p13 | electrogenic | 4-6 |
| *SLC4A7* | NBCn1 | NBC2, NBC3, | 3p22 | electroneutral | 4 |
| *SLC4A8* | NDCBE | NBC3 | 12q13.13 | electroneutral | 1 |
| *SLC4A9* | AE4 | | 5q31 | electroneutral | 2 |
| *SLC4A10* | NBCn2 | NCBE | 2q23-q24 | electroneutral | 2 |
| *SLC4A11* | NaBC1 | BTR1 | 20p12 | Electrogenic; ? electroneutral | 1 |

**Table 1.2. *SLC4* base transporters**: human gene name, protein name, gene locus, function, electrogenicity and splice variants. (Romero MF, 2006, Cordat E, 2009)

| Human Gene | Tissue distribution and cellular/subcellular expression | Link to disease | Phenotype of knockout mouse |
|---|---|---|---|
| *SLC4A1* | RBC, kidney, heart/kAE1 basolateral | Hemolytic anemia, hereditary spherocytosis, southeast asian ovalocytosis, distal renal tubular acidosis, nephrocalcinosis, nephrolithiasis | Haemolytic anaemia in two independent mouse Ae1−/− lines, also seen in spontaneous bovine mutant |
| *SLC4A2* | Widespread/basolateral | Achlorhydria, osteopetrosis | Achlorhydria (loss of stomach acid secretion), failed dentition; altered immune function |
| *SLC4A3* | Brain, heart, retina, pituitary, adrenal gland/non-epithelial | Idiopathic generalized epilepsy, **blindness** | Inner retinal defects, similar to human vitreoretinal degeneration syndromes; sensitivity to chemical-induced seizures |
| *SLC4A4* | Pancreas, kidney, heart, cornea, prostate, colon, stomach, thyroid, brain/basolateral | Proximal renal tubular acidosis, short stature, basal ganglia calcification, mental retardation, **cataracts, band keratopathy, Corneal opacities** (Dinour D *et. al.*, 2004) Mental retardation and **bilateral glaucoma** ( Igarashi T *et. al*, 1999 ) | Metabolic acidosis, runting, splenomegaly, altered dentition, intestinal obstruction; death before weaning |
| *SLC4A5* | Brain (highest in prefrontal cortex), epididymis, cardiac muscle, smooth muscle, kidney, choroid plexus/apical | Hypertension susceptibility | No mouse model |

| SLC4A7 | Heart, kidney, skeletal muscle, smooth muscle, submandibular gland, pancreas, stomach/basolateral | **blindness**, auditory impairment, (breast cancer) | Blindness and auditory defect (Bok D *et. al*, 2003) |
|---|---|---|---|
| SLC4A8 | Prefrontal cortex of brain, testis, cardiac myocytes, oocytes | | No mouse model |
| SLC4A9 | Kidney, testis, pancreas, widespread/apical | | No mouse model |
| SLC4A10 | Cardiac myocytes, neurons, kidney, uterus, adrenal cortex, choroid plexus/basolateral | Partial frontal lobe epilepsy | Epileptic seizures, reduced brain ventricle volume 2° to choroid plexus defect |
| SLC4A11 | Thyroid, trachea, cornea, kidney, salivary gland, testis/apical | **CHED2, FECD, Corneal dystrophy with perceptive deafness (Harboyan syndrome)** | severe morphological alterations in cornea (Gröger N *et. al.,* 2010) |

**Table 1.3. *SLC4* base transporters**: tissue distribution, link to disease, phenotype of knockout mouse. The diseases associated with ophthalmology are shown in bold letter. (Pushkin A et. al., 2006, Cordat E 2009)

Genetic analyses discovered that mutations in *SLC4A4* causes proximal renal tubular acidosis as well as ocular anomalies such as glaucoma, cataracts and band keratopathy. Specifically, nonsense mutation Q29X in the unique 5'-end of *SLC4A4* is related to permanent isolated proximal renal tubular acidosis with mental retardation and bilateral glaucoma. (Igarashi T *et. al.*, 1999) Another anion exchanger AE2 (*SLC4A2*) mRNA expression was also detected in fresh bovine corneal endothelial cells but since AE2 $^{-/-}$ mice did not develop any eye phenotype, the question of whether the function of AE2 is compensated by another gene was raised. (Dinour D *et. al.*, 2004, Salas JT *et. al.*, 2008, Demirci, FY *et. al.*, 2006, Gawenis, LR *et. al.*,

2004, Horita S *et. al*., 2005). Another study reported that mice lacking NBC3 (*SLC4A7*) develop blindness and auditory impairment as in Usher syndrome. (Bok D *et. al,* 2003)

More recently, as a major success to corneal endothelial research, a putative bicarbonate transporter gene (*SLC4A11*) was identified to be responsible for two endothelial dystrophies, recessive CHED (CHED2) (Vithana EN *et. al*., 2006) and late onset FECD (Vithana EN *et. al.,* 2006, 2007). Studies have shown that there is an abnormal localization demonstrated by missense proteins expressed by both CHED2 and FECD mutants. This makes *SLC4A11* gene to become a more clinically significant gene since the previous finding described that Harboyan syndrome (HS) (corneal and auditory defects) is also caused by recessive *SLC4A11* mutations. (Desir J *et. al.,* 2007)

.

**1.2.2 Corneal dystrophies**

Corneal dystrophies are a group of inherited clinical disorders manifested by noninflammatory, bilateral opacity of corneas which cause varying degree of reduction in visual acuity. Based on the anatomical layer predominantly affected, corneal dystrophies can be classified into three groups. They are (1) anterior corneal dystrophies which affect primarily the epithelium, the Bowman layer, (2) stromal corneal dystrophies which affect the stroma and (3) posterior or endothelial corneal dystrophies which involve the Descemet membrane and the endothelium. Most corneal dystrophies follow Mendelian inheritance with some phenotype diversity. The posterior or endothelial corneal dystrophies include Congenital Hereditary Endothelial Dystrophy (CHED [MIM #121700 and #217700]), Posterior Polymorphous Corneal Dystrophy (PPCD; MIM122000) and Fuchs Endothelial Corneal Dystrophy (FECD; MIM136800). This group of diseases, thought to represent defects of neural crest terminal

differentiation (Bahn CF *et. al.*, 1984), share common features of disease such as corneal decompensation, altered morphology of endothelial cells and the secretion of an abnormal Descemet's membrane (McCartney AC *et al.,* 1998, Levy SG *et. al.,* 1996). Several genes have been identified as causatives of posterior dystrophies (table 1.4) and a variety of mutations i.e. missense, deletion/insertion and null mutations were identified in *SLC4A11* gene in the homozygous state in CHED2 cases and in heterozygous state in FECD patients.

| POSTERIOR DYSTROPHIES | Mode of inheritance | Gene |
|---|---|---|
| Fuchs dystrophy (early onset) | AD | *COL8A2* |
| Fuchs dystrophy (late onset) | AD | Unknown |
| Fuchs dystrophy (late onset) | AD | TCF4 |
| Fuchs dystrophy (late onset) | AD | *SLC4A11* |
| Fuchs dystrophy (late onset) | AD | *TCF8* |
| Posterior polymorphous dystrophy type 1 | AD | Unknown |
| Posterior polymorphous dystrophy type 2 | AD | *COL8A2* |
| Posterior polymorphous dystrophy type 3 | AD | *TCF8* |
| Congenital endothelial dystrophy type 1 | AD | Unknown |
| Congenital endothelial dystrophy type 2 | AR | *SLC4A11* |
| X-linked endothelial corneal dystrophy | XR | Unknown |

**Table 1.4. Posterior corneal dystrophies** (Aldave AJ *et. al.*, 2007, Baratz KH *et.al.*, 2010)

FECD, commonest form of endothelial dystrophy in Asian eyes, is a progressive corneal disorder affecting the ageing population.  its prevalence is expected to rise sharply. The characteristic findings are outgrowths on a thickened Descemet membrane (cornea guttae), corneal edema and reduced visual acuity. The initial haziness and glare of vision are followed by painful  corneal erosions which can sometimes lead to  blindness in the elderly population (Klintworth GK, 2009) Since the corneal endothelial cells do not have the ability to proliferate, the only effective treatment for FECD is surgical intervention with corneal transplantation, which is associated with high risk of complications such as high astigmatism, graft rejection,

ocular surface defects, suture related problems and graft failure. In addition, the ever increasing shortage of donor material calls for viable treatment alternatives to allograft surgery, including genetic manipulation of host endothelial cells.

In contrast, recessive CHED (CHED2) is a bilateral corneal disorder affecting the newborns and infants. Its hallmark feature is a finding of markedly thickened corneas with diffuse ground-glass appearance. CHED2 is sometimes associated with progressive postlingual sensorineural hearing loss (Harboyan syndrome) (Desir J *et. al.,* 2008).  Homozygous mutations in the *SLC4A11* gene cause  the CHED2  (Vithana EN *et. al*., 2006, Shah SS *et. al*, 2008, Aldave AJ *et. al.*, 2007, Sultana A *et. al*., 2007, Jiao X *et. al*., 2007) and corneal transplantation (penetrating keratoplasty) is the only definitive treatment for this condition to date.

### 1.2.3. Corneal endothelial cells culture

As corneal transplantation is treatment of choice for many corneal dystrophies and keratopathies that primarily affect the corneal endothelial cell monolayer and due to the fact that specific corneal endothelial cell replacement is a feasible alternative to whole-cornea transplantation, isolation and growing of these cells have been an immense area of interest for researchers. Since several decades ago, primary CECs have been successfully cultured from eyes of many species including human, monkey, bovine, rabbit, rat, and mouse (Gospodarowicz D *et. al.,* 1977, MacCallum DK *et. al.,* 1982, Joo CK *et. al.,* 1994, Engelmann K *et. al.,* 1998, Pistsov MY *et. al.,* 1988, Nayak SK *et. al.,* 1986) but the majority of these cells exhibited limited capacity to proliferate in culture and inability for long term cultures. There was also a question raised on the extent to which these cultivated cells can function as those in uncultured state.

## 1.3 What is bicarbonate?

Bicarbonate is a simple carbon molecule, with alkaline and anionic properties, (Figure 1.4) that serves crucial biochemical roles in many physiological processes. Some examples include the photosynthesis, the energy-producing tricarboxylic acid cycle, the acid-base balance and the volume regulation. (Casey JR, 2006)
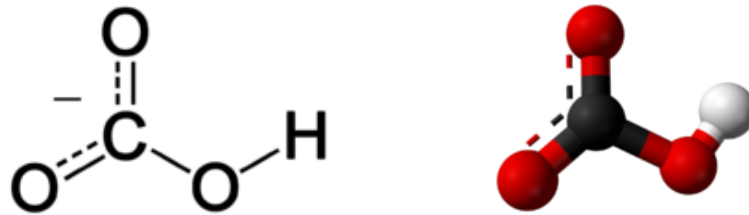


**Figure. 1.4 Structure of bicarbonate and ball and stick model**
<Bicarbonate. Retrieved from Wikipedia: http://en.wikipedia.org/wiki/Bicarbonate>

## 1.3.1 How bicarbonate is produced

The living cells excrete $CO_2$ as a primary waste product. The consumed carbohydrates, proteins and fats are digested into monosacharrides, amino acids and free fatty acids respectively, which undergo different catabolic processes to form the common intermediate product acetyl-CoA. This acetyl CoA subsequently enters the tricarboxylic acid cycle to produce the required energy ATP, with $CO_2$ as a final byproduct (Lehninger AL, 1982).

Most (70-75%) of the $CO_2$ reacts spontaneously with water to form carbonic acid $H_2CO_3$, which is in equilibrium with the bicarbonate ion ($HCO_3^-$) by the acid–base conversion properties of bicarbonate: $H_2CO_3 \Leftrightarrow HCO_3^- + H^+ \Leftrightarrow CO_3^{2-} + H^+$. Unlike $CO_2$, the negatively charged $HCO_3^-$ is not readily permeable to biological membranes by diffusion. Therefore its transport is facilitated by integral membrane proteins.

### 1.3.2 How bicarbonate is excreted

In order to maintain the body's function, the metabolic waste product $CO_2$ must be excreted. However, it has not to be in the form of bicarbonate because the major loss of this base would result in metabolic acidosis which is serious and could be life-threatening. This is the reason why nearly all of the bicarbonate is reabsorbed by various bicarbonate transporters in the kidneys. Instead of secreting the bicarbonate, our bodies exhale the $CO_2$ through the lungs. (Casey JR, 2006)

### 1.3.3 Some physiological roles of bicarbonate

Because of its chemistry and its ability to undergo pH-dependent conversions, the bicarbonate has various physiological roles: regulation of cellular and whole-body pH, disposal of waste $CO_2/HCO_3^-$, acid/base secretion and fluid secretion.

### 1.3.3.1 Bicarbonate and whole-body pH regulation

There are three main buffers in blood which control the shifts of acid and base: (1) proteins, (2) hemoglobin, and (3) the carbonic acid–bicarbonate system.

The third and major buffer system in blood is the **carbonic acid–bicarbonate system:**

$$H^+ + HCO_3^- \Leftrightarrow H_2CO_3$$
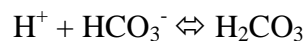
It is one of the most efficient buffer systems in the body since the amount of dissolved $CO_2$ is controlled by respiration. When additional $H^+$ enters the blood, $HCO_3^-$ declines as more $H_2CO_3$ is formed. Unless the extra $H_2CO_3$ were converted to $CO_2$ and $H_2O$ and the $CO_2$ excreted in the lungs, the $H_2CO_3$ concentration would rise. However, not only is all the extra $H_2CO_3$

removed, but also the rise in $H^+$ level stimulates the respiratory center in the brain followed by more $CO_2$ washout with a drop in $pCO_2$, so that some additional $H_2CO_3$ is removed. The pH thus changes very little.

**1.3.3.2 Bicarbonate and the RBC**

The metabolism of our cells continuously produces $CO_2$, which enters the RBC via the plasma. Inside the RBC, the carbonic anhydrase II converts the $CO_2$ and water into the bicarbonate and the $H^+$. The bicarbonate transporter (AE1 or Band 3), a major membrane protein in RBC, exchanges $HCO_3^-$ with $Cl^-$ (the so-called chloride shift) while the deoxygenated haemoglobin buffers the $H^+$, enabling the RBC to take up more $CO_2$. When the RBC reaches the lungs, the reverse process takes place and the $CO_2$ diffuses into the alveoli for excretion.

**1.3.3.3 Bicarbonate and the kidney**

The systemic acid–base balance of the body is chiefly controlled and maintained in the kidneys by three interconnected mechanisms: the reabsorption of bicarbonate, the excretion of acids and the de novo generation of ammonium and bicarbonate. The reabsorption of filtered bicarbonate occurs in the proximal convoluted tubule (approximately 80%), the thick ascending limb of loop of Henle and the distal convoluted tubule (16%) and the collecting duct (4%), using various isoforms of bicarbonate transporters. In the proximal tubule, exit of $HCO_3^-$ from the cell across the basolateral membrane  primarily takes place via the electrogenic sodium-bicarbonate cotransporter (NBCe1) (Aalkjær C *et. al.*, 2004) while in the thick ascending limb, the transport is mediated by the electroneutral another sodium-bicarbonate symporter (NBCn1) and anion

exchanger 2 (AE-2). The intercalated cells of the collecting duct contain Band 3 or anion exchanger proteins AE1 in their basolateral cell membranes, by which $HCO_3^-$ exits the cells in exchange for $Cl^-$. (Koeppen BM, 2009)

## 1.4 Gene characterization study using Real Time qPCR SYBR® Green Technology

### 1.4.1 Quantification of gene expression at transcription level

There are four widely used methods for the quantification of gene transcripts. They are Northern blotting, RNA *in situ* hybridization (Parker, RM *et. al*., 1999), RNAse protection assays (Hod, Y, 1992) and reverse transcription polymerase chain reaction (RT-PCR) (Weis JH, 1992), with each of them having its own advantages and disadvantages. Northern blotting is the only method that provides information about the mRNA size, alternative spliced transcripts and the integrity of the sample but is time-consuming and requires relatively large amounts of RNA. The RNase protection method is most useful for mapping the initiation and termination sites and intron/exon boundaries of transcripts but is not sensitive enough to detect low abundance transcripts. RNA *In situ* hybridization allows the localization of transcripts to specific cellular location within a tissue (Melton, DA *et. al.*, 1984) but its sensitivity is also insufficient. The RT-PCR, an *in vitro* method that involves enzymatic amplification of target mRNA sequence, poses superior sensitivity over these three methods and is now the most commonly used technique for quantification of gene expression.

Quantitative real-time Polymerase Chain Reaction (qRT-PCR) has opened up a new era for researchers to quantify the genetic products (DNA and RNA).  In the past, the conventional PCR measured the final amount of amplified PCR product and its quantification therefore was

only partial and limited (semi-quantitative) In contrast, the qRT-PCR allows researchers to collect the data throughout the amplification process as it occurs (i.e., in real time). The reaction is then characterized in the exponential phase of PCR amplification by the threshold cycle number (Ct) (Gibson *et. al,.* 1996). Thus, the initial copy number of the target determines the time point at which a significant increase in fluorescence is observed.
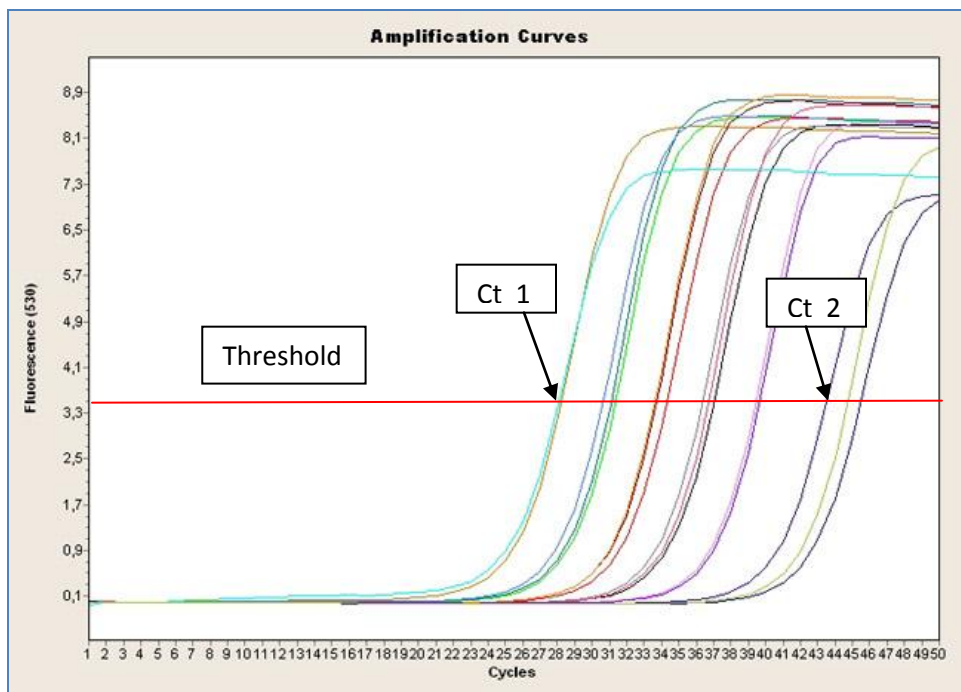


**Figure 1.5. Amplication curve.** Threshold is the point of detection. Cycle threshold (Ct) is the cycle at which sample crosses threshold. For example, the sample with Ct1 requires fewer cycles for fluorescence detection than the sample with Ct2. (Applied Biosystems)

There are two types of chemistry used to detect qPCR products: TaqMan® chemistry and SYBR® Green I dye chemistry. The fluorescence-monitoring system used in our study is the SYBR® Green I dye chemistry. It is a highly specific DNA binding dye which binds to detected minor groove of double stranded DNA and emits the fluorescence. During the PCR, the higher the number of amplified products or 'amplicons' generated by DNA polymerase, the more

amount of fluorescence proportionate to the amount of PCR products is thus produced. Due to its high sensitivity, reproducibility, speed, throughput and accurate quantification of mRNA levels from various samples, qRT-PCR becomes an indispensable tool for researchers in gene expression studies.

### 1.4.2 Relative quantification in real time qPCR

Real-time qPCR data are quantified absolutely or relatively using the Ct number, which therefore is the primary statistical metric of interest. Absolute quantification allows researchers to determine the exact number of transcript copies made. In contrast, relative quantification, which is a comparison between the expression of a gene of interest and that of reference gene or the expression of same gene in two different experimental conditions, is applied in most biological studies. (Pfaffl MW, 2001, Nolan T *et. al.*, 2006, Gutierrez L *et. al.*, 2008, Andersen CL *et. al.*, 2004)

Relative quantification is a method of quantification where the expression of a target gene in a sample is compared with that of another sample. The latter, called a calibrator, can either be an external standard (serial dilution of a positive sample) or a reference sample (a negative or untreated sample) and the results obtained are expressed in target to reference ratios. An internal control gene, often referred to as housekeeping gene (e.g. β-*actin, ribosomal RNA, GADPH*) is co-amplified in order to normalize the input mRNA fraction.

Two similar mathematical models are widely applied for relative quantification of qPCR data: the efficiency calibrated model (Pfaffl MW, 2001) and the ΔΔCt model (Livak KJ *et. al.*, 2001). The comparative Ct (cycle threshold) method is used to calculate changes in gene expression as relative fold difference between an experimental sample and a calibrator sample

using the formula $2^{-\Delta\Delta Ct}$ where 2 is the 'efficiency' of the amplification. $\Delta Ct$ is obtained by subtracting the Ct value of the housekeeping gene from that of the target gene. Then the $\Delta\Delta Ct$ is obtained by subtracting $\Delta Ct$ of treated sample from that of calibrator. The relative fold change between the two samples is then calculated using the formula of $2^{-\Delta\Delta Ct}$.

For the $\Delta\Delta Ct$ calculation to be valid, the efficiencies of both the target amplification and the reference amplification must be approximately equal. A sensitive method for assessing if two amplicons have the same efficiency is to evaluate the variations of $\Delta Ct$ values in calibrated diluted templates. If primer dimers were present, Ct values of all dilutions would fall around the same point. Initially the Ct number is plotted against cDNA input and then the slope of the plot is drawn to calculate the amplification efficiency (E), which can be either expressed as percentage (from 0 to 1) or as time of PCR product increase per cycle (from 1 to 2) by the formula $E = 10^{-1/\text{slope}}$.

### 1.4.3 Accurate normalization of expression level of a target gene using multiple stable reference genes

As mentioned above, housekeeping genes are frequently used for normalization in analysis of qPCR data and therefore they should be expressed uniformly regardless of experimental conditions, sample treatment, origin of tissue/cell types, and developmental staging. However, studies have shown that housekeeping gene expression can vary considerably and there is probably no universal reference gene with a constant expression in all tissues. (Warrington JA *et. al*., 2000, Thellin O *et. al.*, 1999, Suzuki T *et. al*., 2000, Bustin SA, 2000) Hence, using the multiple best reference genes (three in most cases) instead of conventional use of a single one, results in much more accurate and robust normalization and is proved to be a

more valid normalization method.The candidate reference gene stability can be evaluated by many algorithms. One of them is the geNorm$^{TM}$ program, which determines the most stable reference genes from a set of tested genes in a given cDNA sample panel.A gene expression normalization factor for each tissue sample is calculated based on the geometric mean method(Vandesompele J *et. al.*, 2002) Stepwise exclusion of the gene allows ranking of the tested genes according to their expression stability.One major challenge for using multiple housekeeping genes for relative quantification is the requirement for high amplification efficiencies (95 - 105%) across all genes, regardless of amplicon length, complexity or GC content. (Yuan AS *et. al*., 2006)

## 1.5 Aims of study

SLC4A11 and SLC4A4 are important proteins in the cornea as indicated by their involvement in several corneal dystrophies. We hypothesized that this family of proteins are important to the normal function of the corneal endothelium, and that there could be other members of this SLC4 family equally important but as yet unrecognized to be so in the cornea. Furthermore, as important proteins in the cornea, SLC4A11 and SLC4A4 will be subject to study in *in vitro* systems (i.e. corneal endothelial cell culture system), we therefore wanted to explore what gene expression changes take place during cell culturing procedure and the extent to which the normal expression levels remain within the cultured cells. This information will be valuable when interpreting data generated from cultured cells.

Therefore, in this study, the following objectives were undertaken:

- To characterize the expression levels of the entire *SLC4* family of genes relative to those of *SLC4A4* and *SLC4A11* in both human and mouse corneal endothelium, so that we may identify further members from this family of genes that can serve as candidate genes for analysis in corneal dystrophies.

- To characterize/quantify the expressional alterations that occur for *SLC4* genes due to cell culturing procedure involving both early and late subcultures

# II. MATERIALS AND METHODS

## 2.1 Animal experimentation

C57BL6 WT mice were ordered from animal holding unit of National University of Singapore, housed and bred in Singhealth Experimental Medicine Center until the sufficient number for the study was attained. Approval was obtained from the SingHealth International Animal Care and Use Committee (IACUC No. #2008/SHS/372), and all procedures performed in this study were in accordance with the Association for Research in Vision and Ophthalmology (ARVO) resolution for the use of animals in research. The number of animals used in this study as well as any potential distress or discomfort to the animals was kept at minimum in accordance with the above mentioned resolution.

## 2.2 Primer design

PCR primers were designed for all *SLC4* gene family members (*SLC4A1* to *SLC4A11*). The pairs of primers for the target mRNAs were designed based on the mouse and human mRNA sequence using Primer 3 software (Rozen S and Skaletsky H, 2000). The forward and reverse primers were designed in that they were located on separate exons (with a large intron in between) to ensure that the template utilized would be cDNA rather than genomic DNA. Each primer sequence was queried against the human and mouse DNA databases in the National Center for Biotechnology Information (NCBI) website using the Basic Local Alignment Search Tool (BLAST) to ensure that primer sequences were specific for the target mRNA transcript. The primers were synthesized by AIT Biotech (Singapore). The primers were also designed such that they were in a region common to **all known splice variants** of the corresponding transcript

and if they performed poorly in empirical tests then they were redesigned until the ideal primers were obtained. The optimized primer sequences used in the study are shown in the Table 2.1 and 2.2.

| Gene Name | Orientation | Sequence | Amplicon size |
|---|---|---|---|
| *Slc4a1* | Forward<br>Reverse | CTCCTTCCTCATCTCCCTCA<br>TCATCACAACAGGGGCATAA | 104 |
| *Slc4a2* | Forward<br>Reverse | ATGTGGCCTCACTGTCCTTC<br>ATCTGCTCGACCACCTGATG | 124 |
| *Slc4a3* | Forward<br>Reverse | ATTCCCATCTCCATCCTGGT<br>CGCTTATGAGGGGAAGTCAC | 110 |
| *Slc4a4* | Forward<br>Reverse | TCCCTTCATTGCCTTTGTTC<br>CAAGGTGGCGATAGCTCTTC | 151 |
| *Slc4a5* | Forward<br>Reverse | TGAACACAACCACGGTCAAT<br>CGTAGCTCAGGCACTCCTTC | 126 |
| *Slc4a7* | Forward<br>Reverse | CGCATAGAGCCTCCAAAAAG<br>GCATGGTGATCATCCTCCTT | 113 |
| *Slc4a8* | Forward<br>Reverse | GGGCAGCAGTACCATGAGAT<br>GTCCAGGAACTCGTCAATCC | 126 |
| *Slc4a9* | Forward<br>Reverse | CCTTGGCCCACATAGACAGT<br>TGTAAGGACGAACACCACCA | 119 |
| *Slc4a10* | Forward<br>Reverse | TTCAAGACCAGCCGCTATTT<br>GGATCCCAATGGCATAGTCA | 109 |
| *Slc4a11* | Forward<br>Reverse | CTGTGAGGTTCGCTTTGTCA<br>GTGCGAGTCTTCAGGAGCTT | 138 |
| *Gapdh* | Forward<br>Reverse | GCTACACTGAGGACCAGGTTG<br>TGCTCTTAAAAGTCAGGTTTCC | 150 |
| *18S rRNA* | Forward<br>Reverse | AAACGGCTACCACATCCAAG<br>CAATTACAGGGCCTCGAAAG | 112 |
| *βactin* | Forward<br>Reverse | CTAAGGCCAACCGTGAAAAG<br>ACCAGAGGCATACAGGGACA | 104 |
| *Hprt1* | Forward<br>Reverse | CAAACTTTGCTTTCCCTGGT<br>CTGGCCTGTATCCAACACTTC | 100 |
| *AQP1* | Forward<br>Reverse | CTACACTGGCTGCGGTATCA<br>GGGCCAGGATGAAGTCATAG | 143 |
| *Zo1* | Forward<br>Reverse | GGCTTAGAGGAAGGTGATCAAA<br>CTTTAGGGAGGTCAAGGAGGA | 100 |
| *Col8a2* | Forward<br>Reverse | AGGGTCCAGTAGGGGCTAAA<br>CCCTTAGGTCCTGGTTTTCC | 100 |
| *Col1a1* | Forward<br>Reverse | CTTCACCTACAGCACCCTTGTG<br>CTTGGTGGTTTTGTATTCGATGAC | 85 |

**Table 2.1 Sequences of the mouse primers used in the study.**

| Gene Name | Orientation | Sequence | Amplicon size |
|---|---|---|---|
| SLC4A1 | Forward | GTCCCCATCTCCATCCTGA | 273 |
| | Reverse | GGAGCCCTTGACCATCTTG | |
| SLC4A2 | Forward | GAAGAATGCCAAAGGTTCCA | 122 |
| | Reverse | GCAACTCATTCAGCTCCACA | |
| SLC4A3 | Forward | ACTGCTCTGGGTGGTCAAGT | 143 |
| | Reverse | GTTCAGCATCTTCCGAGTCC | |
| SLC4A4 | Forward | TTGGGGAGGTTGACTTTTTG | 143 |
| | Reverse | GGACTTGGCTTTCCCCTTAG | |
| SLC4A5 | Forward | GCTGGTGACCATCCTGATCT | 144 |
| | Reverse | CCCATAAAGGAGCACAAAGC | |
| SLC4A7 | Forward | TCTTCACGGAAATGGATGAA | 102 |
| | Reverse | CGCCATCTTCAACATCCTCT | |
| SLC4A8 | Forward | CATTGCACAGCCTGTTTGAG | 137 |
| | Reverse | GCTGTCATTCAGGTCACTGG | |
| SLC4A9 | Forward | CAGCGACTTCTCCTCAGTCC | 144 |
| | Reverse | GCTCCAAAAGGTGACACCAG | |
| SLC4A10 | Forward | TGCGTTTGTCAGGTTGTCTC | 131 |
| | Reverse | TTGATCTGCCAATCTCATGG | |
| SLC4A11 | Forward | CTGCTTCCCTTGCAGAAAAC | 169 |
| | Reverse | TACTCTCGCCAGACACGATG | |
| GAPDH | Forward | GAAGGTGAAGGTCGGAGTCA | 109 |
| | Reverse | AATGAAGGGGTCATTGATGG | |
| 18S rRNA | Forward | CTTAGAGGGACAAGTGGCG | 71 |
| | Reverse | GGACATCTAAGGGCATCACA | |
| βACTIN | Forward | CCAACCGCGAGAAGATGA | 97 |
| | Reverse | CCAGAGGCGTACAGGGATAG | |
| B2M | Forward | GTGCTCGCGCTACTCTCTCT | 132 |
| | Reverse | TGGATGAAACCCAGACACAT | |

**Table 2.2 Sequences of the human primers used in the study.**

## 2.3 Sample collection

For mouse samples, adult 4-6 week old C57BL6 WT mice (n=5 for primary corneal endothelial cell culture and n=10 for direct corneal endothelial RNA extraction) were sacrificed with an overdose of sodium pentobarbital. Eyes were enucleated and the globes were rinsed with sterile PBS.. The corneas were then dissected from the globe and laid endothelial side uppermost in a sterile Petri dish containing PBS.

For human samples, a total of seven research-grade corneoscleral tissues (five used for direct RNA isolation and two used for cell culture) from cadaver human donors considered unsuitable for transplantation were obtained from Lions Eye Institute for Transplant & Research, Inc. (Tampa, FL, USA) and Sri Lanka Eye Donation Society (Colombo, Sri Lanka). The donors' information are described in the Table 2.3.

| No. | Age | Sex | Race | Cause of death | Elapsed time from death to corneal preservation | Elapsed time from preservation to RNA extraction |
|---|---|---|---|---|---|---|
| **Primary endothelium Sample 1** | 51 | Male | Caucasian | Acute cardiac crisis | 9hr 35mins | 5 days |
| **Primary endothelium Sample 2** | 48 | Male | Asian | Cerebrovascular accident | 13hr 10mins | 2 days |
| **Primary endothelium Sample 3** | 59 | Female | Asian | Hypertension | 11hr 45mins | 2 days |
| **Primary endothelium Sample 4** | 59 | Female | Asian | Hypertension | 21hr 45mins | 2 days |
| **Primary endothelium Sample 5** | 54 | Male | Asian | Myocardial infarction | 18hr 50mins | 2 days |
| **Cultured Cells Sample 1** | 49 | Male | Caucasian | Cerebrovascular accident | 10hr 32mins | 5 days |
| **Cultured Cells Sample 2** | 34 | Female | Caucasian | Metastatic cancer | 8hr 31mins | 5 days |

**Table 2.3. Donors' information of corneas.**

### 2.4 Mouse corneal endothelial cells culture

Several culture media were tested to identify the optimal culture conditions for primary culture of mouse corneal endothelial cells (MCECs). The culture media used by Kaji *et. al.* for the primary culture of bovine corneal endothelial cells was found to be optimal for growth of MCECs. Therefore, primary culture of MCECs was carried out using conditions reported by Kaji

*et. al*. and cells were cultured in minimum essential media (MEM, Invitrogen, CA, USA) with 15% fetal bovine serum (FBS, Invitrogen, CA, USA) and 20 mg/L gentamicin.

Specifically, upon detachment, the mouse eyes were placed in Dulbecco's Modified Eagle's Medium (DMEM, Invitrogen, CA, USA) supplemented with 0.1mg/ml gentamicin and 1.25µg/ml amphotericin B. The Descemet's membranes were then stripped under a dissecting microscope and incubated overnight to stabilize the cells in Opti-MEM I® medium supplemented with 8% FBS, Penicillin/Streptomycin, 0.5mg/ml gentamicin and 1.25µg/ml amphotericin B. After removing the incubating medium, cells were digested away from the Descemet's membranes by a collagenase A treatment (Sigma, MO, USA) carried out at 37°C for 2-3 hours in MEM medium supplemented with 15% FBS, 20µg/ml gentamicin and 2mg/ml collagenase A. Cells were then washed with DMEM medium supplemented with antibiotics before culturing in MEM medium supplemented with 15% FBS and 20µg/ml gentamicin. Cells were grown in a humidified atmosphere of 5% $CO_2$ at 37 °C.

The cultures were passaged on reaching 80% confluence. The MCECs in passage 2 and passage 7 were used for subsequent RNA extraction. The entire experiment was repeated once again independently, to obtain another batch of cells at passage 2 and 7.

## 2.5 Human corneal endothelial cells culture

The HCECs were kindly provided by Dr. Gary Peh Swee Lim of Ocular Tissue Engineering and Stem Cell group from Singapore Eye Research Institute and they were cultured according to the protocol, developed by the group. Briefly, the donor cornea underwent a series of antibiotic washes (3x 15 minutes each). The isolation of HCECs involved a two-step peel-and-digest method. Fristly, the Descement's membrane, together with the corneal endothelium was

carefully peeled and stripped off from the corneal stroma under a dissecting stereomicroscope. The freshly peeled DM-endothelial layers were subjected to an enzymatic digestion using collagenase (2mg/mL) for at least 2 hours, and further dissociated using TrypLE™ Express (Invitrogen, CA, USA) for approximately 5 minutes. Isolated HCECs were plated onto culture dishes coated with FNC coating mix® (Athena Environmental Sciences, MD, USA). The media used were Opti-MEM-I supplemented with 8% FCS, 20ng/ml NGF, 5ng/ml EGF, 20µg/ml ascorbic acid, 200mg/L calcium chloride, 100µg/ml pituitary extract, 50µg/ml gentamicin, 1x antibiotic/antimycotic, 0.08% chondroitin sulphate. The HCECs in passage 2 and passage 5 were used for subsequent RNA isolation..

**2.6 RNA isolation (from corneal endothelium and cultured cells of MCECs and HCECs)**

The Descemet's membranes with corneal endothelial cells were stripped from the periphery of the cornea towards the central region under a dissecting microscope. Total RNA was extracted by TRIZOL™ (Invitrogen, CA, USA) method following manufacturer's protocol with a few modifications. The stripped Descemet's membranes were homogenized in TRIZOL™ reagent using sonicator. In the case of cultured cells, the cells were directly lysed in a culture dish by adding TRIZOL™ reagent and the cell lysate was homogenized several times through a 20-gauge needle. To each 1 ml of TRIZOL™ reagent, 1µl of glycogen (5µg/µl) and 0.2ml chloroform were added, kept at room temperature for 10 minutes and centrifuged at 10,000g for 20 minutes at 4˚C. The aqueous layer (top, clear layer) was transferred to a fresh RNase free tube and mixed with 0.5ml isopropanol and incubated overnight at -20˚C. The reaction was centrifuged at 10,000g for 20 minutes at 4˚C, isopropanol was removed and mixed with 1ml of cold 75% ethanol. Ethanol was removed after centrifugation at 7500g for 4 minutes at 4˚C. The

RNA wash with ethanol was done twice and the resulting pellet dissolved in RNase free water. Genomic DNA was removed by digestion with DNase I (AmpGrade; Invitrogen-Gibco, CA, USA) according to manufacturer's protocol. RNA samples were transferred to RNase-free eppendorf tubes and stored at -70˚C.

## 2.7 Determination of quantity and quality of total RNA

The concentration of RNA was determined by measuring the absorbance at 260 nm ($A_{260}$) in a spectrophotometer (Nanodrop 2000, ThermoFischer Scientific, USA). The quality of extracted RNA was estimated by the $A_{260}/A_{280}$ ratios of the samples.

## 2.8 Reverse transcription

RNA was reverse transcribed using SuperScript™ III First-Strand Synthesis System for RT-PCR (Invitrogen, Carlsbad, CA, USA), according to the manufacturer's protocol. Briefly, one microgram of total RNA with random hexamers and dNTP mix was heat denatured at 65˚C for 5 min and chilled on ice for 1 min. Reverse transcription was carried out in RT buffer, 25mM $MgCl_2$, 0.1M DTT, 40 units of RNaseOUT and 200 units of Superscript™ III reverse transcriptase in a final volume of 20 µl. The reaction was incubated for 10 min at 25˚C, 50 min at 50˚C, 5 min at 85˚C and then chilled on ice. After the reaction was collected by brief centrifugation, any remaining RNA was digested by incubation for 20 min at 37˚C with 1 µl of RNaseH. The resulting cDNA was subsequently used in downstream applications.

**2.9 Polymerase chain reaction (PCR) amplification**

A conventional PCR amplification was performed in a 50 μl reaction volume containing 50-100 ng of cDNA template, 0.1-0.5 μM of each primer, 2mM $MgCl_2$, 0.2 mM dNTP, 1x Green GoTaq® Flexi Buffer (Promega, WI, USA) and 1.25 units of GoTaq® DNA Polymerase (Promega, WI, USA). PCR reaction was carried out after an initial denaturation for 3 min at 95°C followed by 40 cycles of 30sec denaturation at 95°C, 30 sec at 58°C, and 1 min 30 sec extension at 73°C. This was followed by a final cycle for 7 min at 72°C in a thermal cycler (GeneAmp® PCR System 9700, Applied Biosystems USA). The amplified product was analyzed by agarose gel electrophoresis.

**2.10 Agarose gel electrophoresis**

This technique was used to determine/visualize the size of the cDNA fragments generated by PCR. A  2 % (w/v) agarose gel was prepared by melting 2g of powdered agarose (Promega, WI, USA) in 100 ml of 1 x TAE buffer  (0.04 M Tris base, 0.02 M glacial acetic acid and 0.001 M EDTA). The agarose was melted in a microwave oven and then cooled to about 60°C before addition of 10μl of 10mg/ml ethidium bromide (Sigma-Aldrich, MO, USA). The cDNA samples, together with size standard DNA Hyperladder IV (Bioline, UK) were loaded into the wells of the gel and subjected to electrophoresis in 1x TAE buffer. The gel was then viewed under UV illumination and the images were taken by Hamamatsu image detection system. (Japan)

**2.11 Immunocytochemistry**

Immunocytochemistry for HCECs was done according to the protocol provided by the Ocular Tissue Engineering and Stem Cell group from Singapore Eye Research Institute.

Specifically, cover slips were sterilized and placed into organ-culture culture dishes (BD). The cover slips were coated with a FnC Coating Mixture for at least 30 minutes at 37° C. HCEC cells were subcultured and grown in 5 % FBS supplemented medium overnight. The next day, the medium was discarded and the cells were washed with PBS twice. The cells were treated as per experimental requirements, then washed and fixed in 4 % paraformaldehyde for 30 min at 4° C. The cells were washed and permeabilized in a blocking solution made up of 10% normal goat serum containing 0.1% Triton X-100 for 30 minutes at room temperature. The cells were then incubated with primary antibodies diluted in 5 % serum at recommended dilutions (1:40 for Na+K+ ATPase (5µg/mL; Santa Cruz Biotechnology, CA, USA); 1:50 for Zonular Occludens-1 (ZO-1 5µg/mL; BD Biosciences, NJ, USA) overnight at 4° C. The next day, the cells were washed twice for 10min each and incubated with a goat–anti-mouse secondary antibody (1:750, diluted in 5% serum), together with a rhodamine conjugated anti-phalloidin (1:500 (0.5µM); Invitrogen, CA, USA) at room temperature for 1h in the dark. All steps from here on were carried out in the dark. Subsequently, the cells were incubated with DAPI (1:50,000) a nuclear marker, for 5 min at room temperature, washed, and mounted onto slides using anti-fade mounting medium. The slides were examined using a Zeiss Axioplan 2 fluorescence microscope (Zeiss, Germany).

Immunostaining of MCECs was done using the same method as described above except for a few modifications. Briefly, the cells were incubated with primary anti-$Na^+K^+$ ATPase (200µg/mL; Santa Cruz Biotechnology, CA, USA) and anti-ZO-1 antibodies (5µg/mL; Life tech, CA, USA) at recommended dilutions (1:100 for $Na^+K^+$ ATPase and 1:50 for ZO-1) and then incubated with anti-rabbit secondary antibody (1:500, diluted in 5% serum).

**2.12 Selection of most stable housekeeping gene using geNorm™ software**

The downloaded geNorm**™** VBA applet for Microsoft Excel version 3.5 (Biogazelle, Belgium) was installed and applied according to the manufacturer's protocol. Briefly, the expression data matrix with raw data of relative quantities of each housekeeping gene was entered into the geNorm™ software to calculate average expression level stability (M). The genes with the lower M values are considered to have more stable expression levels. The geometric mean of the most stable reference genes were calculated to obtain the normalization factor using the geNorm™ software. The details of the underlying principles and calculations are described in Vandesompele *et* al (2002)

**2.13 Real time qPCR with SYBR® Green I dye for detection**

Real time qPCR with SYBR® Green I dye for detection was performed using the LightCycler® 480 (Roche, Basel, Switzerland). The reaction was performed in a total volume of 10 μl containing 1 x Power SYBR® green PCR master mix (Applied Bisosystems, USA), 80nM-160nM of each primer and 15ng of cDNA template. The threshold cycles (Ct) were calculated using the LightCycler® software v1.5 (Roche, Basel, Switzerland). Real time qPCR was carried out after an initial denaturation for 10 min at 95˚C followed by 45 cycles of 30sec denaturation at 95˚C, 30sec annealing at 58˚C and 45sec extension at 72˚C. These cycling parameters were found to be optimal for amplifications of targets in our study.

Real time qPCR detections of *SLC4* genes and housekeeping genes in mouse primary corneal endothelium and cell culture samples were performed, in parallel with standard templates and negative controls (without the cDNA templates) as described below. In a given experiment, endothelia of 20 mouse corneas were pooled to obtain sufficient RNA quantities representative

of that from the primary endothelium. This RNA was used for two separate first strand synthesis reactions (reverse transcription (RT) reactions) and the resulting cDNA was used for two separate qRT-PCR reactions. In each qRT-PCR run the genes were analyzed in 4 replicates thus yielding 4 data points (i.e Ct values) for each gene. Therefore with the 2 separate qRT-PCR runs 8 data points were obtained for each gene. Similarly, for the cultured cells the experiment was initiated by pooling endothelia from 10 corneas and establishing a growing culture. RNA was then extracted from cells at passage 2 and from cells at passage 7. As described earlier for the primary endothelium, the RNA from passage 2 and passage 7 were also subjected to two separate first strand synthesis reactions and the resulting cDNA used for two separate qRT-PCR reactions. Therefore for each passage, the 2 separate qRT-PCR runs resulted in 8 data points for each gene. The qRT-PCR data from the primary endothelium and cultured cells were paired for analysis purposes when comparing gene expression alterations that take place due to the cell culturing procedure. This paired experiment was then repeated once more independently (for both cultured and primary endothelium) as described to confirm the validity of data. Figure 2.1 diagrammatically depicts the experimental procedure used for the *Slc4* gene expression (via qRT-PCR) analysis, in mice.
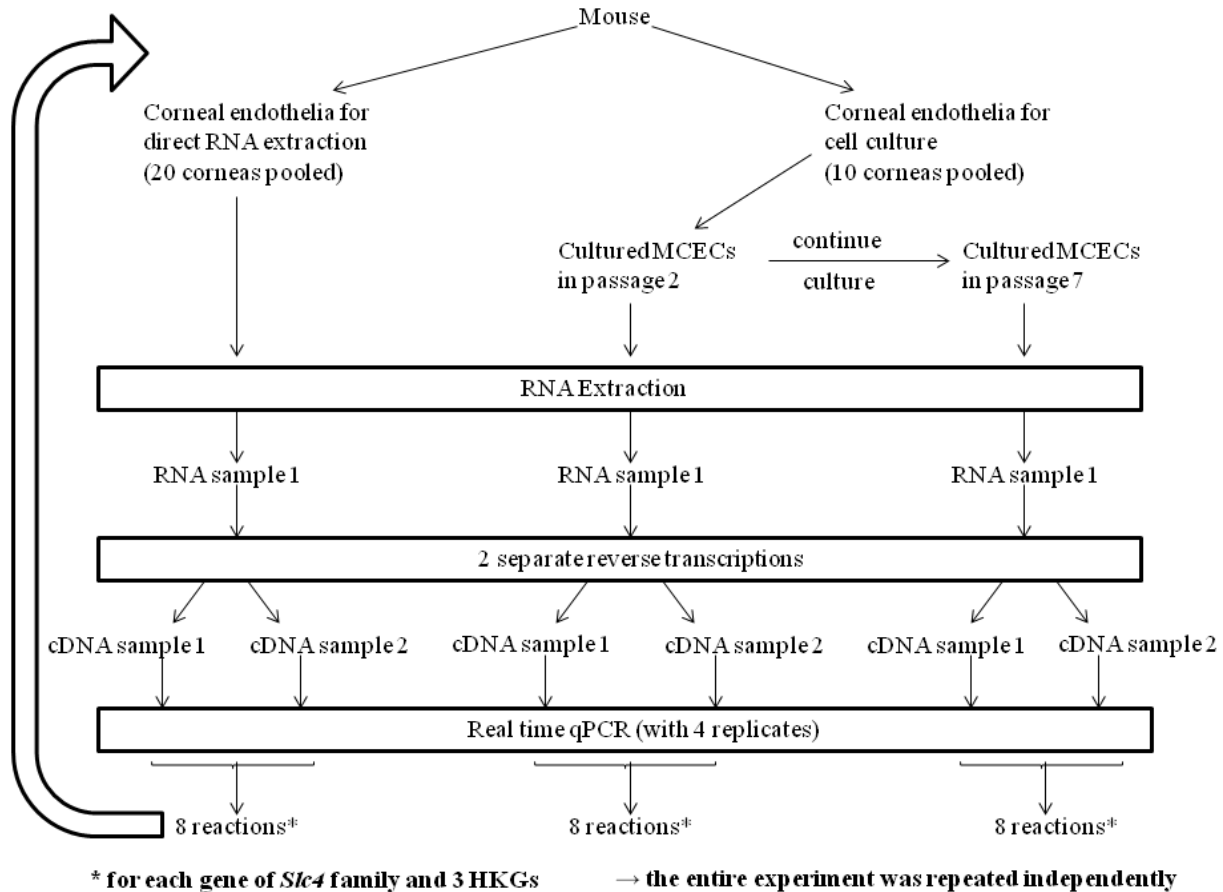
**Figure 2.1. Schematic diagram for experimental workflow used for *SLC4* family gene expression analysis in MCECs.**

For the analysis of *SLC4* gene expression in primary corneal endothelial cells in humans, five donor tissue samples were used. The RNA sample from each donor sample was subjected to two RT reactions and the resulting cDNA samples were used for qPCR with each gene analyzed in 4 replicates. This resulted in 8 qRT-reactions/data points for a given gene in a given donor sample. For human cultured cell samples, the same procedure was followed as described earlier with the cultured mouse samples. Here the cell culture was initiated by endothelia isolated from a single human donor cornea. As with the cultured MCECs, two separate cDNA samples were also prepared from a given RNA sample derived from cells of a given passage (see Figure 2.2 for

more details). Again this resulted in 8 qRT-reactions/data points per given gene for a given passage. The experimental procedure for the cultured cells was repeated once more to test the reproducibility of .data.
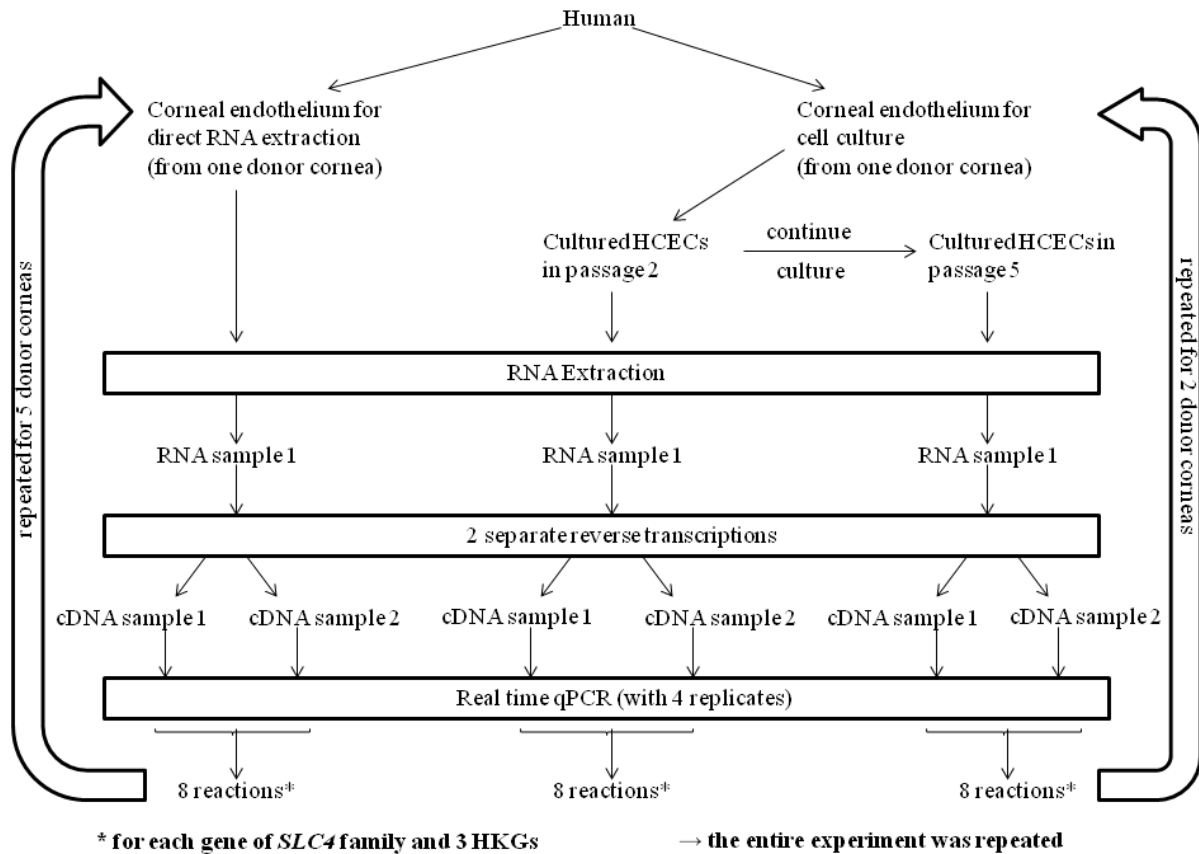


**Figure 2.2. Schematic diagram for experimental workflow used for *SLC4* gene expression analysis in HCECs.**

We carried out the following comparisons:

1. The expression of *SLC4* genes, in both murine and human primary corneal endothelium, was compared against the expression levels of *SLC4A11* and *SLC4A4* genes. Relative quantification of gene expression was carried out using the comparative $C_T$ method (i.e the $2^{-\Delta\Delta Ct}$ method (Livak and Schmittgen, 2001). The expression levels of *SLC4* bicarbonate transporters in each primary

uncultured sample were normalized against the expression levels of the most stable housekeeping gene, i.e., *Hprt1* for mice and *GAPDH* for the human samples. This was determined by using the geNorm™ software as explained in section 2.12. In this analysis, results were reported as a relative gene expression level of a given gene over a control gene, i.e, *SLC4A11* or *SLC4A4*.

   2. The expressional changes that occur in *SLC4* genes due to the culturing procedure were also analyzed by comparing against the gene expression in uncultured/primary cells. In this analysis the samples from the primary endothelium were treated as the control or the calibrator sample while samples from cultured cells served as the experimental samples. Results were reported as relative fold change of experimental sample over control sample. A fold change of >1 meant that experimental samples had increase in expression over the calibrator samples while a fold change of <1 meant a decrease in expression. Here we used a normalizing factor taking into account the expression of several housekeeping genes rather than a single normalizing gene.


## 2.14 Statistical analysis

   When performing expressional analysis of *Slc4* family genes in MCECs, all the data used for statistical analysis were obtained from two independent experiments. In the case of HCECs, when carrying out the analysis of relative mRNA expression levels of *SLC4* genes in human corneal endothelium, we use the data obtained from five donor corneal samples for testing statistical significance. However, when determining the expressional alterations that occur in cultured HCECs, the data used were obtained from two independent experiments. The significance of difference between the groups was determined by the two-tailed Student's t-test using spreadsheet software (Excel 5.0; Microsoft, Redmond, WA), with significance at P <0.05.

# III. RESULTS

## 3.1 Investigation of expression of *Slc4* transporter family in MCECs

In order to compare the mRNA expression levels of *Slc4* gene family members in mouse primary corneal endothelium and to investigate the changes that occur in their expression during cell culture, the primary MCECs were cultured and total RNAs were extracted from primary endothelium and cultured cells (at passage 2 and passage 7). For semi-quantitative analysis of gene expression, reverse transcription-polymerase chain reaction (RT-PCR) was performed and analysed by electrophoresis. For relative quantification of gene expression, real time qPCR with SYBR® green detection was carried out. The current gold standard method for relative quantification was employed, using a combination of several housekeeping genes rather than a single gene. The housekeeping gene which expressed most stably under a given experimental condition (i.e, cell culture in this study) was carefully chosen by geNorm™ software and the normalization factor was used for more accurate normalization.

## 3.1.1 Culture of mouse corneal endothelial cells (MCECs)

Primary MCECs were isolated from corneas of wild type C57BL6 mice. The Descemet's membrane-endothelial layers of 8-10 week old, in-bred mice (n=15) were gently stripped from corneas using a dissecting microscope (Figure 3.1A, 1B) and divided into two groups for both primary cell culture (n=5) and direct RNA extraction (n=10). CECs were grown under optimized culture conditions, as described in section 2.4. Initially, the cultured cells showed stellate morphology at low densities, and upon confluence, they became polygonal in shape, characteristic of endothelial cells (Figure 3.1C, 1D). Cultures were split (i.e. passaged) upon reaching 80% confluence and passaging was carried out until the seventh passage for this study.

In the latter passages, some cells were more elongated in appearance while some appear larger in size with more prominent nuclei (Figure 3.1E, 1F).
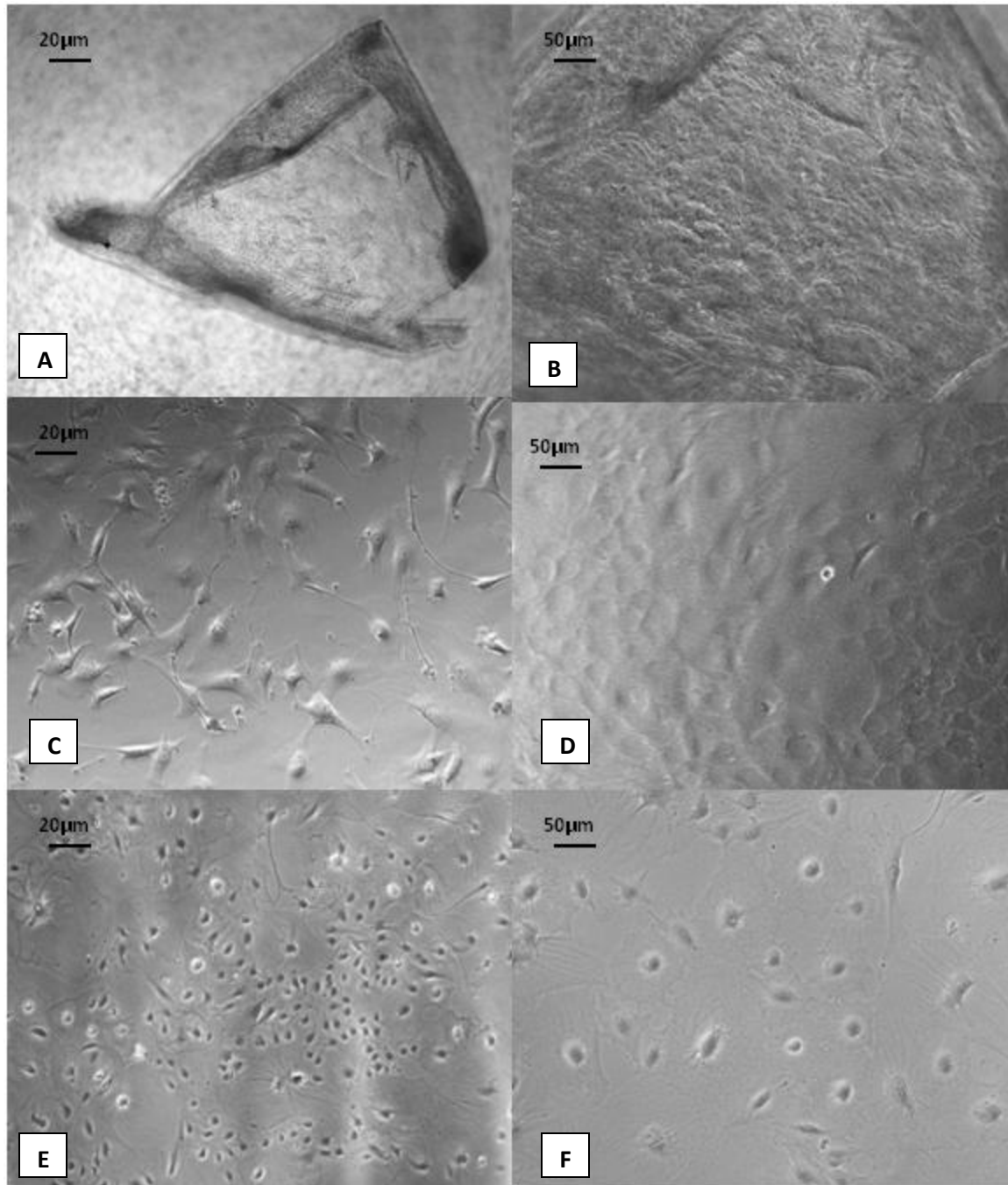


**Figure 3.1. Isolation and establishment of mouse corneal endothelial cells (MCECs).** A. and B. Phase contrast micrographs of descemet's membranesstripped from the corneas of wild type mice. C. and D. MCECs observed in early passage 2 culture E. and F. MCECs in late passage 7.

**3.1.2 RNA extraction and RNA quality**

Total RNA was extracted from primary corneal endothelium as well as from cultured MCECs at passage 2 and 7 (upon confluence) as described in section 2.6. To obtain sufficient amount of RNA for experimentation, a total of 20 mouse corneal endothelia had to be pooled for RNA isolation (See figure 2.1 for experimental workflow). The concentration of RNA was determined by UV spectrophotometry. The ratio of the readings at 260 nm and 280 nm (*A*260/*A*280) provides an estimate of the purity of RNA with respect to contaminants that absorb in the UV, such as protein. Good quality RNA is expected to have an *A*260/*A*280 ratio of 1.9–2.1 in slightly alkaline pH (Sambrook J *et. al.*, 1989). The absorbance readings for all RNA samples extracted from primary corneal endothelium, cultured MCECs at passage 2 and passage 7 were within this range, indicating RNA preparations with sufficient quality suitable for subsequent analyses.

**3.1.3 Determining amplification efficiency and quality of the primers**

When using ΔΔCt model for relative quantification, the formula $2^{-\Delta\Delta Ct}$ is applied where 2 is the 'efficiency' of the amplification. In order for this equation to be valid, the amplification efficiencies of both the gene of interest and the housekeeping gene (HKG) must be optimally equal to 2 (100% efficiency). Thus we initially validated the efficiencies of all the primers of *Slc4* family genes and HKGs by real time qPCR with SYBR® green detection, using mouse kidney cDNA as standard template. Mouse kidney cDNA was used for this purpose since all *Slc4* genes were shown to be expressed in mouse kidney tissue (Nishimura M *et. al.*, 2005) and sufficient quantities of RNA could be extracted from kidney tissue. Amplification analyses using six serial dilutions of template showed high amplification efficiencies for all the primer pairs

employed to amplify the HKGs as well as the *Slc4* genes. The efficiency is described as time of PCR product increase per cycle by the formula $E = 10^{-1/slope}$. Consistent, high amplification efficiencies (95 - 105%) were achieved in all cases, indicating the validity of using $\Delta\Delta Ct$ method (See figure 3.2 and table 3.1)

Furthermore, melting curve analysis was performed for all the primer pairs to ensure that a single specific melting peak was observed without a 'secondary peak', which indicates the presence of primer dimers. As SYBR® green dye can detect all double-stranded DNA, it is important to ascertain that a single product was obtained without primer dimers formation.

*Slc4a1* — $y = -3.5458x + 29.241$, $R^2 = 0.9745$

*Slc4a2* — $y = -3.5107x + 32.983$, $R^2 = 0.9936$

*Slc4a3* — $y = -3.3191x + 31.946$, $R^2 = 0.9296$

*Slc4a4* — $y = -3.5812x + 28.315$, $R^2 = 0.9897$

*Slc4a5* — $y = -3.1672x + 34.544$, $R^2 = 0.9401$

*Slc4a7* — $y = -3.5209x + 32.543$, $R^2 = 0.9506$

*Slc4a8* — $y = -3.4759x + 33.736$, $R^2 = 0.9667$

*Slc4a9* — $y = -3.5555x + 31.667$, $R^2 = 0.9603$

*Slc4a10* — $y = -3.1757x + 39.331$, $R^2 = 0.9469$

*Slc4a11* — $y = -3.1305x + 35.074$, $R^2 = 0.9828$
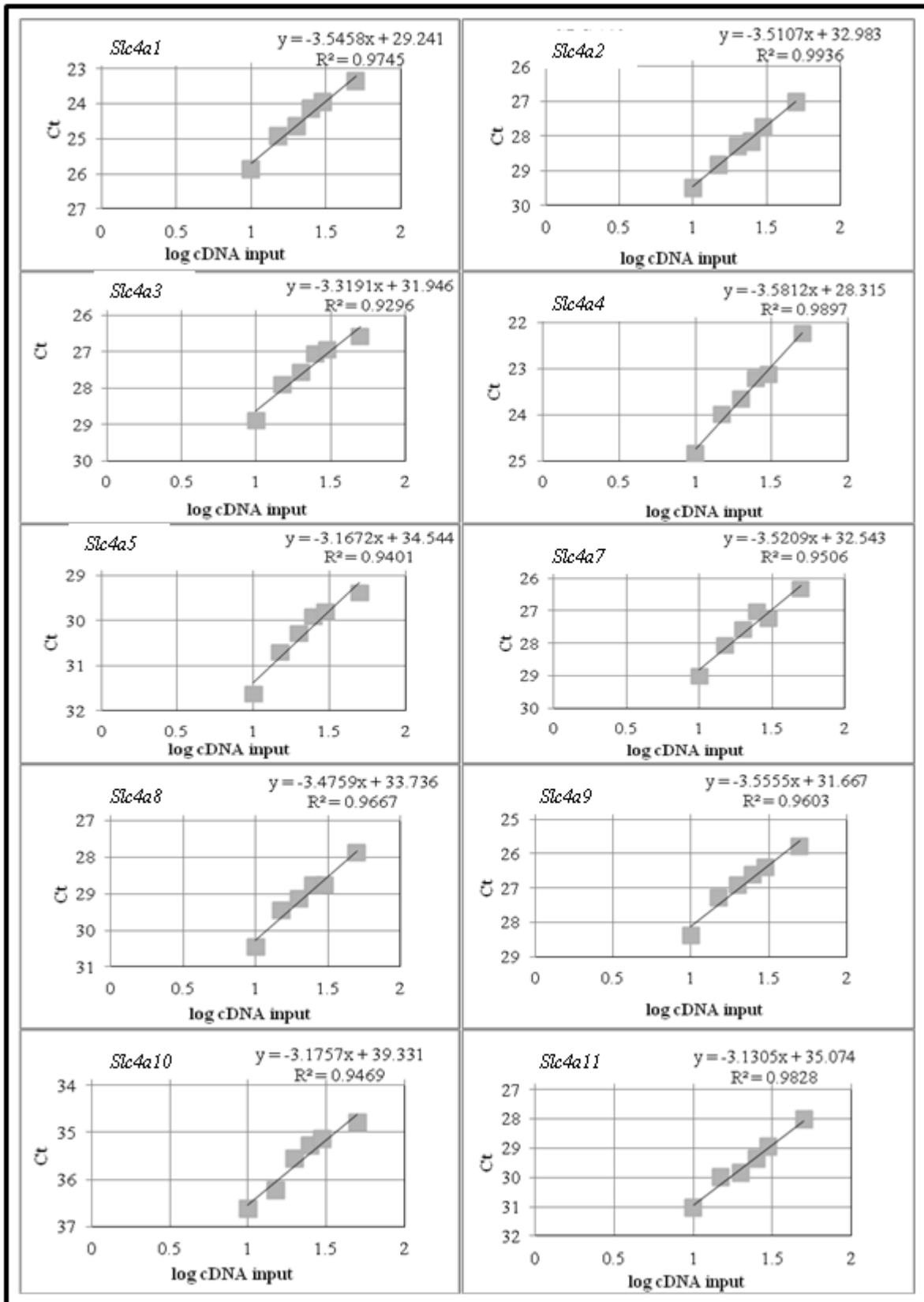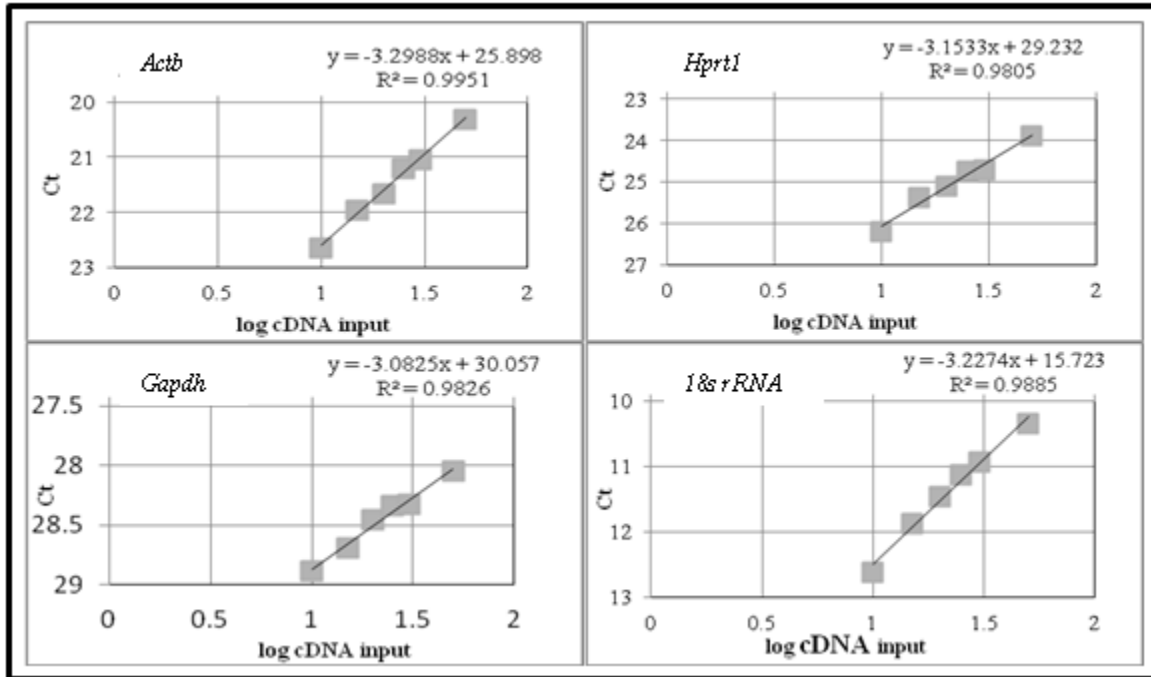
**Figure 3.2. PCR amplification efficiency plots.** The reaction efficiency achieved for each gene was calculated using the Ct slope method, with six data points corresponding to log10-fold mouse kidney cDNA serial dilutions (10 ng - 50 ng/reaction)

| Genes of interest | *Slc4a 1* | *Slc4a 2* | *Slc4a 3* | *Slc4a 4* | *Slc4a 5* | *Slc4a 7* | *Slc4a 8* | *Slc4a 9* | *Slc4a 10* | *Slc4a 11* |
|---|---|---|---|---|---|---|---|---|---|---|
| **Slope** | -3.55 | -3.51 | -3.32 | -3.58 | -3.17 | -3.52 | -3.48 | -3.56 | -3.17 | -3.13 |
| **Efficiency (E)** | **1.91** | **1.92** | **2.00** | **1.90** | **2.07** | **1.92** | **1.94** | **1.91** | **2.06** | **2.08** |

| Housekeeping genes | *β-actin* | *Hprt1* | *Gapdh* | *18S rRNA* |
|---|---|---|---|---|
| **Slope** | -3.30 | -3.15 | -3.08 | -3.23 |
| **Efficiency (E)** | **2.00** | **2.08** | **2.11** | **2.04** |

**Table 3.1. The amplification efficiencies for mouse *Slc4* family genes and housekeeping genes used in the study.** The efficiency is described as time of PCR product increase per cycle by the formula $E = 10^{-1/\text{slope}}$. Consistent, high amplification efficiencies (95 - 105%) were achieved in all cases.

### 3.1.4  Semi-quantitative analysis of *Slc4* family gene expression by reverse transcription polymerase chain reaction (RT-PCR)

First strand cDNA was synthesized from total RNA of mouse primary corneal endothelium as well as cultured cells (in passage 2 and passage 7) as described in methods section 2.8. Equal amount of cDNA template was used for standard PCR with Taq DNA polymerase using primers that were selected specifically to target the mRNA of the said genes. The resulting PCR products were separated by gel electrophoresis and visualized by ethidium bromide staining. The four housekeeping genes (*Gapdh*, *actb*, *hprt1*, *18S rRNA*) were used as amplification (positive) and normalizing controls.

A single RT–PCR product of the predicted size for a *given* mRNA template was observed for each primer pair indicating there was no contamination by genomic DNA and confirmed the amplification of mRNA. This analysis found that all *Slc4* genes were expressed in corneal endothelium and cultured MCECs.  It also indicated *Slc4a11* and *Slc4a2* genes as having the highest expression levels whilst *Slc4a1* and *Slc4a9* appeared to have the lowest expression levels in both primary corneal endothelium and cultured cells. However, it should be noted that this analysis is semi-quantitative and not as sensitive (or always accurate) as real time qPCR for assessment of relative gene expression. RT-PCR is more an accepted methodology for assessing the presence or absence of gene expression in given tissues or cells.
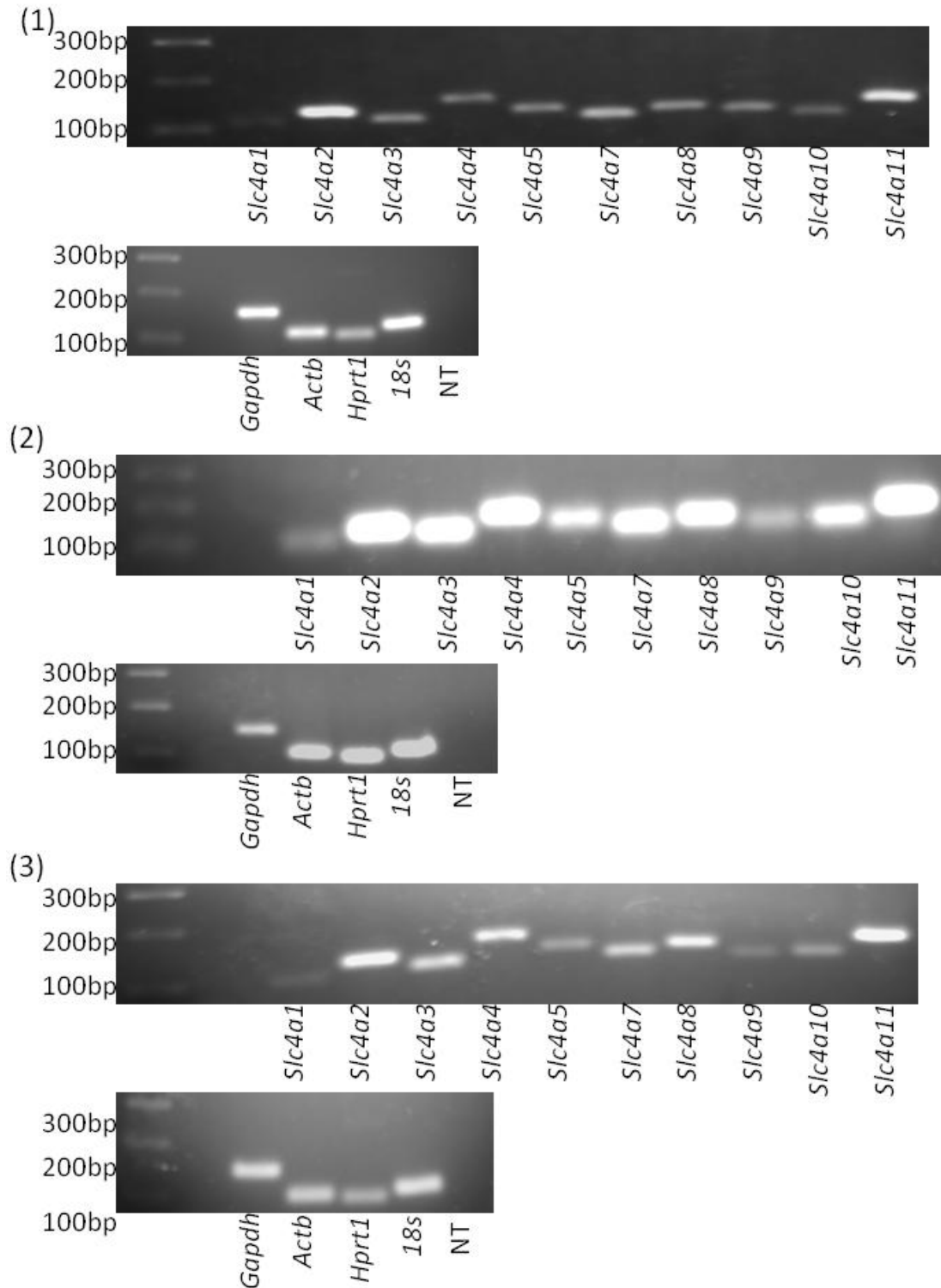
**Figure 3.3.  RT-PCR results from the cDNA samples generated from  (1) mouse primary corneal endothelium (2) cultured passage 2 MCECs (3) cultured passage 7 MCECs.**  100bp size marker is shown in the first lane from the left.  The primers used to generate the PCR products (Table 2.1) are indicated below each lane. The four HKGs (*Gapdh*, *Actb*, *Hprt1* and *18S rRNA*) were used as amplification (positive) controls. Each set of reactions (per gene) included a

no-template negative control, these samples were pooled and the combined sample (NT) was subjected to electrophoresis.


**3.1.5 Assessment of corneal endothelial markers in cultured MCECs**

In order to characterize MCECs, the expressions of several genes normally present in endothelial cells (*Aqp1, Zo-1, Col8a2*) as well as fibroblastic marker *Col1a*1 was examined by reverse transcription PCR. It was observed that MCECs from both early and late passages expressed endothelial markers *Aqp1, Zo-1* and *Col8a2*. However, the fibroblast cell marker *Col1a1* was not expressed in early passage 2 cells but was expressed in late passage 7 cells. (See figure 3.4D)

We further characterized the cells with immunofluorescent analyses on the cultured passage 2 MCECs using antibodies for $Na^+K^+ATPase$ and ZO-1. This analysis was limited to passage 2 MCECs as we were unable to obtain sufficient quantities of cells from passage 7. The activity of $Na^+K^+ATPase$ is required for proper physiological control of corneal thickness by the corneal endothelium [Riley MV (1977), Gerosk DH (1985)]; whilst tight junction-associated protein ZO-1 is involved in the formation of focal tight-junction complexes [Joyce NC (2003), Stiemke MM (1991)]. The cultured MCECs expressed both $Na^+K^+ATPase$ and ZO-1, which are characteristic markers indicative of the corneal endothelium. (See figure 3.4 A,B)
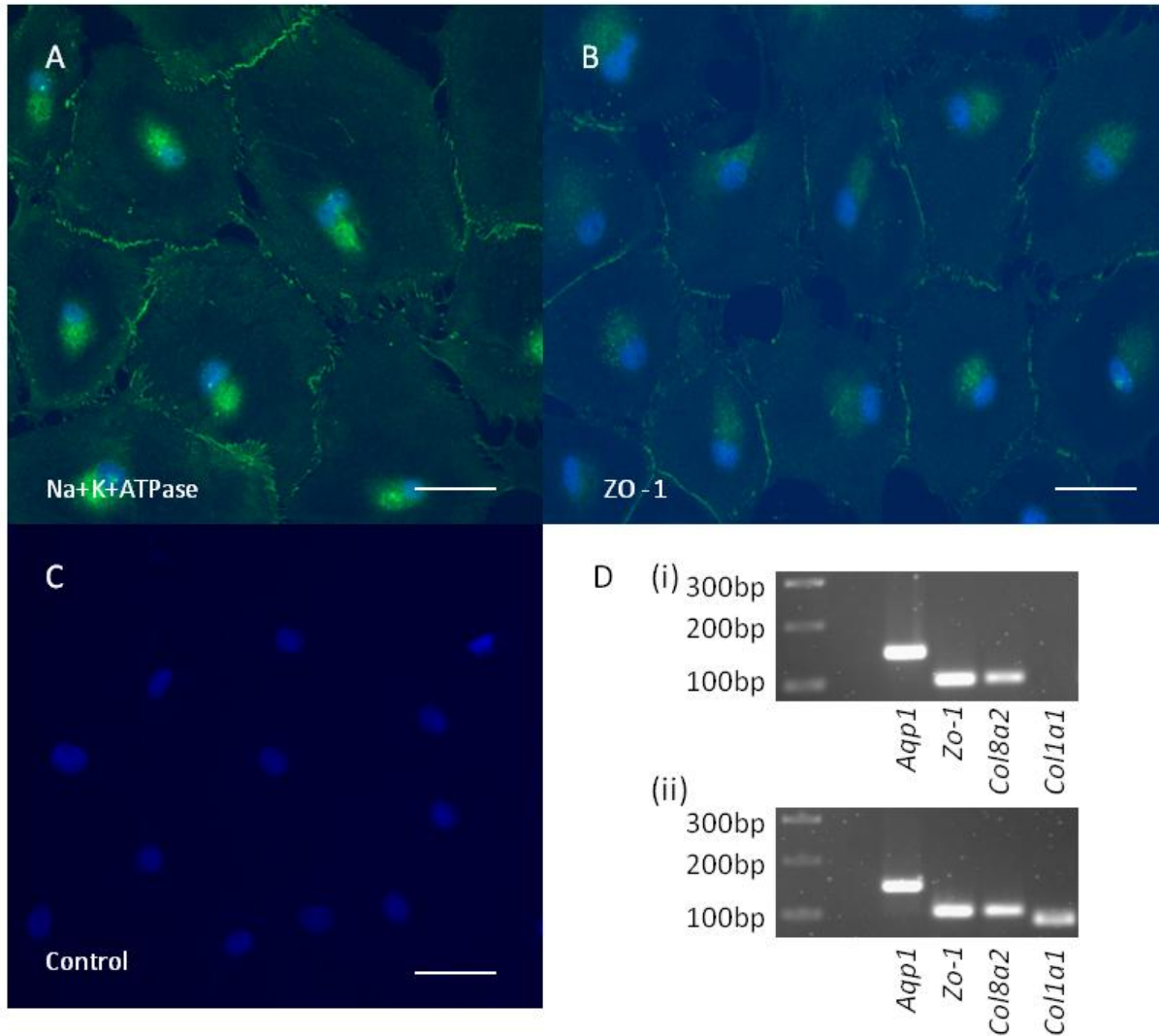
**Figure 3.4. Characterization of MCECs.** Cellular localization of (A) Na$^+$K$^+$ATPase and (B) ZO-1 in MCECs. Cells in passage 2 were immunostained with the indicated antibodies and visualized by fluorescent microscopy. (C) Isotype matched IgG$_1$ negative control. Scale bar: 50μm. (D) mRNA expression of *Aqp1, Zo-1, Col8a2, Col1a1* in (i) passage 2 MCECs and (ii) passage 7 MCECs. Cultured MCECs were harvested and analyzed by reverse transcription PCR. Size markers are shown in the first lane from the left. Note that the fibroblast marker *Col1a1* was not expressed in passage 2 cells but expressed in passage 7 cells.

**3.1.6 Selection of most stable housekeeping gene (HKG) using GeNorm<sup>TM</sup> analysis**

When comparing gene expression across different tissues or conditions, for example primary endothelium versus cultured cells, selection of most stable HKGs from an array of HKGs and use of multiple housekeeping genes have become a norm for more robust and accurate normalization and quantification (see method section 2.12 for more details). In this study, the most stable reference genes were selected from four most commonly used HKGs (*Gapdh, Actb, 18S rRNA and Hprt1*) using the geNorm<sup>TM</sup> software (Biogazelle, Belgium). They were systematically compared with each other and the resulting average expression stability plot was used to rank each HKG in order of expression stability. (See figure 3.5A) According to this analysis, *Hprt1* was found to be the most stable gene whilst *Gapdh* was the least stable gene and therefore unsuitable for normalization. Subsequently, the normalization factor was calculated from three most stable HKGs, namely, *Hprt1*, *actb* and *18S rRNA* (See figure 3.5B).

## A

Average expression stability values of remaining control genes

## B
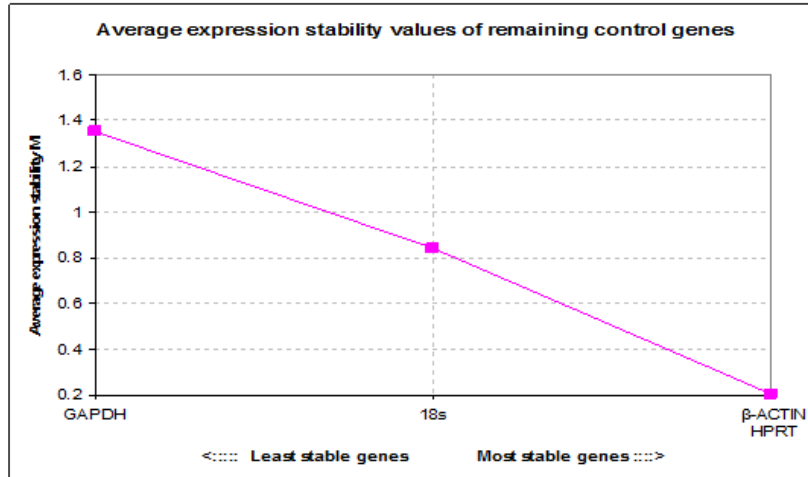
Calculation of normalization factors for most stable reference genes

|  | *18s* | *β-ACTIN* | *HPRT1* | Norm. Factor |
|---|---|---|---|---|
| Cultured MCEC (passage 2) | 1.00 | 1.00 | 1.00 | 1.00 |
| Cultured MCEC (passage 7) | 0.14 | 0.27 | 0.32 | 0.2313 |
| Primary endothelium | 0.76 | 0.34 | 0.37 | 0.4564 |
| M < 1.5 | 1.323 | 0.973 | 0.963 | |

**Figure 3.5. GeNorm™ analysis.** (A) The relative quantities of four HKGs were entered into the geNorm™ software to calculate average expression level stability (M). The genes with the lower M values are considered to have more stable expression levels. (B) The geometric mean of the most stable reference genes were calculated to obtain the normalization factor.

**3.1.7 Relative mRNA expression levels of *Slc4* transporter genes in mouse corneal endothelium**

In order to evaluate the relative expression levels of *Slc4* gene family within the murine corneal endothelium, the expression of each *Slc4* gene was normalized using the most stable housekeeping gene *Hprt1* (obtained by the calculation as described in section 3.1.5), and then compared against the most clinically important genes *Slc4a11* and *Slc4a4*. Therefore data is described as the expression levels of *Slc4* genes relative to that of *Slc4a11* or *Slc4a4*. The relative mRNA expression levels of all *Slc4* genes in mouse corneal endothelium are shown in table 3.2. The ΔCt and ΔΔCt values for a given gene were derived from a single experiment (i.e. 8 qRT-PCR data points/gene) as explained in details in methods section 2.11. However for the calculation of p-values, fold data from the two independent experiments was used (see legend of table 3.2), and in this experimental context indicate the reproducibility of relative expression data.

The same analyses were carried out for cultured passage 2 and passage 7 MCECs (see appendix A and B). However results for the cultured cells are not elaborated here as the aim of this analysis was to identify the order of expression of *Slc4* genes in the uncultured murine corneal endothelium.

**mRNA expression of *Slc4* family genes in mouse corneal endothelium**

| Gene name | $\Delta Ct\,(Ct_{Goi} - Ct_{Hprt1})$ [a] | $\Delta\Delta Ct\,(\Delta Ct_{Goi} - \Delta Ct_{Slc4a11})$ [b] | Normalised expression (rel to *Slc4a11*) [c] | P value [d] | $\Delta\Delta Ct\,(\Delta Ct_{Goi} - \Delta Ct_{Slc4a4})$ [b] | Normalised expression (rel to *Slc4a4*) [c] | P value [d] |
|---|---|---|---|---|---|---|---|
| *Slc4a1* | 7.115±0.3482 | 8.595±0.3482 | 0.0026 (0.0020-0.0033) | 0.00297* | 6.83±0.3482 | 0.0088 (0.0069-0.0112) | 0.00091* |
| *Slc4a2* | -0.63±0.0781 | 0.85±0.0781 | 0.5548 (0.5255-0.5856) | 0.00701* | -0.915±0.0781 | 1.8856 (1.7862-1.9905) | 0.00098* |
| *Slc4a3* | 1.135±0.2393 | 2.615±0.2393 | 0.1632 (0.1383-0.1927) | 0.00219* | 0.85±0.2393 | 0.5548 (0.4700-0.6549) | 0.00253* |
| *Slc4a4* | 0.285±0.0781 | 1.765±0.0781 | 0.2942 (0.2787-0.3106) | 0.00416* | 0±0.0781 | 1.0000 (0.9473-1.0556) | - |
| *Slc4a5* | 3.395±0.0791 | 4.875±0.0791 | 0.0341 (0.0323-0.0360) | 0.00309* | 3.11±0.0791 | 0.1158 (0.1096-0.1223) | 0.00097* |
| *Slc4a7* | 0.56±0.1315 | 2.04±0.1315 | 0.2432 (0.2220-0.2664) | 0.00308* | 0.275±0.1315 | 0.8265 (0.7544-0.9053) | 0.00507* |
| *Slc4a8* | 6.125±0.1151 | 7.605±0.1151 | 0.0051 (0.0047-0.0056) | 0.00300* | 5.84±0.1151 | 0.0175 (0.0161-0.0189) | 0.00096* |
| *Slc4a9* | 5.17±0.2062 | 6.65±0.2062 | 0.0100 (0.0086-0.0115) | 0.00297* | 4.885±0.2062 | 0.0338 (0.0293-0.0390) | 0.00087* |
| *Slc4a10* | 2.815±0.2865 | 4.295±0.2865 | 0.0509 (0.0418-0.0621) | 0.00266* | 2.53±0.2865 | 0.1731 (0.1420-0.2112) | 0.00019* |
| *Slc4a11* | -1.48±0.1373 | 0±0.1373 | 1.0000 (0.9092-1.0998) | - | -1.765±0.1373 | 3.3987 (3.0902-3.7381) | 0.00416* |

**Table 3.2. Relative normalized mRNA expression levels of *Slc4* gene family in mouse corneal endothelium.** Data are described as the expression levels of a given gene relative to that of *Slc4a11* (in column 4) and *Slc4a4* (in column 7).

a. The ΔCt value was determined by subtracting the average *Hprt1 Ct* value from the average Ct value of *gene of interest (Goi)*. The standard deviation (SD) of the difference was calculated from the standard deviations of the Ct values of *Goi* and *Hprt1* by the formula $s = \sqrt{s1^2 + s2^2}$. The mean and SD values were obtained from a data pool of 8 reactions.
b. The calculation of ΔΔCt involved subtraction by the ΔCt calibrator (*Slc4a11* or *Slc4a4*) value. This is subtraction of an arbitrary constant, so the SD of ΔΔCt is the same as the SD of the ΔCt value.
c. The range given for nomalised expression relative to *Slc4a11* or *Slc4a4* was determined by evaluating the expression: $2^{-\Delta\Delta Ct}$ with ΔΔCt + s and ΔΔCt − s, where s = SD of the ΔΔCt value.
d. P values indicate the significance between the normalized expression of given gene and normalized expression of the calibrator gene (*Slc4a11* or *Slc4a4*) from two independent experiments. *P < 0.05

According to this analysis, *Slc4a11* showed the highest expression level whilst *Slc4a1* showed the lowest. This result was supported by the previous semi-quantitative analysis (see section 3.1.3). The exact order of expression level was therefore *Slc4a11* being highest followed by *Slc4a2, Slc4a4, Slc4a7, Slc4a3, Slc4a10, Slc4a5, Slc4a9, Slc4a8* and *Slc4a1*. The expression

of *Slc4a2* was approximately half that of *Slc4a11* (0.55±0.03 [p=0.007]) while the expression of *Slc4a1* was three hundred times less than *Slc4a11*(0.0026±0.0006 [p=0.003]). When comparing the expression levels of the two clinically important genes *(i.e. Slc4a11* and *Slc4a4)*, the expression of *Slc4a11* was found to be approximately three times greater than that of *Slc4a4* (3.4±0.3 [p=0.004]). As the p-values indicate, the above described differences in expression levels between the said genes were statistically significant.

### 3.1.8 Alteration in mRNA expression of *Slc4* genes during MCEC cell culture

Next, we investigated the alterations in gene expression that occur in MCECs during cell culture. This was carried out using multiple housekeeping genes for normalization (figure 3.5A and B). The normalization factor was calculated using expression level data of the three most stable reference genes (*Hprt1, Actb, 18S rRNA*) across the three samples (primary corneal endothelium, passage 2 cells, passage 7 cells). According to this analysis, the expressions of all the *Slc4* transporters except *Slc4a4* and *Slc4a10* were down-regulated in early passage 2. However, in late passage 7, the *Slc4a1, Slc4a2, Slc4a3, Slc4a4, Slc4a7* became up-regulated while the remaining members were still down-regulated. The expression of *Slc4a11* was significantly down regulated 20 fold (0.05±0.001 [p=0.000001]) in passage 2 and by 7 fold (0.14±0.002 [p=0.000002]) in passage 7. Interestingly, the expression of another clinically important gene *Slc4a4* was significantly up-regulated by approximately 2.5 fold (2.52±0.07 [p=0.0007]) in passage 2 and 14 fold (14.57±0.16 [p=0.00005]) in late passage 7.

## A

| Gene name | Fold change in mRNA expression of MCECs (p2) | P value | Fold change in mRNA expression of MCECs (p7) | P value | Significance between p2 and p7 |
|---|---|---|---|---|---|
| Slc4a1 | 0.5697±0.0902 | 0.01433* | 3.5308±0.2449 | 0.00311* | 0.00091* |
| Slc4a2 | 0.5939±0.0130 | 0.00034* | 4.5631±0.0813 | 0.00017* | 0.00010* |
| Slc4a3 | 0.5046±0.0293 | 0.00116* | 7.7543±0.5002 | 0.00182* | 0.00140* |
| Slc4a4 | 2.5286±0.0733 | 0.00077* | 14.5707±0.1649 | 0.00005* | 0.00002* |
| Slc4a5 | 0.0166±0.0028 | 0.00000* | 0.1081±0.0180 | 0.00014* | 0.00914* |
| Slc4a7 | 0.9033±0.1080 | 0.26121 | 6.3643±0.4105 | 0.00195* | 0.00102* |
| Slc4a8 | 0.0847±0.0184 | 0.00013* | 0.4104±0.1147 | 0.01238* | 0.02797* |
| Slc4a9 | 0.0401±0.0093 | 0.00003* | 0.3035±0.0080 | 0.00004* | 0.00001* |
| Slc4a10 | 1.3931±0.0404 | 0.00350* | 0.9428±0.0791 | 0.33701 | 0.00246* |
| Slc4a11 | 0.0525±0.0014 | 0.00000* | 0.1441±0.0020 | 0.00000* | 0.00002* |
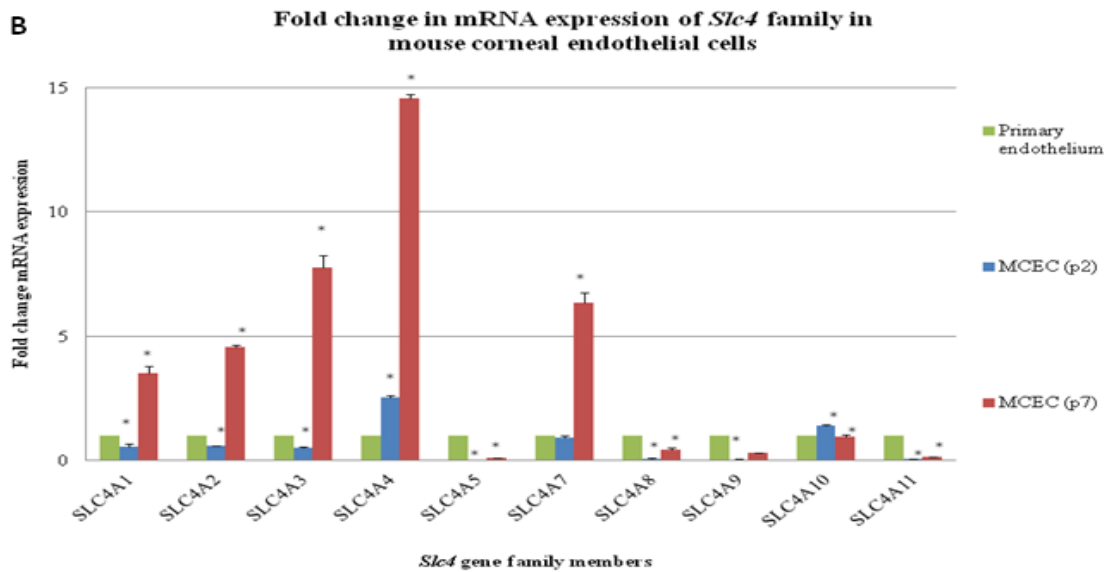


**Fig. 3.6. Alterations in mRNA expressions of *SLC4A* family genes in cultured (passage 2 and 7) mouse corneal endothelial cells compared to the primary endothelium.** A. Data are described as the relative fold change in expression of cultured cells over primary corneal endothelium. Values shown are the mean±SD of two independent culturing experiments. The P values in last column indicate the significance between p2 and p7 change values from two independent experiments. *P < 0.05. B. Data are shown in graph.

50

**3.2 Investigation of mRNA expression of *SLC4* transporter family in human corneal endothelial cells (HCECs)**

Applying the same methodology used for the gene expression analysis in MCECs, the expression levels of *SLC4* gene family members in human corneal endothelium were also compared and the change in their expressions during cell culture was investigated. The whole corneas were ordered from Lions Eye Institute for Transplant & Research, Inc. (Tampa, FL) and Sri Lanka Eye Donation Society (Colombo, Sri Lanka) while the cultured HCECs were kindly provided by Dr. Gary Peh Swee Lim of Ocular Tissue Engineering and Stem Cell group from Singapore Eye Research Institute.

**3.2.1 Cultivation of human corneal endothelial cells (HCECs)**

The HCECs were cultivated according to the protocol developed by Dr Gary Peh's group. Briefly, the isolation of HCECs involved a two-step peel-and-digest method and then the isolated HCECs were plated onto culture dishes coated with FNC coating mix®. The protocol is elaborated in section 2.5. Phase contrast micrographs of HCECs showed that in early passage 2, the cells were polygonal in shape (Figure 3.7A and B) but in late passage 5, their morphology became more elongated (Figure 3.7C and D). It was reported that in some late subcultures, HCECs turned fibroblast-like and appeared to have lost contact inhibition. (Peh GSL et al, 2011)
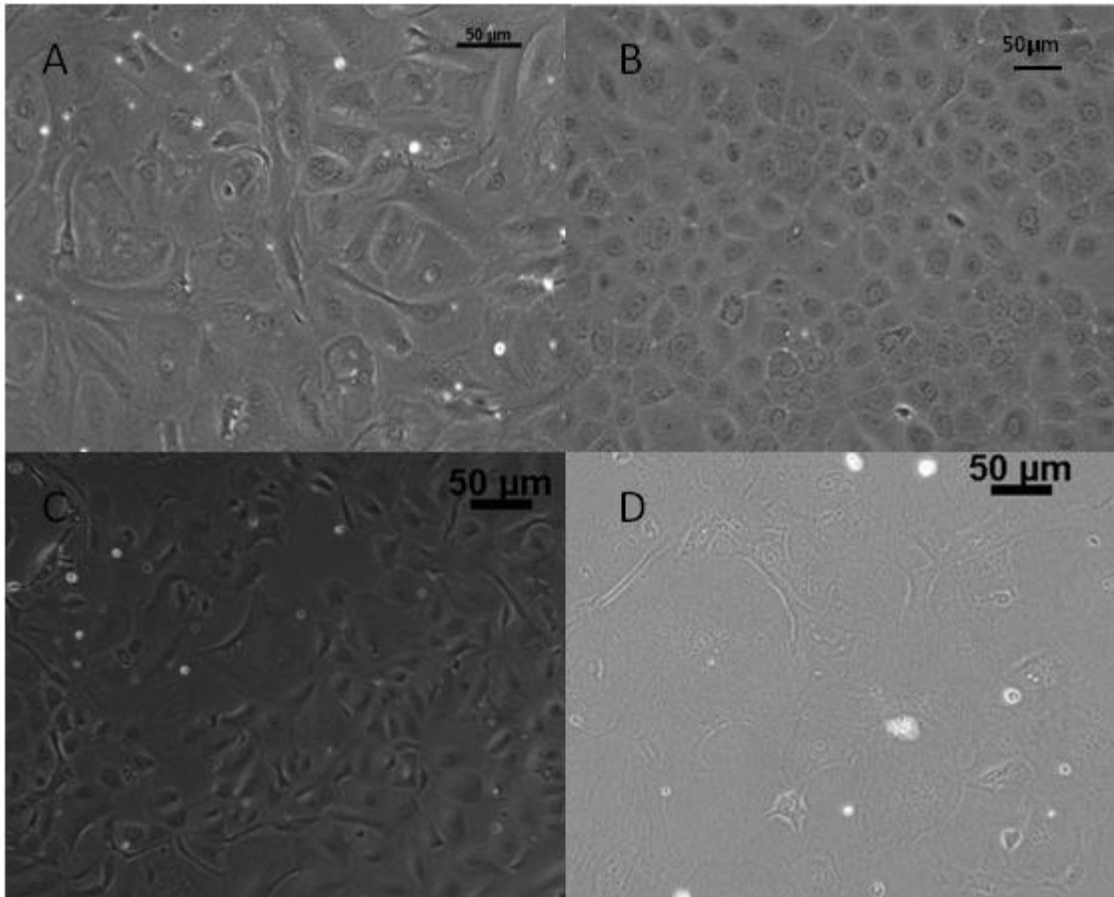
**Figure 3.7. Morphology of cultured human corneal endothelial cells (HCECs).** (A) and (B) show HCECs observed in early passage 2 of culture while (C) and (D) show those in late passage 5 .

### 3.2.2. Immunostaining with endothelial cell markers for cell identification

Immunocytochemistry revealed that HCECs in early passage 2 expressed endothelial cell markers, $Na^+$-$K^+$ ATPase and ZO 1. The images were also kindly provided by Dr Gary Peh. Immunostaining for $Na^+$-$K^+$-ATPase (Figure 3.8A), an integral membrane protein complex responsible for regulating pump functions, reavealed that it was located at the basolateral memebrane while ZO-1, junctional molecule, (Figure 3.8B) was located at the cell boundaries of the cultivated HCECs.
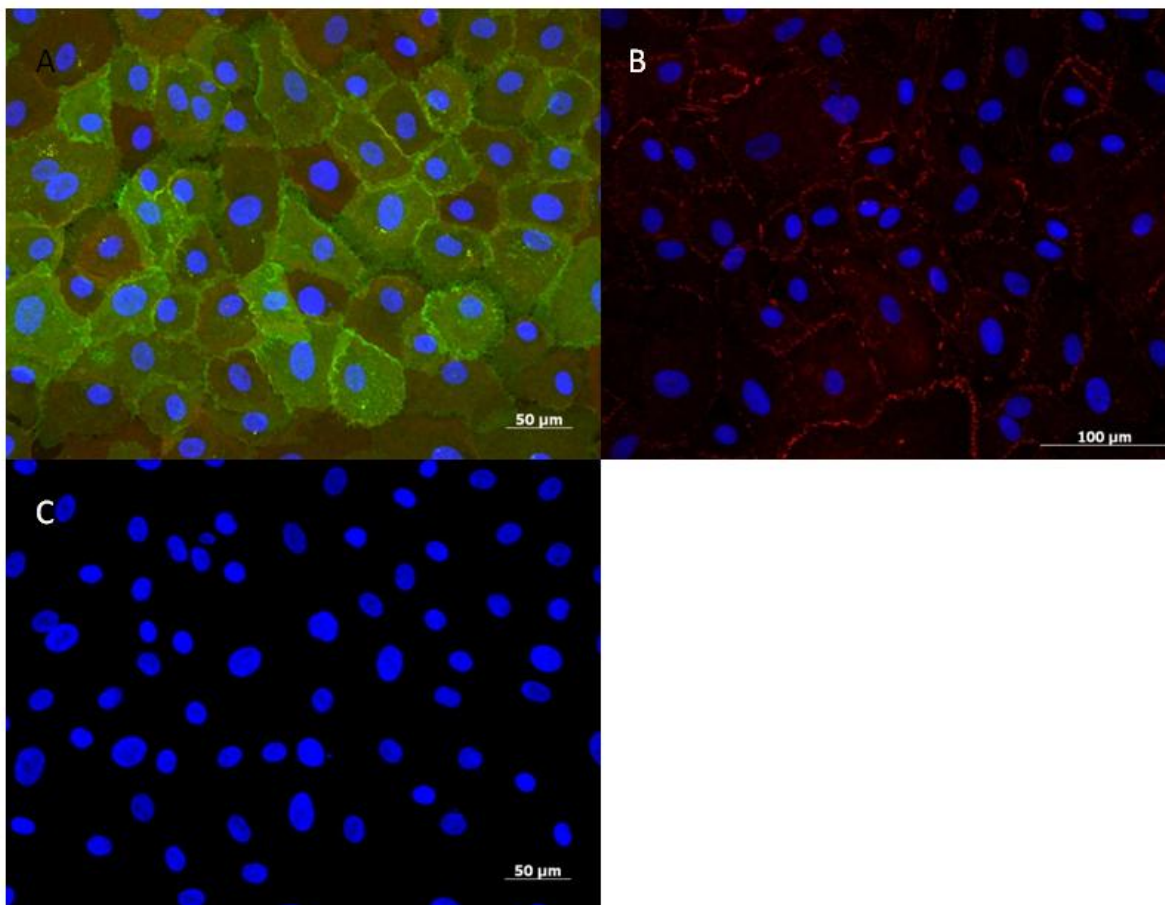
**Figure 3.8. Cellular localization of Na$^+$K$^+$ ATPase and ZO-1 in HCECs.** (A) Na$^+$K$^+$ ATPase shown in green, nucleus in DAPI blue and cytoskeletal network in Phalloidin red. (B) ZO-1 in red and nucleus in DAPI blue (C) Isotype matched IgG$_1$ negative control. (Courtesy of Dr Gary Peh, Singapore Eye Research Institute)

### 3.2.3 RNA isolation and RNA quality

Total RNA was extracted from primary corneal endothelia of five donor cornea samples (n=5; donors' information can be found in table 2.3) as well as from cultured cells in passage 2 and 5 (upon confluence) using TRIzol™ reagent as described in section 2.6. The concentration of RNA was determined by UV spectrophotometry (See section 2.7). Absorbance ratios (A$_{260/280}$) for all RNA samples (primary endothelium, cultured passage 2 and passage 5 cells) were within the range of 1.9 - 2.1, indicating good quality RNA preparations suitable for downstream applications.

**3.2.4 Determining amplification efficiency and quality of the primers**

The efficiencies of amplifying all the primers of *SLC4* family as well as the housekeeping genes were initially validated as described in the section 3.1.4, using the immortalized human corneal endothelial cell line (IHCEn) cDNA as template. Amplification of serial dilution of template showed high amplification efficiency (95% - 105%) by all primers. (See figure 3.9 and table 3.3)

Again, a single specific melting peak observed on melting curve analysis for each primer ruled out the possibility of primer dimer formation.

SLC4A1: $y = -3.2424x + 39.047$, $R^2 = 0.9902$

SLC4A2: $y = -3.4285x + 27.653$, $R^2 = 0.9662$

SLC4A3: $y = -3.2176x + 33.318$, $R^2 = 0.9758$

SLC4A4: $y = -3.5149x + 35.074$, $R^2 = 0.9747$

SLC4A5: $y = -3.2039x + 35.013$, $R^2 = 0.9886$

SLC4A7: $y = -3.4749x + 27.258$, $R^2 = 0.965$

SLC4A8: $y = -3.2588x + 34.716$, $R^2 = 0.9915$

SLC4A9: $y = -3.2482x + 36.745$, $R^2 = 0.9839$

SLC4A10: $y = -3.3631x + 35.333$, $R^2 = 0.9919$

SLC4A11: $y = -3.259x + 35.636$, $R^2 = 0.9827$

55
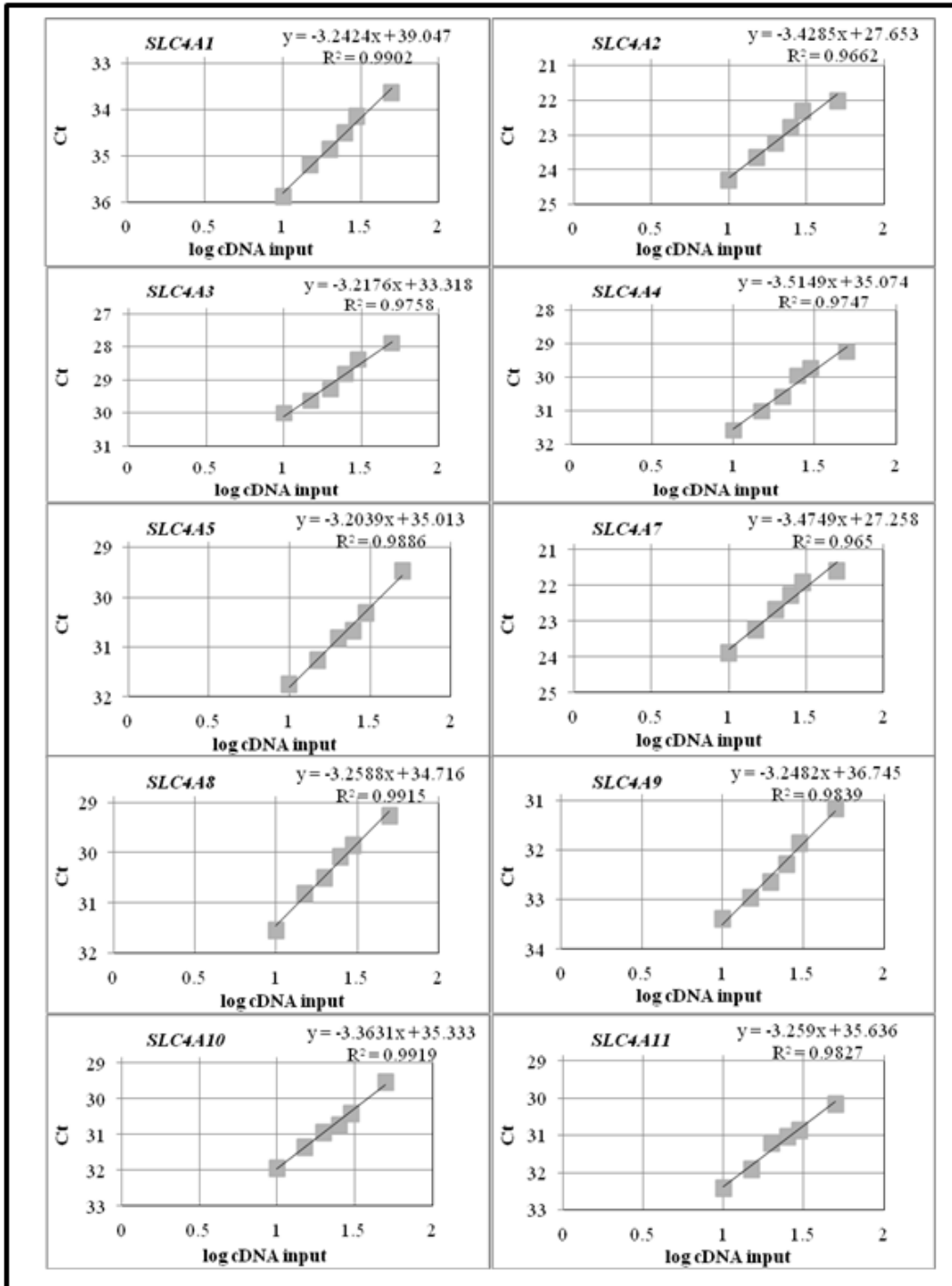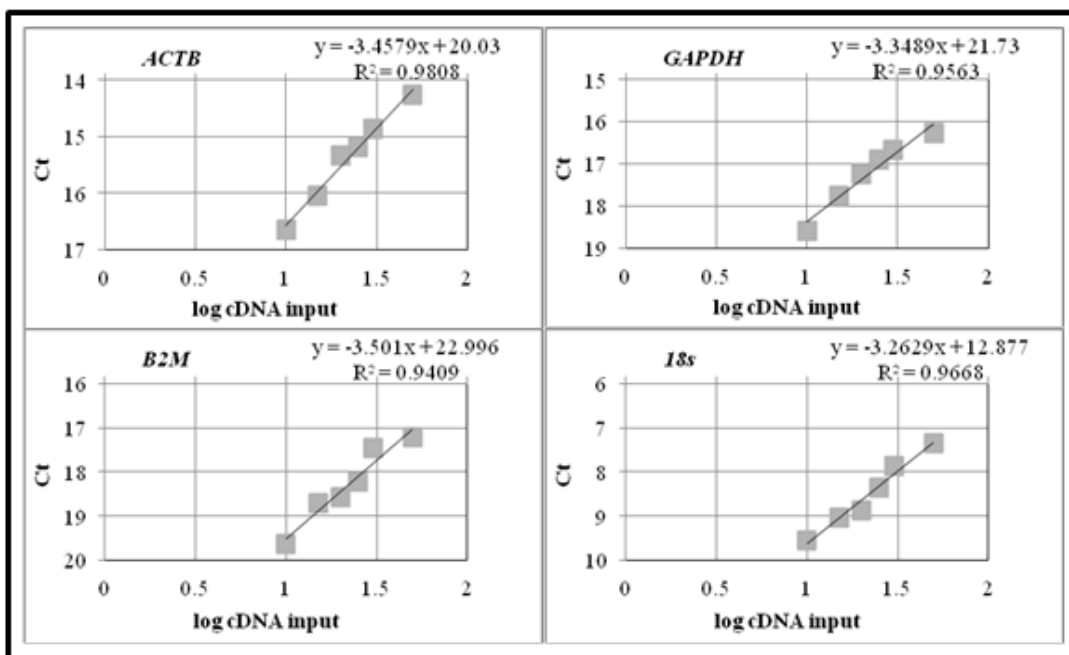
**Figure 3.9. PCR efficiency plots.** The efficiency for each gene was calculated using the Ct slope method, with six data points corresponding to log10-fold cDNA serial dilutions (10 ng - 50 ng/reaction)

| Genes of interest | SLC4 A1 | SLC4 A2 | SLC4 A3 | SLC4 A4 | SLC4 A5 | SLC4 A7 | SLC4 A8 | SLC4 A9 | SLC4 A10 | SLC4 A11 |
|---|---|---|---|---|---|---|---|---|---|---|
| Slope | -3.24 | -3.43 | -3.22 | -3.52 | -3.20 | -3.48 | -3.26 | -3.25 | -3.36 | -3.26 |
| Efficiency | 2.04 | 1.96 | 2.04 | 1.92 | 2.05 | 1.94 | 2.03 | 2.03 | 1.98 | 2.03 |

| Housekeeping genes | ACTB | GAPDH | B2M | 18S rRNA |
|---|---|---|---|---|
| Slope | -3.46 | -3.35 | -3.50 | -3.27 |
| Efficiency | 1.95 | 1.99 | 1.93 | 2.02 |

**Table 3.3. The amplification efficiencies for human *SLC4* family genes and housekeeping genes used in the study.** All primer pairs displayed consistent, high amplification efficiencies.

**3.2.5 Semi-quantitative analysis by reverse transcription polymerase chain reaction (RT-PCR)**

First strand cDNA was synthesized from total RNA of human primary corneal endothelium as well as from cultured HCECs (in passage 2 and passage 5) as described in the methods section 2.8. Equal amount of cDNA template was used for standard PCR with Taq DNA polymerase and the resulting PCR products were separated by gel electrophoresis and visualized by ethidium bromide staining. The four housekeeping genes (*ACTB, GAPDH, B2M, 18S rRNA*) were used as amplification and normalizing controls. A single RT–PCR product of expected size for a *given* mRNA template was observed for each *SLC4* gene and housekeeping gene, ruling out the possibility of primer dimer inclusions (See figure 3.10).

**3.2.6 Selection of most stable housekeeping gene (HKG) using GeNorm$^{TM}$ analysis**

Selection of most stable housekeeping gene was carried out as described in the section 3.1.5, using the four widely used housekeeping genes (*ACTB, GAPDH, B2M, 18S rRNA*). The ubiquitously used *GAPDH* was found to be the most stable HKG while *B2M* was not suitable to be used for normalization (See figure 3.11A) Then the normalization factor was calculated using three most stable HKGs (*ACTB, GAPDH* and *18S rRNA)* (Figure 3.11B).
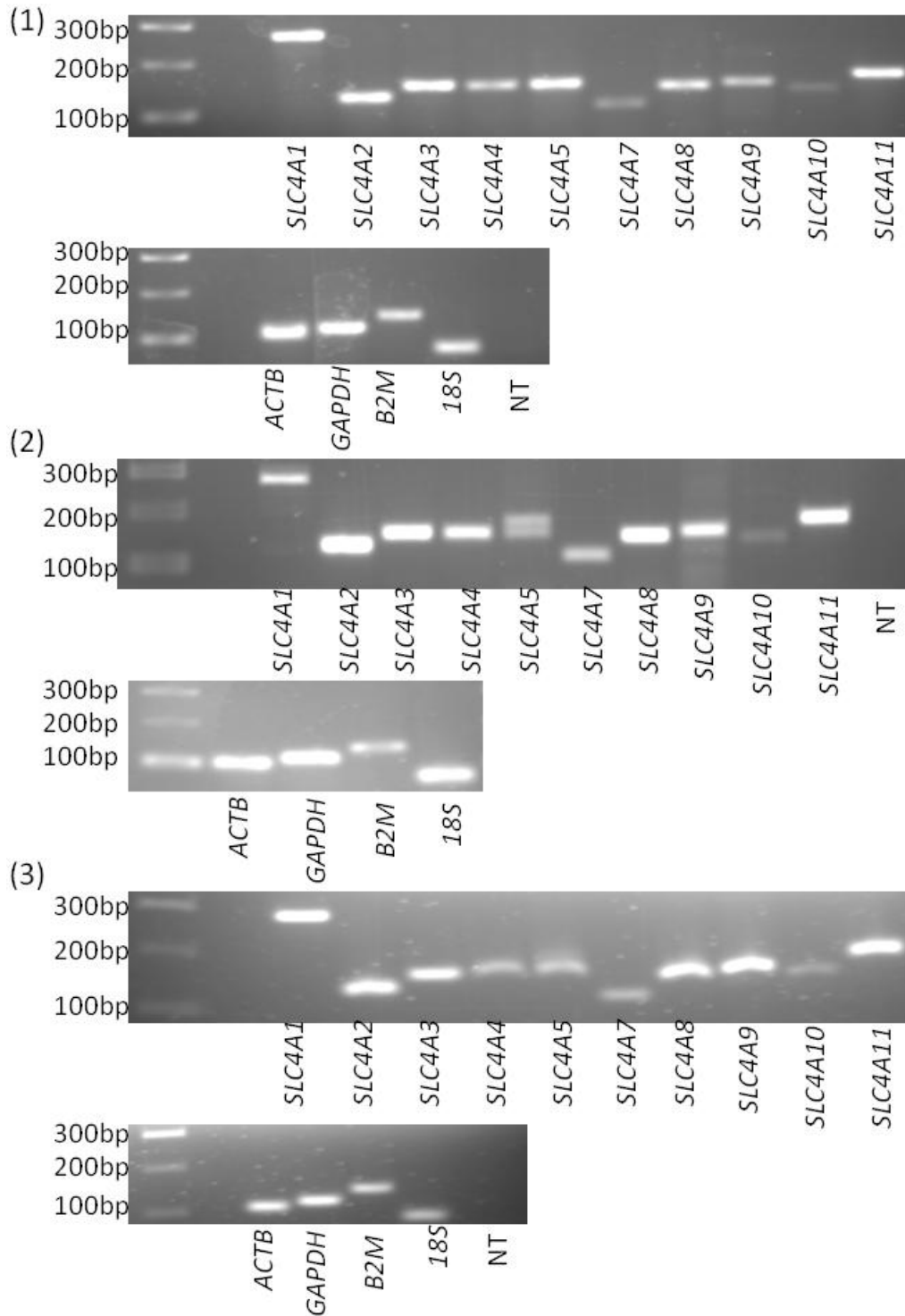
**Figure 3.10. RT-PCR results from the cDNA samples generated from (1) human primary corneal endothelium (2) cultured passage 2 HCECs, (3) cultured passage 5 HCECs.** 100bp size marker is shown in the first lane from the left. The primers used to generate the PCR products (Table 2.2) are indicated below each lane. The four HKGs (*ACTB, GAPDH, B2M, 18S rRNA*) were used as amplification (positive) controls. Each set of reactions (per gene) included a

no-template negative control, these samples were pooled and the combined sample (NT) was subjected to electrophoresis.

A

Average expression stability values of remaining control genes



B
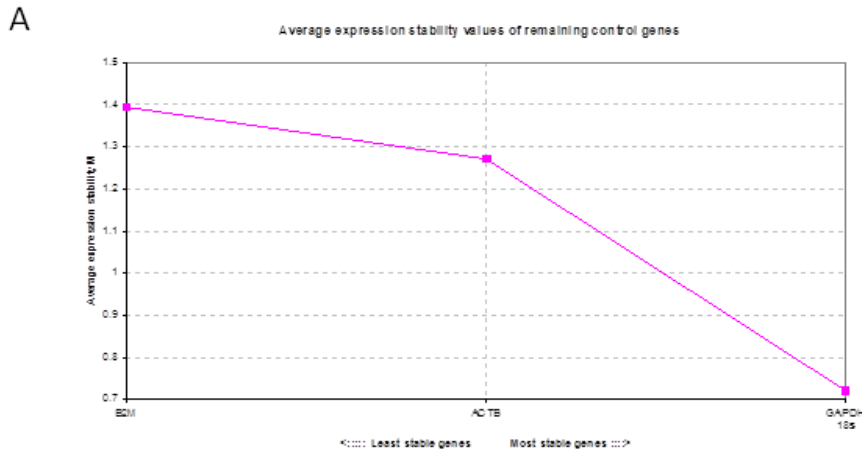
| Calculation of normalization factors for most stable reference genes | | | | |
|---|---|---|---|---|
| | *ACTB* | *GAPDH* | *18S* | Norm. Factor |
| Cultured HCEC (passage 2) | 0.87 | 1.00 | 8.83 | 0.8858 |
| Cultured HCEC (passage 5) | 1.00 | 0.50 | 1.00 | 0.7946 |
| Primary endothelium | 0.45 | 0.16 | 0.36 | 0.1384 |
| M < 1.5 | 1.359 | 1.211 | 1.489 | |

**Figure 3.11 GeNorm™ analysis. (A)** The analysis gave average expression level stability (M). The genes with the lower M values were considered to have more stable expression levels. **(B)** The geometric means of the most stable reference genes were calculated to obtain the normalization factors.

**3.2.7 Relative mRNA expression levels of *SLC4* genes in the human corneal endothelium**

In order to evaluate the relative mRNA expression levels of *SLC4* gene family within the human corneal endothelium, the expression of each *SLC4* gene was normalized using *GAPDH* (obtained by the calculation as described in section 3.2.6), and then compared against *SLC4A11* and *SLC4A4*. The five donor corneas were used in this study. (See table 2.3 of methods section for donors' information) To demonstrate that all the 5 donor corneas had comparable relative expression levels and the validity of the experiment, we depicted the data in terms of $\Delta Ct$ values after normalization against the most stable internal reference gene *GAPDH* (Figure. 3.12). Although the five donor cornea samples had discrepancy in age, race, cause of death and elapsed time from death to corneal preservation, the expression levels of *SLC4* family members in five corneal samples followed the same pattern of relative abundance, i.e., *SLC4A11* having the highest expression followed by *SLC4A4, SLC4A2, SLC4A3, SLC4A7, SLC4A5, SLC4A8, SLC4A1, SLC4A10* and *SLC4A9*.
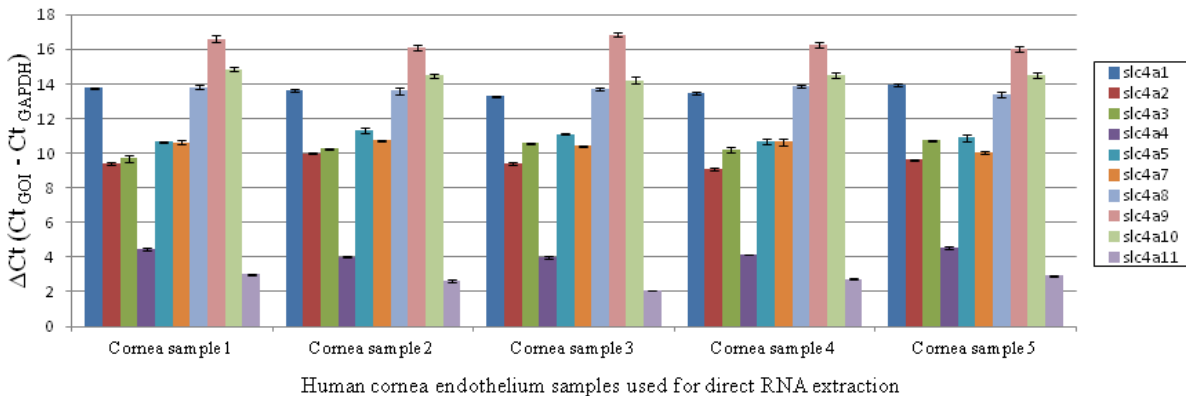


**Figure 3.12. $\Delta Ct$ values obtained from qRT-PCR analysis on *SLC4* family gene expression in five human donor cornea samples.** The $\Delta Ct$ value was determined by subtracting the average *GAPDH* Ct value from the average Ct value of *gene of interest (GOI)*. The mean and SD values were obtained from a data pool of 8 reactions. Note that the expression levels of *SLC4* family members in five corneal samples followed the same pattern of relative abundance. The lower the $\Delta Ct$ value, the higher the expression level.

The relative mRNA expression levels of all *SLC4* genes in the human corneal endothelium are shown in table 3.4. Here the $\Delta$Ct and $\Delta\Delta$Ct values for a given gene were derived using qRT-PCR data from a single sample (i.e. 8 qRT-PCR data points/gene), representative of five samples, as explained in detail in methods section 2.11. However for the calculation of p-values, fold data from 5 independent samples (i.e. 5 corneas) were used (see legend of table 3.4), and in this experimental context indicate the reproducibility of relative expression data.

According to this analysis, *SLC4A11* showed the highest expression and its expression was approximately 2.75 times higher (2.75±0.1 [p=0.0004]) than that of *SLC4A4*. The order of abundance for expression of *SLC4* gene family in the human corneal endothelium was as follows: *SLC4A11, SLC4A4, SLC4A2, SLC4A3, SLC4A7, SLC4A5, SLC4A8, SLC4A1, SLC4A10* and *SLC4A9*. Hence, based on their level of expression in human corneal endothelium, the *SLC4* family members can be categorized into three groups: *SLC4A11* and *SLC4A4* in 'high expression', *SLC4A2, SLC4A3, SLC4A7* and *SLC4A5* in 'moderate expression', *SLC4A1, SLC4A8, SLC4A10* and *SLC4A9* in 'very low expression'. The expression level of *SLC4A9* gene was found to be negligible (0.00008±0.00001 [p=0.0004]) relative to that of *SLC4A11*.

Once again, for the sake of completion we also analyzed the relative expression levels of *SLC4* genes in cultured HCECs (see appendix C and D). These results are however not elaborated upon as the purpose of this analysis was to identify the abundance of *SLC4* gene members in primary **<u>uncultured</u>** corneal endothelial cells in comparison to the clinically relevant *SLC4A11* and *SLC4A4* genes.

**mRNA expression of *SLC4* family genes in human corneal endothelium**

| Gene name | $\Delta Ct$ ($Ct_{GOI}-Ct_{GAPDH}$) [a] | $\Delta\Delta Ct$ ($\Delta Ct_{GOI}-\Delta Ct_{SLC4A11}$) [b] | Normalised expression (rel to *SLC4A11*) [c] | P value [d] | $\Delta\Delta Ct$ ($\Delta Ct_{GOI}-\Delta Ct_{SLC4A4}$) [b] | Normalised expression (rel to *SLC4A4*) [c] | P value [d] |
|---|---|---|---|---|---|---|---|
| *SLC4A1* | 13.765±0.0652 | 10.77±0.0652 | 0.00057 (0.00055-0.00060) | 0.000424* | 9.31±0.0652 | 0.00158 (0.00151-0.00165) | 0.000520* |
| *SLC4A2* | 9.39±0.0700 | 6.395±0.0700 | 0.01188 (0.01132-0.01247) | 0.000420* | 4.935±0.0700 | 0.03269 (0.03114-0.03432) | 0.000512* |
| *SLC4A3* | 9.715±0.2871 | 6.72±0.2871 | 0.00949 (0.00777-0.01157) | 0.000387* | 5.26±0.2871 | 0.02610 (0.02139-0.03184) | 0.000413* |
| *SLC4A4* | 4.455±0.0570 | 1.46±0.0570 | 0.36349 (0.34941-0.37814) | 0.000374* | 0±0.0570 | 1.00000 (0.96126-1.04031) | - |
| *SLC4A5* | 10.67±0.0500 | 7.675±0.0500 | 0.00489 (0.00473-0.00507) | 0.000424* | 6.215±0.0500 | 0.01346 (0.01300-0.01394) | 0.000522* |
| *SLC4A7* | 10.63±0.1432 | 7.635±0.1432 | 0.00503 (0.00456-0.00556) | 0.000416* | 6.175±0.1432 | 0.01384 (0.01253-0.01528) | 0.000498* |
| *SLC4A8* | 13.805±0.2041 | 10.81±0.2041 | 0.00056 (0.00048-0.00064) | 0.000423* | 9.35±0.2041 | 0.00153 (0.00133-0.00177) | 0.000516* |
| *SLC4A9* | 16.61±0.1836 | 13.615±0.1836 | 0.00008 (0.00007-0.00009) | 0.000424* | 12.155±0.1836 | 0.00022 (0.00019-0.00025) | 0.000525* |
| *SLC4A10* | 14.87±0.2247 | 11.875±0.2247 | 0.00027 (0.00023-0.00031) | 0.000423* | 10.415±0.2247 | 0.00073 (0.00063-0.00086) | 0.000518* |
| *SLC4A11* | 2.995±0.0515 | 0±0.0515 | 1.00000 (0.96495-1.03633) | - | -1.46±0.0515 | 2.75108 (2.65465-2.85102) | 0.000374* |

**Table 3.4. Relative normalized mRNA expression of *SLC4* gene family in human primary corneal endothelium.** The expression levels are described in relative to that of *SLC4A11* (in column 4) and *SLC4A4* (in column 7).

a. The $\Delta Ct$ value was determined by subtracting the average *GAPDH Ct* value from the average Ct value of *gene of interest (GOI)*. The standard deviation (SD) of the difference was calculated from the standard deviations of the Ct values of *GOI* and *GAPDH* by the formula $s = \sqrt{s1^2 + s2^2}$. The mean and SD values were obtained from a data pool of 8 reactions.

b. The calculation of $\Delta\Delta Ct$ involved subtraction by the $\Delta Ct$ calibrator (*Slc4a11* or *Slc4a4*) value. This is subtraction of an arbitrary constant, so the SD of $\Delta\Delta Ct$ is the same as the SD of the $\Delta Ct$ value.

c. The range given for nomalised expression relative to *SLC4A11* or *SLC4A4* was determined by evaluating the expression: $2^{-\Delta\Delta Ct}$ with $\Delta\Delta Ct + s$ and $\Delta\Delta Ct - s$, where s = SD of the $\Delta\Delta Ct$ value.

d. P values indicate the significance between the normalized expression of given gene and normalized expression of calibrator gene from five donor samples. *P < 0.05

### 3.2.8 Alteration in mRNA expression of *SLC4* genes during HCEC culture

As done earlier with MCECs, we also investigated the alterations in gene expression that occur in HCECs during cell culture. This was also carried out using multiple housekeeping genes for normalization (figure 3.12A, B). The normalization factor was obtained from the expression of three most stable reference genes (*GAPDH, ACTB, 18S rRNA*) across three samples (primary endothelium, passage 2 cells, passage 5 cells).

According to this analysis, in the cultured cells (passage 2 as well as 5), the expressions of the *SLC4A2, SLC4A4, SLC4A7, SLC4A8 and SLC4A9* were significantly up-regulated while those of *SLC4A1, SLC4A3, SLC4A5, SLC4A10* and *SLC4A11* were significantly down-regulated. The expression of most important gene in primary corneal endothelium *SLC4A11* was significantly reduced by approximately 40% ($0.59\pm0.04$ [p=0.0026]) in early passage and by approximately 70% ($0.31\pm0.01$ [p=0.00007]) in late passage. Meanwhile, the expression of another important gene *SLC4A4* showed a significant 3-fold increase ($3.74\pm0.16$ [p=0.0011]) in early passage and 4-fold increase ($4.04\pm0.5$ [p=0.0088]) in late passage.

**A**

| Gene name | Fold change in mRNA expression of HCECs (p2) | P value | Fold change in mRNA expression of HCECs (p5) | P value | Significance between p2 and p5 |
|---|---|---|---|---|---|
| *SLC4A1* | 0.0978±0.0619 | 0.00156* | 0.1357±0.0785 | 0.00274* | 0.05859 |
| *SLC4A2* | 4.4280±0.3554 | 0.00356* | 5.3270±0.0816 | 0.00012* | 0.02955* |
| *SLC4A3* | 0.2816±0.0096 | 0.00006* | 0.4858±0.0199 | 0.00050* | 0.00085* |
| *SLC4A4* | 3.7364±0.1599 | 0.00114* | 4.0371±0.4970 | 0.00881* | 0.26234 |
| *SLC4A5* | 0.3820±0.0146 | 0.00019* | 0.1434±0.0275 | 0.00034* | 0.00096* |
| *SLC4A7* | 11.4056±0.5397 | 0.00090* | 8.2726±0.6961 | 0.00304* | 0.00083* |
| *SLC4A8* | 14.0419±0.2772 | 0.00015* | 11.4982±0.1467 | 0.00007* | 0.00088* |
| *SLC4A9* | 3.8018±0.0990 | 0.00042* | 3.4303±0.1566 | 0.00138* | 0.00793* |
| *SLC4A10* | 0.0466±0.0187 | 0.00013* | 0.5484±0.0382 | 0.00237* | 0.00050* |
| *SLC4A11* | 0.5912±0.0362 | 0.00261* | 0.3096±0.0098 | 0.00007* | 0.00292* |
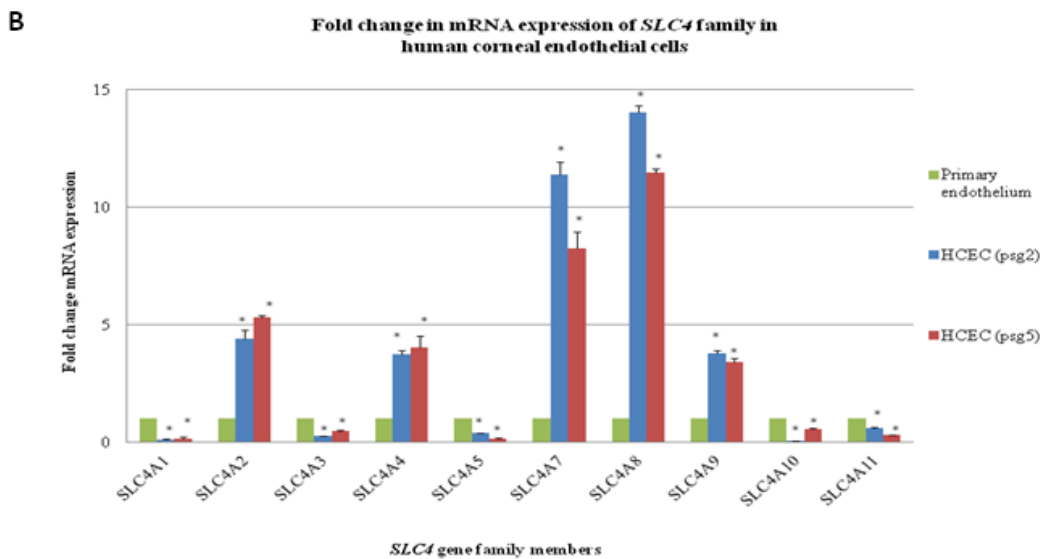


**Figure 3.13. Fold change in mRNA expressions of *SLC4* family genes in cultured human corneal endothelial cells (in passage 2 and 5).** A. Data are described as the relative fold change in expression of cultured cells over primary corneal endothelium. Values shown are the mean±SD of two independent experiments. The P values in last column indicate the significance between p2 and p5 change values from two independent experiments. *P < 0.05. B. Data are shown in graph.

# IV. DISCUSSION

## 4.1 Discussion of results

### 4.1.1 Characterization of mRNA expression levels of *SLC4* family in corneal endothelium

The *SLC4A* family is comprised of integral membrane proteins that mediate chloride/bicarbonate exchange or sodium-coupled bicarbonate co-transport across plasma membrane. *SLC4A11* is the most divergent member of the family and was described as an electrogenic $Na^+$-coupled borate co-transporter and as an electrogenic $Na^+/OH^-$ co-transporter when borate is absent (Park M *et al*, 2004). Our investigation discovered that all members of the *SLC4* bicarbonate transporter family are expressed in both MCECs and HCECs but some more than others can serve as potential candidate genes for corneal endothelial diseases. Previous studies have investigated their expression in other tissues (Gottsch JD *et. al*., 2003, Damkier HH *et. al*., 2007), but not in ocular tissues. Amongst the family, the *SLC4A11* showed the highest expression in both mouse and human corneal endothelium, therefore it is highly possible that it plays the most pivotal role in transporting solutes in the corneal endothelium although we did not establish functional correlation with its expression. The function of *SLC4A11* in the corneal endothelium is unknown so far. Nevertheless, corneal endothelial function is highly dependent on the presence of bicarbonate, bicarbonate transport, and intracellular pH regulation (Bonanno JA, 2012), suggesting that any putative bicarbonate transport or $Na^+/OH^-$ cotransport activity by *SLC4A11* is important.

It has been well known that homozygous mutations in the *SLC4A11* cause two early-onset corneal dystrophies: congenital hereditary endothelial dystrophy (CHED) (Vithana EN *et. al*., 2006, Aldahmesh MA *et. al.,* 2009, Shah SS *et. al.,* 2008, Jiao X et. *al.,* 2007) and Harboyan syndrome (Desir J *et. al*., 2007, 2008) whereas heterozygous mutations in *SLC4A11* are

responsible for familial cases of late-onset FCD. (Vithana EN *et. al.,* 2007, 2008, Riazuddin SA *et. al.,*2010). Recent study on *Slc4a11* mutant mice revealed severe morphological alterations in endothelial cell layer, such as thickening and malfunctions in ion homeostasis such as a dramatic increase in sodium and chloride concentrations in the corneal stroma. (Gröger N *et. al.,* 2010)

Our study found that the *SLC4A4, SLC4A2* and *SLC4A7* genes were expressed significantly higher than other members of the family in the corneal endothelium and hence they can become the important foci of future genetic studies for corneal endothelial diseases. Interestingly, previous studies have identified homozygous mutations in the kNBC1 gene (*SLC4A4*) in patients with permanent isolated proximal renal tubular acidosis and bilateral glaucoma. (Igarashi T *et. al.*, 2003, Dinour D *et. al.,* 2004, Inatomi J *et. al.,* 2004, Demirci FY *et. al.,* 2006). The importance of *SLC4A7* in vision was also highlighted by the finding that the *Slc4a7*$^{-/-}$ mice develop blindness and auditory impairment because of degeneration of sensory receptors in the eye and inner ear (Bok D *et. al.,* 2003). AE2 (*SLC4A2*) has been found to be expressed in fresh human, rabbit and bovine corneal endothelium (Sun XC *et al,* 2001) but there is still little evidence for its association with corneal diseases so far.

The *SLC4* family, except *SLC4A11*, can be functionally divided into three main groups (Fig. 1.3), namely anion exchangers (AEs), Na bicarbonate cotransporters (NBCs), sodium-driven chloride/bicarbonate exchangers (NDCBE). We found that the expression of genes encoding the two NBCs (*SLC4A4* and *SLC4A7*) to be next highly expressed after *SLC4A11* indicating that the NBCs are the main bicarbonate transporters in corneal endothelium.

|  | Primary | Secondary |
|---|---|---|
| Na bicarbonate cotransporters (NBCs) | NBCe1 (*SLC4A4)* | NBCn1 (*SLC4A7)* |
| anion exchangers (AEs) | AE2 (*SLC4A2*) | AE3 (*SLC4A3*) |
| Na-driven $Cl^-/HCO_3^-$ exchangers (NDCBEs) | AE1 (*SLC4A1)* | NDCBE *(SLC4A8)* |

**Table 4.1. Proposed hierarchy for *SLC4* family members within a given functional group categorized thus according to their relative levels of expression in human corneal endothelium**

If one was to consider a group at a time, our data indicate that for NBCs, NBCe1 (*SLC4A4)* is the primary member in the corneal endothelium and that NBCn1 (*SLC4A7)* is secondary. Similarly for AEs, AE2 (*SLC4A2*) appears to be primary to AE3 (*SLC4A3*). In the case of NDCBE family of proteins, AE1 (*SLC4A1)* is primary to NDCBE *(SLC4A8)*. The redundancy seen with this family of genes is perhaps indicative of the important role that these genes play in ion transport within the corneal endothelium. It will also be interesting to explore the compensatory role played by the secondary gene in the event of a defect, i.e. mutation, involving the primary member of each class.

Another notable factor about the *SLC4* family is the expression of different splice variants and their tissue distribution. The pNBC1 (pancreatic variant) is expressed in cornea, conjunctiva, lens, ciliary body, and retina, whereas the expression of kNBC1 (kidney variant) is restricted to the conjunctiva in rat eye. (Bok D *et. al.,* 2001) In human eye, the long isoform of the sodium bicarbonate cotransporter (pNBC-1) is expressed on the basolateral side of fresh human corneal endothelium (Sun XC *et. al.,* 2003). In our study, we utilized primers that recognize the common 'region' amongst the splice variants for a given gene rather than focusing

on a particular splice variant. Therefore we are not able to draw conclusions about the expressions of a particular splice form.

Our investigation established, on a small scale, expression profiles of all members of the *SLC4* family in both MCECs and HCECs using real-time qPCR. Although there are limitations on the number of targeted genes that can be analyzed at a time, real-time qPCR can provide the simultaneous measurement of gene expression in many different samples (Schena M *et. al*., 1995, Fink L *et. al.,* 1998, Higuchi R *et. al.*, 2003). Nowadays, microarray analysis is becoming popular as a relatively rapid technique that allows parallel analysis of thousands of genes in a number of tissues (Lipshutz RJ *et. al.*, 1999, Duggan DJ *et. al.,* 1999). The expression of approximately 1200 genes have been identified using duplicate microarrays and a preliminary database of human corneal gene expression has been compiled (Jun AS *et. al.,* 2001). However, the use of microarrays is limited by the finite number of oligonucleotide sequences localized on a chip and are not able to identify the expression of novel genes, unlike in the case of real time qPCR.

**4.1.2 Comparison of mouse and human gene expression pattern in corneal endothelium**

Often, rodents serve as a convenient model in many acid-base as well as genetic studies. Although studies on human gene expression of some acid-base transporters have been reported (Abuladze N *et. al.,* 1998, Marino CR *et. al.,* 1999, Amlal H *et. al.,* 1999, Nishimura M *et al* 2005, 2008),  few studies have compared the human expression pattern of these transporters with that of rodents. One study concluded that some selected human tissues display distinct expression patterns of $HCO_3^-$ transporters, which closely resemble that of rodent tissues

(Damkier HH *et. al.,* 2007). Another study found, in mice, a similar pattern of corneal endothelial cell loss with aging and a comparable process of Descemet's thickening over time (Joyce NC, 2003, Jun AS *et al* 2006). According to our study, in mouse corneal endothelium, the mRNA expression levels of *SLC*4 family in descending order of abundance is *Slc4a11> Slc4a2> Slc4a4> Slc4a7> Slc4a3> Slc4a10> Slc4a5> Slc4a9> Slc4a8> Slc4a1* whilst in human corneal endothelium, the order is *SLC4A11> SLC4A4> SLC4A2> SLC4A3> SLC4A7> SLC4A5> SLC4A1> SLC4A8> SLC4A10> SLC4A9*, notably showing much similarity between mouse and human gene expression for this gene family. Interestingly, the complete resemblance is seen when they are divided into two main groups: high expression group with *SLC4A11, SLC4A2, SLC4A4, SLC4A7, SLC4A3* and low expression group with *SLC4A10, SLC4A5, SLC4A9, SLC4A8, SLC4A1*. This suggests similar evolutionary forces at play in the regulation of expression of these genes in these two mammalian species as well as possible conservation of the functional role played by each member in solute transport in the corneal endothelium through evolution.

### 4.1.3 Alteration in gene expression during corneal endothelial cell culture

In our investigation, we observed that during MCEC culture, there was a transformation to a more fibroblastic-like phenotype in late passage 7 while in the case of HCECs, the cells could not grow well beyond passage 5. Furthermore, our qRT-PCR analyses also indicated marked changes in expression pattern of *SLC4* transporter genes in both cultured MCECs and HCECs. One study stated that the cultured cells were not a good model for corneal endothelial transport studies since it was found thatAE2 was absent in cultured cells which is otherwise present in corneal endothelium . (Bonanno JA 2003) There were also two contradictory reports,

with one indicating activity of the $Na^+$-$K^+$-$2Cl^-$ cotransporter in cultured bovine corneal endothelial cells (Diecke F *et. al.,* 1998)  while the other (Riley M *et. al.,* 1997) being unable to show any cotransporter activity in the intact rabbit corneal preparations. Although culturing has some convenience and practical advantages over the native tissue, caution must be exercised when extending the results from the cultured cells to the native tissue. (Bonanno JA *et. al.,* 1998) It can be postulated that the changed environmental conditions of culture media for the cells, for example high salt content, could be the key factor for altered expression seen for some genes, especially those of solute transporters, in  cultured cells.

In this study, we found the *SLC4A11* gene to be the most highly expressed member of the *SLC4* gene family in the human cornea endothelium. Moreover, during cell culture *SLC4A11* gene expression was reduced by more than 70% in late passages. The morphology of endothelial cells was also less 'endothelial like' in late passages. A recent study showed that *SLC4A11* gene was important for corneal endothelial cell survival and viability (Liu J *et al*, 2012). In this study, the authors used small hairpin RNAs (shRNAs) against *SLC4A11* in a human corneal endothelial cell line (HCECs) to investigate the effects of *SLC4A11* gene depletion. *SLC4A11* knockdown was shown to suppress HCECs' growth and reduce cell viability. This was associated with increased apoptosis in *SLC4A11*-silenced cells. The loss of 'endothelial like' state of cells and reduced expression of *SLC4A11* gene seen in our current study also makes it tempting to speculate if the maintenance of endothelial cellular phenotype is one of the roles of *SLC4A11* gene as well as the maintenance of cell viability and survival.

Another possible explanation for the observed gene expressional alterations is the so-called Epithelial/endothelial-to-mesenchymal transition (E/EnMT) during which endothelial cells lose endothelial markers and obtain mesenchymal markers, as suggested by the elevated level of

*Col1A1* in late passage cells. In vitro studies have shown that endothelial cells can undergo EMT, a process which is speculated to depend on transforming growth factor TGFß1 (Leask A et al, 2004). Being the major cytokine in the anterior chamber of the eye (Melles GR 2006), high TGFß levels can lead to myofibroblast formation in the corneal endothelial layer (Reneker LW *et. al.,* 2010). The drastically altered expression levels of the main genes *SLC4A11* and *SLC4A4*, seen in late endothelial cell culture passages co-incident with altered cellular morphology indicate that further study should be undertaken to explore the possible link between *SLC4* gene expression and EMT.

## 4.2. Clinical relevance of the study

Several *SLC4* bicarbonate transporter genes have been linked to a wide range of diseases (Table 1.3) including some eye disorders. The *SLC4* gene family members expressed in the cornea, which are not yet identified as being involved in any corneal diseases, are potential candidate genes to be interrogated in corneal endothelial diseases. Identification and characterization of more genes causative of corneal endothelial diseases would further our understanding of pathologic mechanisms underlying this group of disorders and may lead to novel ways to treat these conditions. In this study the expression profiles of *SLC4* family members were characterised in both the mouse and human corneal endothelium. Understanding the hierarchy of expression of bicarbonate transporters within the same functional group has also opened up the interesting possibility of compensatory therapeutics. For instance, if mutations in *SLC4A4* lead to functional loss of the protein (NBCe1), one can explore whether up regulating the expression of its related secondary member of same functional group, NBCn1, encoded by

*SLC4A7,* can have possible therapeutic benefit. This would of course require the identification of pharmaceutical drugs that can specifically up regulate these *SLC4* transporter genes/proteins.

Some solute carriers are also responsible for drug transport in various tissues and they may be key determinants of the pharmacokinetic characteristics of drugs (Mizuno N *et. al.,* 2003, 2002, Katsura T *et. al.,* 2003). Similarly, *SLC4A* bicarbonate transporters may become promising candidates for drug delivery (Nishimura M *et. al.,* 2008).

Corneal blindness, a second leading cause of visual blindness (Whitcher JP *et al*, 2001), is caused by corneal endothelial dysfunction (Carlson KH *et al*, 1988) and restoration of vision is possible only by corneal transplantation (Engelmann K *et al*, 2004). However, shortage of transplant-grade donor corneas is a current pressing matter worldwide (McColgan K, 2009) and hence the development of tissue-engineered constructs is an urgent requirement. Understanding the gene expression profile of the corneal endothelium, with regard to important genes like *SLC4A11*, will lead to the development of high quality tissue-engineered constructs with more expressional resemblance to native tissue. Such constructs will eventually be able to replace donor corneas in transplantation.

## 4.3. Technical difficulties and limitations of current study

The use of mice in corneal research is technically challenging due to the small size of the murine eye globe and the fragility of the cornea. Stripping of Descemet's membrane from a cornea, especially from the mouse cornea, under a dissecting microscope was a very time-consuming and tedious work. Extreme care also had to be taken not to contaminate with the stromal layers and fibroblast cells.

The high cost of human corneal samples also posed no room for errors throughout the entire experiment, from Descement's membrane stripping to real time qPCR. Much practice had to be exercised using cadaveric corneal rims before performing actual tests with ordered corneas. Due to the small size of the specimen, which is merely a single layer of endothelial cells, RNA yield was very low as expected; therefore a number of corneal endothelia from the same litter of mice had to be pooled to obtain sufficient quantities of RNA. The quality of primers also plays a significant role in the performance of qRT-PCR. The primer pair for each gene was therefore carefully designed to be sensitive and specific for the gene of interest. If any non-specificity was observed in empirical experiments, primers were redesigned until optimal results were obtained.

The main limiting factor in this study is that gene expression levels were only tested at the RNA level and not at the protein level. Ideally, the expression levels should have been confirmed by using specific antibodies to the various *SLC4* genes in western analysis. The small number of human corneal samples (n=5) was another limitation in this study. Thirdly, the use of a few housekeeping genes for normalization is also not ideal although we applied three stable housekeeping genes out of four, instead of traditional use of a single gene. Only four HKGs were chosen due to the small yield of RNA and cDNA. With the gradual realization that the expression of traditionally used HKGs like *ACTB* and *GAPDH* are not stable in all tissues/cells or under all conditions (Thellin O *et. al.,* 1999, Barber RD *et. al.,* 2005, Selvey S *et. al.*, 2001, Suzuki T *et. al.,* 2000, Glare EM *et. al.,* 2002), the use of a combination of multiple stable HKGs for proper normalization is advocated. A panel of at least eight or ten HKGs should therefore be ideally set up to select the most stable HKGs in tissue of interest under desired conditions.

**4.4. Possible future work/experiments**

➢ Further studies, involving larger number of both human samples and HKGs, can be carried out to validate this pilot project.

➢ The protein expression and distribution of *SLC4* family members in human corneal endothelium can be confirmed by Western and immunohistochemical analyses.

➢ The expression pattern of all splice variants for each *SLC4* transporter in CECs can be studied to gain more knowledge on different splice variants.

➢ Mutational screening of this study's candidate genes can be performed on a panel of FECD patients' DNA samples.

➢ Specific endothelial cell markers and mesenchymal cell markers can be applied on cultured corneal endothelial cells to gain more insight into endothelial mesenchymal transition.

## V. CONCLUSION

To the best of our knowledge, this is the first ever study to investigate the expression levels of the entire *SLC4* bicarbonate transporter family in corneal endothelial cells of both human and mouse. We could establish expression profiles for each member in primary corneal endothelium of human and mouse. We could also quantify the expressional alterations that occur for *SLC4* genes due to cell culturing procedure involving both early and late subcultures. Interestingly, the two members, *SLC4A11* and *SLC4A4*, already known for their involvement in corneal endothelial dystrophies, were found to be the most highly expressed in corneal endothelium. Thus we speculate that the other two highly expressed genes, *SLC4A2* and *SLC4A7* are worthy of being considered next as potential candidate genes for corneal endothelial diseases. The drastically altered expression levels of the main genes *SLC4A11* and *SLC4A4*, seen in late endothelial cell culture passages co-incident with altered cellular morphology indicate that further study should be undertaken to explore the possible link between *SLC4* gene expression and EMT.

## Presentation

Part of this study "Investigation of the relative expression levels of *SLC4* bicarbonate transporter family members in mouse corneal endothelial cells (MCECs)" was selected for poster presentation at the Inaugural SingHealth Duke-NUS Scientific Congress, held at Concourse, Level 3 Suntec International Convention and Exhibition Centre on 15 – 16 October 2010.

# REFERENCES

Aalkjær C, Frische S, Leipziger J, Nielsen S and Praetorius J. Sodium coupled bicarbonate transporters in the kidney, an update. Acta Physiol Scand 2004, 181, 505–512

Abuladze N, Lee I, Newman D, Hwang J, Boorer K, Pushkin A, Kurtz I. Molecular cloning, chromosomal localization, tissue distribution, and functional expression of the human pancreatic sodium bicarbonate cotransporter. *J Biol Chem* 273: 17689–17695, 1998.

Aldahmesh MA, Khan AO, Meyer BF, Alkuraya FS. Mutational spectrum of SLC4A11 in autosomal recessive CHED in Saudi Arabia. Invest Ophthalmol Vis Sci. 2009 Sep;50(9):4142-5.

Aldave AJ, Yellore VS, Bourla N, Momi RS, Khan MA, Salem AK, Rayner SA, Glasgow BJ, Kurtz I: Autosomal recessive CHED associated with novel compound heterozygous mutations in SLC4A11. *Cornea* 2007, 26:896-900.

Alper SL. Molecular physiology of SLC4 anion exchangers. *Exp Physiol* 91.1 pp 153–161, 2005.

Amlal H, Burnham CE, Soleimani M. Characterization of Na_/HCO3– cotransporter isoform NBC-3. *Am J Physiol Renal Physiol* 276: F903–F913, 1999.

Andersen C.L., Jensen J.L., Orntoft T.F. Normalization of real time quantitative reverse transcription-PCR data: a model based variance estimation approach to identify genes suited for normalization, applied to bladder and colon cancer data sets, Cancer Res. 64 (2004) 5245–5250.

Bahn CF, Falls HF, Varley GA, Meyer RF, Edelhauser HF, Bourne WM. Classification of corneal endothelial disorders based on neural crest origin. Ophthalmology. 1984; 91(6):558-63.

Baratz KH, Tosakulwong N, Ryu E, Brown WL, Branham K, Chen W, Tran KD, Schmid-Kubista KE, Heckenlively JR, Swaroop A, Abecasis G, Bailey KR, Edwards AO. E2-2 protein and Fuchs's corneal dystrophy.N Engl J Med. 2010 Sep 9;363(11):1016-24.

Barber RD, Harmer DW, Coleman RA, Clark BJ. GAPDH as a housekeeping gene: analysis of GAPDH mRNA expression in a panel of 72 human tissues. Physiol Genomics 2005; 21:389-95.

Barrett KE, Barman SM, Boitano S, Brooks H, "Chapter 36. Gas Transport & pH in the Lung" (Chapter). Barrett KE, Barman SM, Boitano S, Brooks H: Ganong's Review of Medical Physiology, 23e:

Barrett KE, Barman SM, Boitano S, Brooks H, "Chapter 40. Acidification of the Urine & Bicarbonate Excretion" (Chapter). Barrett KE, Barman SM, Boitano S, Brooks H: Ganong's Review of Medical Physiology, 23e:

Bender David A, Mayes Peter A, "Chapter 16. Overview of Metabolism & the Provision of Metabolic Fuels" (Chapter). Murray RK, Bender DA, Botham KM, Kennelly PJ, Rodwell VW, Weil PA: Harper's Illustrated Biochemistry, 28e:

Bok D, Galbraith G, Lopez I, Woodruff M, Nusinowitz S, BeltrandelRio H, Huang W, Zhao S, Geske R, Montgomery C, Van Sligtenhorst I, Friddle C, Platt K, Sparks MJ, Pushkin A, Abuladze N, Ishiyama A, Dukkipati R, Liu W, Kurtz I. Blindness and auditory impairment caused by loss of the sodium bicarbonate cotransporter NBC3. Nat Genet. 2003 Jul;34(3):313-9.

Bok D, Schibler MJ, Pushkin A, Sassani P, Abuladze N, Naser Z, and Kurtz I. Immunolocalization of electrogenic sodium-bicarbonate cotransporters pNBC1 and kNBC1 in the rat eye. *Am J Physiol Renal Physiol* 281: F920–F935, 2001.

Bonanno JA, Yi G, Kang XJ, Srinivas SP. Reevaluation of Cl-/HCO3- exchange in cultured bovine corneal endothelial cells. Invest Ophthalmol Vis Sci. 1998 Dec;39(13):2713-22.

Bonanno JA. Identity and regulation of ion transport mechanisms in the corneal endothelium. Prog Retin Eye Res. 2003 Jan;22(1):69-94.

Bonnano JA and Giasson C. Intracellular pH regulation in fresh and cultured bovine corneal endothelium. II. Na1:HCO3 2 cotransport and Cl2/HCO3 2 exchange. *Invest Ophthalmol Vis Sci* 33: 3069–3079, 1992

Bonanno, J.A. (2012) Molecular mechanisms underlying the corneal endothelial pump, *Experimental Eye Research 95*, 2-7.

Bourne WM, Nelson LR, Hodge DO (1997) Central corneal endothelial cell changes over a ten-year period. Invest Ophthalmol Vis Sci 38: 779–782.

Bowes Rickman C, Ebright JN, Zavodni ZJ, Yu L, Wang T, Daiger SP, Wistow G, Boon K, Hauser MA (2006) DeWning the human macula transcriptome and candidate retinal disease genes using Eye-SAGE. Invest Ophthalmol Vis Sci 47(6):2305–2316

Bustin SA: Absolute quantification of mRNA using real-time reverse transcription polymerase chain reaction assays. *J Mol Endocrinol* 2000, 25:169-193.

K. H. Carlson, W. M. Bourne, J. W. McLaren, and R. F.Brubaker, "Variations in human corneal endothelial cell morphology and permeability to fluorescein with age," *Experimental Eye Research*, vol. 47, no. 1, pp. 27–41, 1988.

Carlson KH, Bourne WM, McLaren JW, et al. Variations in human corneal endothelial cell morphology and permeability to fluorescein with age. *Exp Eye Res* 1988; 47: 27.

Casey JR. Why bicarbonate? Biochem. Cell Biol. **84**: 930–939 (2006)

Cicinnati V.R., Shen Q., Sotiropoulos G.C., Radtke A., Gerken G., Beckebaum S., Validation of putative reference genes for gene expression studies in human hepatocellular carcinoma using real-time quantitative RT-PCR, BMC Cancer 8 (2008) 350–355.

Cordat E, Casey JR. Bicarbonate transport in cell physiology. Biochem.J. (2009) 417, 423-439.

Damkier HH, Nielsen S, Praetorius J. Molecular expression of SLC4-derived Na+-dependent anion transporters in selected human tissues. Am J Physiol Regul Integr Comp Physiol. 2007 Nov;293(5):R2136-46.

Demirci FY, Chang MH, Mah TS, Romero MF, Gorin MB. Proximal renal tubular acidosis and ocular pathology: a novel missense mutation in the gene (SLC4A4) for sodium bicarbonate cotransporter protein (NBCe1). Mol Vis. 2006 Apr 10;12:324-30.

Desir J, Abramowicz M: Congenital hereditary endothelial dystrophy with progressive sensorineural deafness (Harboyan syndrome). *Orphanet J Rare Dis* 2008, 3:28

Desir J, Moya G, Reish O, Van Regemorter N, Deconinck H, David KL, Meire FM, Abramowicz MJ. Borate transporter SLC4A11 mutations cause both Harboyan syndrome and non-syndromic corneal endothelial dystrophy. J Med Genet. 2007 May;44(5):322-6.

Diecke F, Zhu Z, Kang F, Kang K, Fischbarg J. Sodium, potassium, two chloride cotransport in corneal endothelium: characterization and possible role in volume regulation and fluid transport. *Invest Ophthalmol Vis Sci.* 1998;39:104-110.

Dinour D, Chang MH, Satoh J, Smith BL, Angle N, Knecht A, Serban I, Holtzman EJ, Romero MF. A novel missense mutation in the sodium bicarbonate cotransporter (NBCe1/SLC4A4) causes proximal tubular acidosis and glaucoma through ion transport defects. J Biol Chem. 2004 Dec 10;279(50):52238-46.

Duggan DJ, Bittner M, Chen Y, Meltzer P, Trent JM. Expression profiling using cDNA microarrays. *Nat Genet.* 1999;21(suppl):10-14.

Engelmann K, Bohnke M, Friedl P. Isolation and long-term cultivation of human corneal endothelial cells. Invest Ophthalmol Vis Sci 1988; 29:1656-62.

Engelmann K, Bednarz J, Valtink M (2004) Prospects for endothelial transplantation. Exp Eye Res 78: 573–578.

Ensembl genome browser. http://www.ensembl.org/index.html

Fink L, Seeger W, Ermert L, Hanze J, Stahl U, Grimminger F, Kummer W, Bohle RM: Real-time quantitative RT-PCR after laser-assisted cell picking. *Nat Med* 1998, 4:1329-1333.

Fishchberg J, Morice DM. An update on corneal hydration control. 2003

Fischbarg J. On the mechanism of fluid transport across corneal endothelium and epithelia in general. Journal of experimental zoology 300a:30–40 (2003)

Gawenis, L. R., Ledoussal, C., Judd, L. M., Prasad, V., Alper, S. L., Stuart-Tilley, A., Woo, A. L., Grisham, C., Sanford, L. P., Doetschman, T. et al. (2004) Mice with a targeted disruption of the AE2 Cl−/HCO3− exchanger are achlorhydric. J. Biol. Chem. 279, 30531–30539

GeNorm website. http://medgen.ugent.be/genorm/

Geroski DH, Matsuda M, Yee RW, Edelhauser HF (1985) Pump function of the human corneal endothelium. Effects of age and cornea guttata. Ophthalmology 92: 759–763.

Gibson, U. E. M., et al. (1996). "A novel method for real time quantitative RT-PCR." Genome Research 6(10): 995-1001.

Glare EM, Divjak M, Bailey MJ, Walters EH. beta-Actin and GAPDH housekeeping gene expression in asthmatic airways is variable and not suitable for normalising mRNA levels. Thorax 2002; 57:765-70.

Gospodarowicz D, Mescher AL, Birdwell CR. Stimulation of corneal endothelial cell proliferations in vitro by fibroblast and epidermal growth factors. Exp Eye Res 1977; 25:75-89.

Gottsch JD, Seitzman GD, Margulies EH, Bowers AL, Michels AJ, Saha S, Jun AS, Stark WJ, Liu SH. Gene expression in donor corneal endothelium. Arch Ophthalmol. 2003 Feb;121(2):252-8.

Gröger N, Fröhlich H, Maier H, Olbrich A, Kostin S, Braun T, Boettger T. SLC4A11 prevents osmotic imbalance leading to corneal endothelial dystrophy, deafness, and polyuria. J Biol Chem. 2010 May 7;285(19):14467-74.

Gutierrez L, Mauriat M, Pelloux J, Bellini C, Wuytswinkel VO, Towards a systematic validation of references in real-time RT-PCR, Plant Cell 20 (2008) 1734–1735.

Heid CA, Stevens J, Livak KJ, Williams PM: Real time quantitative PCR. *Genome Res* 1996, 6:986-994.

Higuchi R, Fockler C, Dollinger G, Watson R: Kinetic PCR analysis: real-time monitoring of DNA amplification reactions. *Biotechnology* 1993, 11:1026-1030.

Hod, Y. (1992). "A simplified ribonuclease protection assay." Biotechniques 13(6): 852-4.

Horita, S., Yamada, H., Inatomi, J., Moriyama, N., Sekine, T., Igarashi, T., Endo, Y., Dasouki, M., Ekim, M., Al-Gazali, L. et al. (2005) Functional analysis of NBC1 mutants associated with proximal renal tubular acidosis and ocular abnormalities. J. Am.Soc. Nephrol. 16, 2270–2278

Huggett J., Dheda K., Bustin S., Zumla A., Real-time RT-PCR normalization: strategies and considerations, Genes Immun. 6 (2005) 279–284.

Igarashi T, Inatomi J, Sekine T, Cha SH, Kanai Y, Kunimi M, Tsukamoto K, Satoh H, Shimadzu M, Tozawa F, Mori T, Shiobara M, Seki G, Endou H. Mutations in SLC4A4 cause permanent isolated proximal renal tubular acidosis with ocular abnormalities. Nat Genet. 1999 Nov;23(3):264-6.

Inatomi J, Horita S, Braverman N, Sekine T, Yamada H, Suzuki Y, Kawahara K, Moriyama N, Kudo A, Kawakami H, Shimadzu M, Endou H, Fujita T, Seki G, Igarashi T. Mutational and functional analysis of SLC4A4 in a patient with proximal renal tubular acidosis. Pflugers Arch. 2004 Jul;448(4):438-44.

Jentsch TJ, Keller SK, Koch M, and Wiederholt M. Evidence for coupled transport of bicarbonate and sodium in cultured bovine corneal endothelial cells. *J Membr Biol* 81: 189– 204, 1984.

Jiao X, Sultana A, Garg P, Ramamurthy B, Vemuganti GK, Gangopadhyay N, Hejtmancik JF, Kannabiran C: Autosomal recessive corneal endothelial dystrophy (CHED2) is associated with mutations in SLC4A11. *J Med Genet* 2007, 44:64-68.

Johnson LR, Jacobson ED, Christensen J, Alpers D, and Walsh JH. New York: Raven, 1994, p.1285–1309.

Joo CK, Pepose JS and Fleming TP. *In vitro* propagation of primary and extended life span murine corneal endothelial cells. Invest Ophthalmol Vis Sci. 1994;35:3952–7.

Joyce NC, Navon SE, Roy S, Zieske JD. Expression of cell cycle associated proteins in human and rabbit corneal endothelium in situ. Invest Ophthalmol Vis Sci. 1996;37:1566–1575.

Joyce NC (2003) Proliferative capacity of the corneal endothelium. Prog Retin Eye Res 22: 359– 389.

Jun AS, Liu SH, Koo EH, Do DV, Stark WJ, Gottsch JD. Microarray analysis of gene expression in human donor corneas. Arch Ophthalmol. 2001 Nov;119(11):1629-34.

Jun AS, Chakravarti S, Edelhauser HF, Kimos M. Aging changes of mouse corneal endothelium and Descemet's membrane. Exp Eye Res. 2006 Oct;83(4):890-6.

Kaji Y, Amano S, Usui T, Oshika T, Yamashiro K, Ishida S, Suzuki K, Tanaka S, Adamis AP, Nagai R and Horiuchi S. Expression and function of receptors for advanced glycation end products in bovine corneal endothelial cells. Invest Ophthalmol Vis Sci. 2003;44:521–528.

Katsura T, Inui K. Intestinal absorption of drugs mediated by drug transporters: mechanisms and regulation. Drug Metab Pharmacokinet. 2003;18(1):1-15.

Klintworth, G.K. (2009). Corneal dystrophies. Orphanet J. Rare Dis. 4, 7.

Koeppen BM The kidney and acid base regulation. *Adv Physiol Educ* 33: 275–281, 2009.

Leask A, Abraham DJ (2004) TGF-beta signaling and the fibrotic response. FASEB J 18(7):816– 827

Lehninger, A.L. 1982. Principles of biochemistry. Worth Publishers, Inc., New York.

Levy, S.G., Moss, J., Sawada, H., Dopping-Hepenstal, P.J. and McCartney, A.C. The composition of wide spaced collagen in normal and diseased Descemet's membrane. Curr. Eye. Res.1996; 15, 45-52.

Li Y.L., Ye F., Hu Y.. Lu, W.G, Xie X., Identification of suitable reference genes for gene expression studies of human serous ovarian cancer by real-time polymerase chain reaction, Anal. Biochem. 394 (2009) 110–116.

Lipshutz RJ, Fodor SP, Gingeras TR, Lockhart DJ. High density synthetic oligonucleotide arrays. *Nat Genet.* 1999;21(suppl):20-24.

Liu J, Seet LF, Koh LW, Venkatraman A, Venkataraman D, Mohan RR, Praetorius J, Bonanno JA, Aung T, Vithana EN. Depletion of SLC4A11 causes cell death by apoptosis in an immortalized human corneal endothelial cell line. Invest Ophthalmol Vis Sci, 2012 Jun, 53(7):3270-9.

Livak KJ, Schmittgen TD: Analysis of relative gene expression data using real-time quantitative PCR and the 2-ΔΔCT method. *Methods* 2001, 25:402-408.

MacCallum DK, Lillie JH, Scaletta LJ, Occhino JC, Frederick WG, Ledbetter SR. Bovine corneal endothelium in vitro. Elaboration and organization and of a basement membrane. Exp Cell Res 1982; 139:1-13.

Marino CR, Jeanes V, Boron WF, Schmitt BM. Expression and distribution of the Na(+)-HCO(-)(3) cotransporter in human pancreas. *Am J Physiol Gastrointest Liver Physiol* 277: G487–G494, 1999.

Maurice DM. The permeability to sodium ions of the living rabbit's cornea. J. Physiol. (I95I) II2, 367-39I

McCartney, A.C. and Kirkness, C.M. Comparison between posterior polymorphous dystrophy and congenital hereditary endothelial dystrophy of the cornea. Eye.1998; 2, 63-70.

McColgan K, "Corneal transplant surgery," *Journal of perioperative practice*, vol. 19, no. 2, pp. 51–54, 2009.

Melles GR (2006) Posterior lamellar keratoplasty: DLEK to DSEK to DMEK. Cornea 25(8):879–881

Melton, D.A. (1984). "Efficient in vitro synthesis of biologically active RNA and RNA hybridization probes from plasmids containing a bacteriophage SP6 promoter." Nucleic Acids Res 12(18): 7035-56.

Mescher AL, "Chapter 23. The Eye and Ear: Special Sense Organs" (Chapter). Mescher AL: Junqueira's Basic Histology: Text & Atlas, 12e:

Mizuno N, Niwa T, Yotsumoto Y, Sugiyama Y. Impact of drug transporter studies on drug discovery and development. Pharmacol Rev. 2003 Sep;55(3):425-61.

Mizuno N, Sugiyama Y. Drug transporters: their role and importance in the selection and development of new drugs. Drug Metab Pharmacokinet. 2002;17(2):93-108.

Nayak SK, Samples JR, Deg JK, Binder PS. Growth characteristics of primate (baboon) corneal endothelium in vitro. Invest Ophthalmol Vis Sci 1986; 27:607-11.

Nishimura M, Naito S. Tissue-specific mRNA expression profiles of human solute carrier transporter superfamilies. Drug Metab Pharmacokinet. 2008;23(1):22-44.

Nishimura M, Naito S. Tissue-specific mRNA expression profiles of human ATP-binding cassette and solute carrier transporter superfamilies. Drug Metab Pharmacokinet. 2005 Dec;20(6):452-77.

Nolan T, Hands RE, Bustin SA, Quantification of mRNA using real-time PCR, Nat. Protoc. 1 (2006) 1559–1582.

Park, M., Li, Q., Shcheynikov, N., Zeng, W., and Muallem, S. (2004) NaBC1 is a ubiquitous electrogenic Na$^+$-coupled borate transporter essential for cellular boron homeostasis and cell growth and proliferation, *Molecular Cell 16*, 331-341

Parker, R.M. and N. M. Barnes (1999). "mRNA: detection by in Situ and northern hybridization." Methods Mol Biol 106: 247-83.

Peh GSL, R. W. Beuerman, A. Colman, D. T. Tan, and J. S.Mehta, "Human corneal endothelial cell expansion for corneal endothelium transplantation: an overview," *Transplantation*, vol. 91, no. 8, pp. 811–819, 2011.

Peh GS, Toh KP, Wu FY, Tan DT, Mehta JS. Cultivation of human corneal endothelial cells isolated from paired donor corneas. PLoS One. 2011;6(12):e28310.

Pfaffl MW: A new mathematical model for relative quantification in real-time RT-PCR. *Nucl Acids Res* 2001, 29:2002-2007.

Pistsov MY, Sadovnikova EY, Danilov SM. Human corneal endothelial cells: isolation, characterization and long-term cultivation. Exp Eye Res 1988; 47:403-14.

Primer 3 primers design. Rozen S and Skaletsky H, 2000. http://frodo.wi.mit.edu/primer3/

Pushkin A, Kurtz I. SLC4 base (HCO3-, CO32-) transporters: classification, function, structure, genetic diseases and knockout models. Am J Physiol Renal Physiol 290: F580-F599. 2006

Reneker LW, Bloch A, Xie L, Overbeek PA, Ash JD. Induction of corneal myofibroblasts by lens-derived transforming growth factor beta1 (TGFbeta1): a transgenic mouse model. Brain Res Bull. 2010 Feb 15;81(2-3):287-96.

Riazuddin SA, Vithana EN, Seet LF, Liu Y, Al-Saif A, Koh LW, Heng YM, Aung T, Meadows DN, Eghrari AO, Gottsch JD, Katsanis N. Missense mutations in the sodium borate cotransporter SLC4A11 cause late-onset Fuchs corneal dystrophy. Hum Mutat. 2010 Nov;31(11):1261-8.

Riley M, Winkler B, Starnes C, Peters M. Fluid and ion transport in corneal endothelium: insensitivity to modulators of Na-K-2C1 cotransport. *AmJ Physiol.* 1997;273:Cl480-Cl486.

Riley MV (1977) Anion-sensitive ATPase in rabbit corneal endothelium and its relation to corneal hydration. Experimental eye research 25: 483–494.

Roisin E.M., Nicola M., Michael J.K., Evaluation and validation of candidate endogenous control genes for real-time quantitative PCR studies of breast cancer, BMC Mol. Biol. 8 (2007) 107–120

Romero MF. Molecular pathophysiology of SLC4 bicarbonate transporters. Curr Opin Nephrol Hypertens 14:495–501. (2005)

Romero MF, Fulton CM, Boron WF. The SLC4 family of $HCO_3^-$ transporters. Pflugers Arch - Eur J Physiol (2004) 447:495–509.

Salas, J. T., Banales, J. M., Sarvide, S., Recalde, S., Ferrer, A., Uriarte, I., Oude Elferink, R. P., Prieto, J. and Medina, J. F. (2008) Ae2a,b-deficient mice develop antimitochondrial antibodies and other features resembling primary biliary cirrhosis. Gastroenterology 134, 1482–1493

Sambrook J, Fritsch EF and Maniatis T (1989) Molecular Cloning: A Laboratory Manual, Cold Spring Harbor Laboratory Press., New York.

Schena M, Shalon D, Davis RW, Brown PO: Quantitative monitoring of gene expression patterns with a complementary DNA microarray. *Science* 1995, 270:467-470.

Selvey S, Thompson EW, Matthaei K, Lea RA, Irving MG, Griffiths LR. Beta-actin–an unsuitable internal control for RT-PCR. Mol Cell Probes 2001; 15:307-11.

Shah SS, al-Rajhi A, Brandt JD, Mannis MJ, Roos B, Sheffield VC, Syed NA, Stone EM, Fingert JH: Mutation in the SLC4A11 gene associated with autosomal recessive congenital hereditary endothelial dystrophy in a large Saudi family. *Ophthalmic Genet* 2008, 29:41-45.

Stiemke MM, McCartney MD, Cantu-Crouch D, Edelhauser HF (1991) Maturation of the corneal endothelial tight junction. Investigative ophthalmology & visual science 32: 2757–2765.

Sultana A, Garg P, Ramamurthy B, Vemuganti GK, Kannabiran C: Mutational spectrum of the SLC4A11 gene in autosomal recessive congenital hereditary endothelial dystrophy. *Mol Vis* 2007, 13:1327-1332.

Sun XC, Bonanno JA. Identification and cloning of the Na/HCO(3-) cotransporter (NBC) in human corneal endothelium. Exp Eye Res. 2003 Sep;77(3):287-95.

Sun XC, McCutheon C, Bertram P, Xie Q, Bonanno JA. Studies on the expression of mRNA for anion transport related proteins in corneal endothelial cells. Curr Eye Res. 2001 Jan;22(1):1-7.

Suzuki T, Higgins PJ, Crawford DR. Control selection for RNA quantitation. Biotechniques 2000; 29:332-7.

Thellin O, Zorzi W, Lakaye B, De Borman B, Coumans B, Hennen G, Grisar T, Igout A, Heinen E: Housekeeping genes as internal standards: use and limits. *J Biotechnol* 1999, 75:291-295.

UCSC genome browser. http://genome.ucsc.edu/

UCSC genome blat search. http://genome.ucsc.edu/cgi-bin/hgBlat

Vandesompele J, Preter KD, Pattyn F, Poppe B, Roy NV, Paepe AD, Speleman F. Accurate normalization of real-time quantitative RT-PCR data by geometric averaging of multiple internal control genes. *Genome Biology* 2002, 3(7):research0034.1–0034.11

Vithana EN, Morgan PE, Ramprasad V, Tan DT, Yong VH, Venkataraman D, Venkatraman A, Yam GH, Nagasamy S, Law RW, Rajagopal R, Pang CP, Kumaramanickevel G, Casey JR, Aung T. SLC4A11 mutations in Fuchs endothelial corneal dystrophy. Hum Mol Genet. 2008 Mar 1;17(5):656-66.

Vithana EN, Morgan PE, Ramprasad V, Tan DTH, Yong VHK, Venkataraman D, Venkatraman A, Yam GHF, Nagasamy S,  Law RWK, Rajagopal R,  Pang CP, Kumaramanickevel K, Casey JR , Aung T. *SLC4A11* Mutations in Fuchs Endothelial Corneal Dystrophy (FECD). Hum. Mol. Genet 2007; doi: 10.1093/hmg/ddm337.

Vithana EV, Morgan P, Sundaresan P, Ebenezer N, Tan DT, Anand S, Khine KO, Venkataraman D, Yong V, Salto-Tellez M, Venkataraman A, Guo K, Heemadevi B, Mohamad M, Srinivasan M, Prajna V, Khine M, Casey JR, Inglehearn C, Aung T. Mutations in Na-borate co-transporter SLC4A11 cause recessive Congenital Hereditary Endothelial Dystrophy, CHED2. Nature Genetics, 2006; 38:755-7

Wain, H. M., Lush, M. J., Ducluzeau, F., Khodiyar, V. K. and Povey, S. (2004) Genew: the Human Gene Nomenclature Database, 2004 updates. Nucleic Acids Res. 32, D255–D25)

Warrington JA, Nair A, Mahadevappa M, Tsyganskaya M: Comparison of human adult and fetal expression and identification of 535 housekeeping/maintenance genes. *Physiol Genomics* 2000, 2:143-147.

Weis, J. H., et al. (1992). "Detection of rare mRNAs via quantitative RT-PCR." Trends Genet 8(8): 263-4.

Whitcher JP, Srinivasan M, Upadhyay MP. Corneal blindness: a global perspective. Bulletin of the World Health Organization, 2001, 79: 214–221

Yuan JS, Reed A, Chen F, Stweart CN. Statistical analysis of real-time PCR data. *BMC Bioinformatics* 2006, **7**:85

Zhu Q, Lee, D. W. and Casey, J. R. (2003). Novel topology in C-terminal region of the human plasma membrane anion exchanger, AE1. J. Biol. Chem. 278, 3112-v3120.

**Appendix A. mRNA expression of *Slc4* family genes in cultured mouse corneal endothelial cells (passage 2)**

| Gene name | $\Delta Ct$ ($Ct_{Goi}$-$Ct_{Hprt1}$) [a] | $\Delta\Delta Ct$ ($\Delta Ct_{Goi}$-$\Delta Ct_{Slc4a11}$) [b] | Normalised expression (rel to *Slc4a11*) [c] | P value [d] | $\Delta\Delta Ct$ ($\Delta Ct_{Goi}$-$\Delta Ct_{Slc4a4}$) [b] | Normalised expression (rel to *Slc4a4*) [c] | P value [d] |
|---|---|---|---|---|---|---|---|
| *Slc4a1* | 8.235±0.2332 | 5.155±0.2332 | 0.0281 (0.0239-0.0330) | 0.000492* | 8.98±0.2332 | 0.0020 (0.0017-0.0023) | 0.000633* |
| *Slc4a2* | 0.43±0.0570 | -2.65±0.0570 | 6.2767 (6.0335-6.5297) | 0.000508* | 1.175±0.0570 | 0.4429 (0.4257-0.4607) | 0.000744* |
| *Slc4a3* | 2.43±0.0962 | -0.65±0.0962 | 1.5692 (1.4680-1.6773) | 0.004005* | 3.175±0.0962 | 0.1107 (0.1036-0.1184) | 0.000559* |
| *Slc4a4* | -0.745±0.0632 | -3.825±0.0632 | 14.1723 (13.5644-14.8074) | 0.000644* | 0±0.0632 | 1.0000 (0.9571-1.0448) | - |
| *Slc4a5* | 9.615±0.2470 | 6.535±0.2470 | 0.0108 (0.0091-0.0128) | 0.000545* | 10.36±0.2470 | 0.0008 (0.0006-0.0009) | 0.000636* |
| *Slc4a7* | 1.015±0.1789 | -2.065±0.1789 | 4.1843 (3.6964-4.7367) | 0.007350* | 1.76±0.1789 | 0.2952 (0.2608-0.3342) | 0.000035* |
| *Slc4a8* | 9.995±0.3162 | 6.915±0.3162 | 0.0083 (0.0067-0.0103) | 0.000544* | 10.74±0.3162 | 0.0006 (0.0005-0.0007) | 0.000637* |
| *Slc4a9* | 10.12±0.3371 | 7.04±0.3371 | 0.0076 (0.0060-0.0096) | 0.000543* | 10.865±0.3371 | 0.0005 (0.0004-0.0007) | 0.000636* |
| *Slc4a10* | 2.645±0.0632 | -0.435±0.0632 | 1.3519 (1.2939-1.4125) | 0.000813* | 3.39±0.0632 | 0.0954 (0.0913-0.0997) | 0.000639* |
| *Slc4a11* | 3.08±0.0604 | 0±0.0604 | 1.0000 (0.9590-1.0428) | - | 3.825±0.0604 | 0.0706 (0.0677-0.0736) | 0.000644* |

**Appendix B. mRNA expression of *Slc4* family genes in cultured mouse corneal endothelial cells (passage 7)**

| Gene name | $\Delta$Ct (Ct$_{Goi}$ - Ct$_{Hprt1}$) [a] | $\Delta\Delta$Ct ($\Delta$Ct$_{Goi}$ - $\Delta$Ct$_{Slc4a11}$) [b] | Normalised expression (rel to *Slc4a11*) [c] | P value [d] | $\Delta\Delta$Ct ($\Delta$Ct$_{Goi}$ - $\Delta$Ct$_{Slc4a4}$) [b] | Normalised expression (rel to *Slc4a4*) [c] | P value [d] |
|---|---|---|---|---|---|---|---|
| *Slc4a1* | 6.085±0.1557 | 3.98±0.1557 | 0.0634 (0.0569-0.0706) | 0.002245* | 8.875±0.1557 | 0.0021 (0.0019-0.0024) | 0.006460* |
| *Slc4a2* | -2.03±0.1221 | -4.135±0.1221 | 17.5695 (16.1441-19.1207) | 0.002376* | 0.76±0.1221 | 0.5905 (0.5426-0.6426) | 0.015596* |
| *Slc4a3* | -1.03±0.1513 | -3.135±0.1513 | 8.7847 (7.9100-9.7562) | 0.003825 | 1.76±0.1513 | 0.2952 (0.2658-0.3279) | 0.007859* |
| *Slc4a4* | -2.79±0.2022 | -4.895±0.2022 | 29.7538 (25.8621-34.2311) | 0.006633* | 0±0.2022 | 1.0000 (0.8692-1.1505) | - |
| *Slc4a5* | 7.395±0.2688 | 5.29±0.2688 | 0.0256 (0.0212-0.0308) | 0.002187* | 10.185±0.2688 | 0.0009 (0.0007-0.0010) | 0.006453* |
| *Slc4a7* | -1.32±0.1513 | -3.425±0.1513 | 10.7406 (9.6711-11.9284) | 0.003787* | 1.47±0.1513 | 0.3610 (0.3250-0.4009) | 0.008380* |
| *Slc4a8* | 8.2±0.4206 | 6.095±0.4206 | 0.0146 (0.0109-0.0196) | 0.002163* | 10.99±0.4206 | 0.0005 (0.0004-0.0007) | 0.006449* |
| *Slc4a9* | 7.68±0.1253 | 5.575±0.1253 | 0.0210 (0.0192-0.0229) | 0.001496* | 10.47±0.1253 | 0.0007 (0.0006-0.0008) | 0.006456* |
| *Slc4a10* | 3.69±0.17 | 1.585±0.1700 | 0.3333 (0.2963-0.3750) | 0.001489* | 6.48±0.1700 | 0.0112 (0.0100-0.0126) | 0.006481* |
| *Slc4a11* | 2.105±0.121 | 0±0.1210 | 1.0000 (0.9195-1.0875) | - | 4.895±0.1210 | 0.0336 (0.0309-0.0366) | 0.006632* |

**Appendix C. mRNA expression of *SLC4* family genes in human corneal endothelial cells (passage 2)**

| Gene name | $\Delta Ct$ ($Ct_{GOI} - Ct_{GAPDH}$) [a] | $\Delta\Delta Ct$ ($\Delta Ct_{GOI} - \Delta Ct_{SLC4A11}$) [b] | Normalised expression (rel to *SLC4A11*) [c] | P value [d] | $\Delta\Delta Ct$ ($\Delta Ct_{GOI} - \Delta Ct_{SLC4A4}$) [b] | Normalised expression (rel to *SLC4A4*) [c] | P value [d] |
|---|---|---|---|---|---|---|---|
| *SLC4A1* | 17.28±0.0738 | 12.725±0.0738 | 0.00015 (0.00014-0.00016) | 0.001222* | 13.925±0.0738 | 0.00006 (0.000061-0.000068) | 0.000584* |
| *SLC4A2* | 8.045±0.1151 | 3.49±0.1151 | 0.08900 (0.08218-0.09640) | 0.001147* | 4.69±0.1151 | 0.03874 (0.035770-0.041959) | 0.000542* |
| *SLC4A3* | 12.345±0.0474 | 7.79±0.0474 | 0.00452 (0.00437-0.00467) | 0.001227* | 8.99±0.0474 | 0.00197 (0.001903-0.002032) | 0.000584* |
| *SLC4A4* | 3.355±0.0604 | -1.2±0.0604 | 2.29740 (2.20318-2.39565) | 0.000250* | 0±0.0604 | 1.00000 (0.958988-1.042766) | - |
| *SLC4A5* | 12.86±0.0539 | 8.305±0.0539 | 0.00316 (0.00305-0.00328) | 0.001225* | 9.505±0.0539 | 0.00138 (0.001326-0.001429) | 0.000584* |
| *SLC4A7* | 7.92±0.0671 | 3.365±0.0671 | 0.09706 (0.09265-0.10168) | 0.001283* | 4.565±0.0671 | 0.04225 (0.040328-0.044258) | 0.000578* |
| *SLC4A8* | 10.795±0.0738 | 6.24±0.0738 | 0.01323 (0.01257-0.01393) | 0.001227* | 7.44±0.0738 | 0.00576 (0.005472-0.006061) | 0.000582* |
| *SLC4A9* | 15.485±0.0354 | 10.93±0.0354 | 0.00051 (0.00050-0.00053) | 0.001222* | 12.13±0.0354 | 0.00022 (0.000218-0.000229) | 0.000584* |
| *SLC4A10* | 20.095±0.5802 | 15.54±0.5802 | 0.00002 (0.00001-0.00003) | 0.001221* | 16.74±0.5802 | 0.00001 (0.000006-0.000014) | 0.000584* |
| *SLC4A11* | 4.555±0.0875 | 0±0.0875 | 1.00000 (0.94118-1.06250) | - | 1.2±0.0875 | 0.43528 (0.409670-0.462480) | 0.000250* |

**Appendix D. mRNA expression of *SLC4* family genes in human corneal endothelial cells (passage 5)**

| Gene name | $\Delta Ct$ ($Ct_{GOI}$ − $Ct_{GAPDH}$) [a] | $\Delta\Delta Ct$ ($\Delta Ct_{GOI}$ - $\Delta Ct_{SLC4A11}$) [b] | Normalised expression (rel to *SLC4A11*) [c] | P value [d] | $\Delta\Delta Ct$ ($\Delta Ct_{GOI}$ - $\Delta Ct_{SLC4A4}$) [b] | Normalised expression (rel to *SLC4A4*) [c] | P value [d] |
|---|---|---|---|---|---|---|---|
| *SLC4A1* | 16.61±0.2650 | 11.96±0.2650 | 0.00025 (0.00021-0.00030) | 0.000575* | 14.205±0.2650 | 0.00005 (0.00004-0.00006) | 0.005231* |
| *SLC4A2* | 6.94±0.0447 | 2.29±0.0447 | 0.20448 (0.19823-0.21091) | 0.000654* | 4.535±0.0447 | 0.04313 (0.04182-0.04449) | 0.005571* |
| *SLC4A3* | 10.72±0.0707 | 6.07±0.0707 | 0.01488 (0.01417-0.01563) | 0.000573* | 8.315±0.0707 | 0.00314 (0.00299-0.00330) | 0.005251* |
| *SLC4A4* | 2.405±0.1818 | -2.245±0.1818 | 4.74037 (4.17913-5.37698) | 0.007236* | 0±0.1818 | 1.00000 (0.88160-1.13430) | - |
| *SLC4A5* | 13.435±0.2790 | 8.785±0.2790 | 0.00227 (0.00187-0.00275) | 0.000566* | 11.03±0.2790 | 0.00048 (0.00039-0.00058) | 0.005228* |
| *SLC4A7* | 7.545±0.1275 | 2.895±0.1275 | 0.13444 (0.12307-0.14686) | 0.000392* | 5.14±0.1275 | 0.02836 (0.02596-0.03098) | 0.005321* |
| *SLC4A8* | 10.245±0.0430 | 5.595±0.0430 | 0.02069 (0.02008-0.02131) | 0.000583* | 7.84±0.0430 | 0.00436 (0.00424-0.00450) | 0.005266* |
| *SLC4A9* | 14.795±0.0765 | 10.145±0.0765 | 0.00088 (0.00084-0.00093) | 0.000576* | 12.39±0.0765 | 0.00019 (0.00018-0.00020) | 0.005232* |
| *SLC4A10* | 15.7±0.1077 | 11.05±0.1077 | 0.00047 (0.00044-0.00051) | 0.000575* | 13.295±0.1077 | 0.00010 (0.00009-0.00011) | 0.005231* |
| *SLC4A11* | 4.65±0.0600 | 0±0.0600 | 1.00000 (0.95926-1.04247) | - | 2.245±0.0600 | 0.21095 (0.20236-0.21991) | 0.007236* |